# MANAGING RANDOMNESS IN WIRELESS NETWORKS: RANDOM POWER CONTROL AND SUCCESSIVE INTERFERENCE CANCELLATION

A Dissertation

Submitted to the Graduate School
of the University of Notre Dame
in Partial Fulfillment of the Requirements
for the Degree of

Doctor of Philosophy

by

Xinchen Zhang

---

Martin Haenggi, Director

Graduate Program in Electrical Engineering
Notre Dame, Indiana
September 2013

MANAGING RANDOMNESS IN WIRELESS NETWORKS: RANDOM POWER CONTROL AND SUCCESSIVE INTERFERENCE CANCELLATION

Abstract

by

Xinchen Zhang

Considering wireless networks whose channel quality and node distribution are random, this thesis studies two types of techniques that can potentially significantly boost the network performance: random power control and successive interference cancellation (SIC).

Random power control generalizes conventional (deterministic) power control by allowing the transmitters to randomly vary their transmit power. In the first part of the thesis, we study random power control in two types of wireless networks: the noise-limited networks and the interference-limited networks. In noise-limited networks, we show that random power control can significantly reduce the local delay, and the optimal power control policies are ALOHA-type random on-off policies. In interference-limited networks, we take a game theoretic framework and focus on two sets of strategies: single-node optimal power control (SNOPC) strategies and Nash equilibrium power control (NEPC) strategies. SNOPC strategies maximize the expected throughput of the power controllable link given that all the other transmitters do not use power control. Under NEPC strategies, no individual node of the network can achieve a higher expected throughput by unilaterally deviating from these strategies. We prove that under mean and peak power constraints at each transmitter, the SNOPC and NEPC strategies are ALOHA-type random on-off power control policies.

Successive interference cancellation (SIC) allows the receiver to decode and cancel signal components from users sequentially and thus can potentially significantly boost the network throughput. However, the feasibility of SIC depends on the received signal power ordering which further depends on the fading distribution, network geometry, and many other system parameters. In the second part of the thesis, we provide a unified framework to study the performance of SIC in $d$-dimensional wireless networks with arbitrary fading distribution and power-law path loss. Using this framework, we are able to analytically characterize the performance of SIC. The results suggest that the marginal benefit of enabling the receiver to successively decode $k$ users diminishes very fast with $k$, especially in networks of high dimensions and small path loss exponent. On the other hand, SIC is highly beneficial when the users are clustered around the receiver and/or very low-rate codes are used, and with multiple packet reception, a lower per-user information rate always results in higher aggregate throughput in interference-limited networks. In contrast, there exists a positive optimal per-user rate that maximizes the aggregate throughput in noisy networks.

The analytical results serve as useful tools to understand the potential gain of SIC in heterogeneous cellular networks (HCNs). Using these tools, we quantify the gain of SIC on the coverage probability in HCNs with non-accessible base stations. An interesting observation is that, for contemporary narrow-band systems (*e.g.,* LTE and WiFi), most of the gain of SIC is achieved by canceling a single interferer.

CONTENTS

FIGURES . . . . . v

TABLES . . . . . ix

ACKNOWLEDGMENTS . . . . . x

SYMBOLS . . . . . xii

CHAPTER 1: INTRODUCTION AND THESIS ORGNIZATION . . . . . 1
1.1 Random Power Control . . . . . 1
1.2 Successive Interference Cancellation . . . . . 4

CHAPTER 2: RANDOM POWER CONTROL IN NOISE-LIMITED NETWORKS . . . . . 6
2.1 Motivation and Main Contribution . . . . . 6
2.2 Related Work . . . . . 7
2.3 Applications to Wireless Networks . . . . . 8
2.4 Chapter Organization . . . . . 8
2.5 Problem Formulation . . . . . 9
2.5.1 Reception Model . . . . . 9
2.5.2 Delay Definitions . . . . . 9
2.5.3 The Optimal Stationary Power Control Policy . . . . . 11
2.6 Rayleigh Fading . . . . . 13
2.6.1 ALOHA Is the Optimal Policy . . . . . 13
2.6.2 Comparison of Random Power Control Schemes . . . . . 18
2.7 General Fading Distributions . . . . . 21
2.7.1 The Optimality of ALOHA . . . . . 21
2.7.2 Peak-power-limited and Mean-power-limited Regimes . . . . . 24
2.7.3 Numerical Approach . . . . . 26
2.7.4 Examples . . . . . 26
2.8 Conclusions . . . . . 31

CHAPTER 3: RANDOM POWER CONTROL IN INTERFERENCE-LIMITED NETWORKS . . . 34
3.1 The SNOPC and NEPC Strategies . . . 34
3.2 Relation to Other Work . . . 35
3.3 Chapter Organization . . . 36
3.4 System Model . . . 37
3.4.1 Network Model . . . 37
3.4.2 Game-Theoretic Formulation . . . 37
3.5 Case 1: Unknown Link Distances . . . 39
3.6 Case 2: Known Link Distance . . . 42
3.6.1 General $f_R$ . . . 42
3.6.2 Bipolar Networks . . . 44
3.7 Case 3: Static Network . . . 47
3.8 Performance Evaluation . . . 52
3.8.1 The Single-node Optimal Power Control (SNOPC) Strategies . . . 52
3.8.2 Nash Equilibrium Power Control (NEPC) Strategies . . . 55
3.9 Conclusions . . . 59

CHAPTER 4: THE PERFORMANCE OF SUCCESSIVE INTERFERENCE CANCELLATION . . . 61
4.1 Successive Interference Cancellation and Related Work . . . 61
4.2 Contributions and Organization . . . 63
4.3 System Model and Metrics . . . 64
4.3.1 The Power-law Poisson Network with Fading (PPNF) . . . 64
4.3.2 SIC Model and Metrics . . . 65
4.4 The Path Loss Process with Fading (PLPF) . . . 66
4.5 Bounds on the Probability of Successive Decoding . . . 68
4.5.1 Basic Bounds . . . 69
4.5.2 The Lower Bounds . . . 70
4.5.2.1 High-rate lower bound . . . 70
4.5.2.2 Low-rate lower bound . . . 72
4.5.3 The Upper Bound . . . 73
4.5.4 The Sequential Multi-user Decoding (SMUD) Bounds . . . 74
4.5.5 Two General Outage Results . . . 79
4.5.6 Numerical Results . . . 80
4.6 The Expected Gain of SIC . . . 82
4.6.1 The Mean Number of Successively Decoded Users . . . 82
4.6.2 The Aggregate Throughput . . . 86
4.6.3 A Laplace Transform-based Approximation . . . 90
4.7 The Effect of Noise . . . 91
4.8 Conclusions . . . 96

CHAPTER 5: SIC IN HETEROGENEOUS CELLULAR NETWORKS . . . . 98
5.1 Modeling Heterogeneous Cellular Networks Using PPP . . . . . 98
5.2 The Marked Path Loss Process with Fading . . . . . 99
5.3 The Coverage Probability . . . . . 100
5.3.1 Without SIC . . . . . 101
5.3.2 With SIC . . . . . 101
5.4 The Effect of the Path Loss Exponent $\alpha$ . . . . . 105
5.5 Average Throughput . . . . . 106
5.6 Finite SIC Capabilty . . . . . 107
5.6.1 The High SIR Case . . . . . 110
5.6.2 More Realistic Cases . . . . . 112
5.7 Conclusions . . . . . 115

CHAPTER 6: CONCLUDING REMARKS AND FUTURE WORK . . . . . 117
6.1 Random Power Control in Networks with Both Noise and Interference 117
6.2 Practical Aspects of Random on-off Power Control . . . . . 118
6.2.1 Adaptive Modulation . . . . . 118
6.2.2 RF Constraints . . . . . 118
6.3 More Detailed Modeling of SIC in Random Wireless Networks . . . . 119
6.3.1 Centralized Rate Assignment and Scheduling . . . . . 119
6.3.2 Power Control and SIC . . . . . 119
6.3.2.1 Deterministic Power Control . . . . . 119
6.3.2.2 Random Power Control . . . . . 120

BIBLIOGRAPHY . . . . . 121

FIGURES


2.1 A collection of links with random distances. Transmitters are denoted by x and receivers are denoted by o. The distances $r_k, k \in [5]$ are iid drawn from some distribution $f_R(x)$. . . . . 12

2.2 Broadcast in wireless network. Transmitters are denoted by x and receivers are denoted by o. The distances $r_k, k \in [5]$ are deterministic and known to the transmitter. . . . . 12

2.3 Comparison of the conditional local delay for different power control schemes. Here, $P_{\max} = 4$, $\theta = 1$, $\alpha = 2$. . . . . 20

2.4 Minimum conditional local delay for Nakagami-$m$ fading, where $P_{\max} = 4$, $\theta = 1$, $\alpha = 2$. . . . . 27

2.5 Numerically obtained $F_P^*(x)$ for Rician fading. $P_{\max} = 4$, $\theta = 1$, $\alpha = 2$, $K = 1$. . . . . 29

2.6 Numerically obtained $F_P^*(x)$ for lognormal fading. $P_{\max} = 4$, $\theta = 1$, $\alpha = 2$, $\sigma = 1$. . . . . 29

2.7 Minimum local anycast delay in the Rayleigh fading case. $P_{\max} = 4$, $\theta = 1$, $\alpha = 2$. . . . . 32

3.1 Comparison of throughput using 1) constant power transmission (no power control) 2) GOPT ALOHA 3) the best response to the GOPT ALOHA and 4) NEPC strategy. Here, $\lambda = 1$, $P_{\max} = 2$, $\alpha = 2$, $\theta = 10$. To the right of the two vertical lines, the transmit power of the GOPT and NEPC strategies hits their corresponding peak power limits. . . 47

3.2 The NEPC in a Poisson bipolar network in case 3. Each transmitter-receiver pair is linked by a line, where a circle is centered at the transmitter and the receiver is labeled by x. The radius of each circle is proportional to the Nash equilibrium transmit probability (Fig. 3.2a) or the throughput (Fig. 3.2b) at the corresponding link. Here, $\lambda = 1$, $r \equiv 0.3$, $P_{\max} = 2$, $\theta = 10$. . . . . 53

3.3 Comparison of throughput using three different SNOPC strategies. Here, $\lambda = 1$, $P_{\max} = 10$, $\alpha = 4$, $\theta = 10$. The throughput of case 3 is averaged over 10,000 realizations of the PPP. . . . . 54

3.4 Comparison of throughput in bipolar network using constant power transmission, NEPC strategies in case 2 and case 3, the case where all nodes transmit with power $P_{\max}$ and probability $P_{\max}^{-1}$ ($\gamma = P_{\max}$), and SNOPC strategy in case 2. Here, $\lambda = 1$, $P_{\max} = 2$, $\alpha = 4$, $\theta = 10$. . . 57

3.5 Comparison of the spatial throughput under NEPC when link distance are Rayleigh distributed with mean $1/2\sqrt{\lambda_r}$ in three cases. Here, $\lambda = \lambda_r = 1$, $P_{\max} = 2$, $\alpha = 4$, $\theta = 10$. The throughput in case 3 is averaged over 10,000 PPP realizations. . . . . 59

4.1 Realizations of two non-uniform PPP with intensity function $\lambda(x) = 3\|x\|^b$ with different $b$, where × denotes an active transmitter and ○ denotes the receiver at the origin. . . . . 64

4.2 Comparison of $\mathbb{P}(\xi_k^{-1} > \theta I_k)$ between simulation and the analytical value according to Corollary 9 for $k = 1, 2, 3, 4, 5$. . . . . 78

4.3 Combined upper bound (Proposition 11), high-rate lower bound (Proposition 9), and SMUD upper bound (Proposition 12) for $p_k$ ($k = 1, 2, 3$, from top to bottom) in a 2-d uniform network with path loss exponent $\alpha = 3$. . . . . 81

4.4 Upper and (high-rate) lower bounds (in Proposition 11 and 9, respectively) for $p_k$ ($k = 1, 2, 3$) in a 2-d network with with path loss exponent $\alpha = 4$, $\theta = 1$ and density function $\lambda(x) = a\|x\|^b$. $b = 0$ is the uniform case. . . . . 82

4.5 SMUD bounds (in Proposition 12) for $p_k$ ($k = 1, 2, 3$) in a 2-d network with path loss exponent $\alpha = 4$, $\theta = 1$ and density function $\lambda(x) = a\|x\|^b$. $b = 0$ is the uniform case. . . . . 83

4.6 The mean number of users that can be successively decoded in a 2-d uniform network with path loss exponent $\alpha = 4$. Here, the upper bound, lower bound, low-rate lower bound, SMUD upper bound refer to the bounds in Proposition 13, 15, 14 and 16, respectively. . . . . 86

4.7 Aggregate throughput at $o$ in a 2-d uniform network with with path loss exponent $\alpha = 4$, *i.e.,* $\beta = \delta = 2/\alpha = 1/2$. The upper bound, lower bound, low-rate lower bound and SMUD upper bound come from Propositions 15, 13, 14 and 16 respectively. . . . . 87

4.8 Simulated and approximated, by (4.20), aggregate throughput at $o$ in a 2-d uniform network. . . . . 92

4.9 Aggregate throughput at $o$ in a 2-d uniform network with noise. Here, the path loss exponent $\alpha = 4$. Three levels of noise are considered: $W = 0.1$, $W = 1$ and $W = 10$. . . . . 95

5.1 An 2-tier HCN with 10% of Tier 1 (macrocell) BSs (denoted by +) overloaded and 30% of Tier 2 (femtocell) BSs (denoted by ×) configured as closed. A box is put on the BS whenever it is non-accessible (*i.e.,* either configured as closed or overloaded). The o at origin is a typical receiver. . . . . 99

5.2 The coverage probability (with infinite SIC capability) as a function of SIR threshold $\theta$ in HCNs with $\eta = 0.6$ and $\alpha = 4$. The (Laplace-transform-based) approximation, lower bound and upper bounds of $P_c^{\mathrm{SIC}}$ is calculated according to (5.6), (5.4) and (5.5), respectively. The coverage probability in the case without SIC (a problem also studied in [23, 24]) is also plotted for comparison, where the $\theta \geq 0$dB part is analytically obtained by (5.2) and the $\theta < 0$dB part is based on simulation. . . . . 104

5.3 Comparison between coverage probability with and without SIC in HCNs with $\eta = 0.8$, $\theta = 1$. Here, the upper and lower bounds are based on (5.9) and (5.7), respectively. . . . . 106

5.4 The average throughput as a function of SIR threshold $\theta$ in HCNs with $\eta = 0.6$ and $\alpha = 4$. The (Laplace-transform-based) approximation, lower bound and upper bounds of $P_c^{\mathrm{SIC}}$ is calculated according to (5.6), (5.4) and (5.5), respectively. The non-outage throughput in the case without SIC is plotted for comparison, where the $\theta \geq 0$dB part is analytically obtained by (5.2) and the $\theta < 0$dB part is based on simulation. . . . . 107

5.5 Comparison between the upper bound on the coverage probabilities and the simulated coverage probability of femto-cell networks with different levels of SIC capability when $\alpha = 4$. The upper bounds on $P_{c,n}^{\mathrm{SIC}}$ is calculated according to (5.12) for $n = 1, 2$ (coverage probability is higher for larger $n$). The upper bound on $P_c^{\mathrm{SIC}}$ is calculated by (5.13). The simulated value of $P_{c,n}^{\mathrm{SIC}}$ is plotted for $n = 1, 2, 10$. When $\theta = 2$dB, the curves for $n = 2$ and $n = 10$ almost completely overlap. 111

5.6 Comparison between the upper bound on the coverage probabilities and the simulated coverage probability of femto-cell networks with different path loss exponent $\alpha$ when $\theta = 0$dB. The upper bounds on $P_{c,n}^{\mathrm{SIC}}$ is calculated according to (5.14) for $n = 1, 2$ (coverage probability is higher for larger $n$). The upper bound on $P_c^{\mathrm{SIC}}$ is calculated by (5.15). The simulated value of $P_{c,n}^{\mathrm{SIC}}$ is plotted for $n = 1, 2, 10$. For $\alpha \leq 3.5$, the curves for $n = 2$ and $n = 10$ almost completely overlap. . 113

5.7 Coverage probability of femto-cell networks with SIR threshold $\theta \geq -5$dB with $\alpha = 4$. The solid lines are calculated for $n = 1, 2$ according to (5.14) (the lines are higher for larger $n$), which are an upper bounds on $P_{c,n}^{\text{SIC}}$ when $\theta \geq 0$dB. For $\theta \leq 0$, these lines should be considered as approximations. The upper bound on $P_c^{\text{SIC}}$ is calculated by (5.15). The simulated value of $P_{c,n}^{\text{SIC}}$ is plotted for $n = 1, 2, 10$. For $\eta \leq 0.9$, the curves for $n = 2$ and $n = 10$ almost completely overlap throught the simulated SIR range. . . . . 114

TABLES

2.1 OPTIMAL TRANSMIT POWER $\xi$ FOR ANYCAST WITH RAYLEIGH FADING, WHERE $P_{\max} = 4$, $\alpha = 2$, $\theta = 1$. . . . . 32

# ACKNOWLEDGMENTS

Foremost, I want to thank my advisor, one of the best teachers I have ever known, Dr. Martin Haenggi. He has been extremely supportive throughout my research, offering inspiration, advices and encouragement. His emphasis in mathematical rigor and conciseness shaped my style and improved my skills in presenting complex technical ideas on papers. It has been such a pleasure and honor working with Dr. Haenggi.

I thank my defense committee: Dr. Thomas Fuja, Dr. Bertrand Hochwald and Dr. Yih-Fang Huang for the inspirations resulted from the defense and their kind suggestions, which perfected the dissertation. I need to thank all the professors from the EE and the Math departments who have taught or advised me. They built up my knowledge and shaped who I am. Also, I thank all the staff in the EE department, espeically, Tracy, the best graduate coordinator I could ever imagine.

I would like to thank my colleagues and friends Jing Huang, Zhenhua Gong, Zhanwei Sun, Lai Wei, Zhen Tong, Krishnan Padmanabhan, Sunil Srinivasa, Sundeep Venkatraman, Sundar Vanka, Feng Zhu, Utsaw Kumar, Jiao Wang, Anjin Guo, Ding Nie - to name just a few - for all the discussions we had and all the things I learned from them. I also want to thank all the other wonderful friends I made in ND. They gave this 5 years so much fun.

This dissertation is not possible without all the support from my parents Mr. Kejian Zhang and Ms. Guoji Yan and my wife Mi Zhou. They encouraged me to set goals, work hard and pay attention to everyday life. They made this PhD journey organized and enjoyable.

Last but not least, the financial support from National Science Foundation is gratefully acknowledged. I also want to thank Broadcom Corp. and FutureWei Technologies, Inc. for the internship opportunities. These experiences complemented what I learned in the university.

# SYMBOLS

| | |
|---|---|
| $\mathbb{P}$ | probability measure |
| $\mathbb{E}$ | expectation |
| $\mathbb{E}^{!x}$ | expectation with respect to the reduced Palm measure |
| $[n]$ | the set $\{1,2,\cdots,n\}$ |
| $\mathbb{N}$ | natural numbers $\{1, 2, \cdots\}$ |
| $\mathbb{R}^d$ | $d$-dimensional Euclidean space |
| $o$ | origin of $\mathbb{R}^d$ |
| $\|\cdot\|$ | Euclidean metric of $x \in \mathbb{R}^d$ |
| $\mathbb{R}^+$ | non-negative real numbers |
| $1(\cdot)$ | indicator function |
| $1_A(x)$ | $\equiv 1(x \in A)$ |
| $\stackrel{\mathrm{d}}{=}$ | equality in distribution |
| $\triangleq$ | definition |

# CHAPTER 1

# INTRODUCTION AND THESIS ORGNIZATION

Wireless networks are becoming ubiquitous in modern society. The exponentially increasing data demand and number of wireless devices requires not only novel techniques to improve the efficiency of wireless networks but also network-wide analytical tools to generate insights on the design of truly robust and scalable wireless systems.

Focusing on random power control and successive inteference cancellation and using tools from stochastic geometry [39, 41, 63], this thesis explores the design insights of the two promising techniques in the context of large-scale random wireless networks.

## 1.1 Random Power Control

Power control benefits wireless communication in many different ways (see [48, 52, 57, 59] and the references therein).

In the context of point-to-point communication, typical power control policies include water-filling, dynamic programming, channel inversion, etc. Water-filling is typically used to maximize the throughput [16, 30, 31, 49, 65]. Power control policies based on dynamic programming are useful in reducing the queueing delay under power constraints, or, conversely, reducing energy consumption under queueing delay constraints [13, 19, 28, 51, 59].

In wireless networks, two main approaches have been used to analyze and design sensible power control policies: the optimization approach and the game theory approach. The optimization approach takes a global point of view and aims at finding

the power assignment that maximizes some global metric [17, 27, 44, 61]. Recent efforts concentrate on finding such assignment by distributed algorithms, and algorithms with different merit have been proposed in both infrastructure (cellular) networks [43] and infrastructureless (ad hoc) networks [27, 44, 45]. Instead of modeling network users as cooperative individuals, the game theory approach views the network as a collection of selfish users with conflicting interests [53]. Many forms of games have been introduced to facilitate the analysis and design (see [2, 56, 62] and the references therein). Although properly designed the games (*e.g.,* by designing pricing structures) are often used to find solutions that maximize some global utility (*e.g.,* [3, 8, 25, 45]), the key merit of game theory arguments lies in revealing the robust power control strategies such that malicious users cannot benefit from deviating from them, which can hardly be achieved by other approaches. A detailed survey of existing power control schemes is presented in [18].

Most of the works listed above characterize power control strategy by a set of deterministic power levels across frequency, time, and transmitters. While it is intuitive that the deterministic treatment of transmit power is good enough when the complete channel state information (CSI) is available at the transmitters, it is unclear, without perfect CSI, whether randomness in the transmit power can be beneficial. This thesis answers this question by studying the case where the transmit power at each node is allowed to be a random variable with arbitrary distribution subject to a (unit) mean power and a peak power constraint. Our results show that this additional randomness can be highly beneficial.

We focuses on two different types of networks: noise-limited networks and interference limited networks. Although they are different in nature, it turns out that the resulting (optimal) power control strategies are closely related and are all ALOHA-type random on-off policies, whose transmit power and probability is a function of the transmitters' knowledge of the networks.

Chapter 2 considers noise-limited networks, and we focus on the *delay till success* (DTS), defined as the time until a packet is successfully received (decoded) at the receiver. We derive the optimal power control policies that minimize the DTS over the network for different fading statistics. It is shown that DTS is closely related to the local delay [9, 36, 37] in wireless networks. In fact, DTS can be viewed as the local delay conditioned on the link distance. Therefore, a direct application of our results is the minimization of the local delay. Our results also indicate a way of minimizing the local *anycast* delay, *i.e.,* the mean delay for a transmission to any node[1].

In Chapter 3, we consider interference-limited networks and focus on the expected throughput of each node. Modeling power control as a non-cooperative game where each transmitter tries to maximize its expected throughput, we characterize two types of power control strategies: 1. Single-node optimal power control (SNOPC) strategies when only one node in the network uses power control; 2. Nash equilibrium power control (NEPC) strategies when all the nodes in the network use power control. SNOPC strategies maximize the expected throughput of the power-controllable link, whereas NEPC strategies ensure that no individual node of the network can achieve a higher expected throughput by unilaterally deviating from these strategies. In the discussion of each type of strategy, we consider three different levels of information available at the transmitters, which can be interpreted as corresponding to three levels of mobility of the network. It turns out that, in many cases, ALOHA-type random on-off power control policies are single-node optimal and constitute Nash equilibria.

[1]In the literature, the local anycast delay is sometimes also referred to as exit delay, *e.g.* [11].

## 1.2 Successive Interference Cancellation

The analysis of interference-limited networks in Chapter 3 takes the conventional approach of treating interference as noise. This approach complies with the implementation of most of the existing wireless devices. However, interference is fundamentally different from noise in that interference is generated by other transmitters and thus has much more known structure than noise. Such structure can be exploited to design better receivers and thus improve the network performance [12, 14, 15, 20, 46, 47, 58, 71].

Amongst the many possible techniques to exploit the interference structure, successive interference cancellation (SIC) is a promising one mainly because of its relatively manageable complexity [12, 71]. First introduced in [21], the idea of SIC is to decode different users sequentially, *i.e.,* the interference due to the decoded users is subtracted before decoding other users. Although not always being the optimal multiple access scheme in wireless networks [12, 14], SIC is especially amenable to implementation [4, 68] and does attain boundaries of the capacity regions in multiuser systems in many cases [12, 22, 60].

In a network without centralized power control, *e.g.,* ad hoc networks, the use of SIC hinges on the ordering of the received power from different users (active transmitters), which further depends on the spatial distribution of the users as well as many other network parameters. Therefore, it is important to quantify the gain of SIC with respect to different system parameters. Nonetheless, although the performance of SIC is well-understood for fixed network topology without out-of-the-system interference, the fundamental limits of SIC in the context of large random wireless networks is difficult to characterize [71].

Chapter 4 provides a unified framework to study the performance of SIC in $d$-dimensional wireless networks. Modeling the active transmitters in the network by a Poisson point process (PPP) with power-law density function (which includes the

uniform PPP as a special case), we analytically characterize the performance of SIC as a function of many system parameters including the path loss exponent, fading, coding rate and user distribution. The results suggest that the marginal benefit of enabling the receiver to successively decode $k$ users diminishes very fast with $k$, especially in networks of high dimensions and small path loss exponent. On the other hand, SIC is highly beneficial when the users are clustered around the receiver and/or very low-rate codes are used, and with multiple packet reception, a lower per-user information rate always results in higher aggregate throughput in interference-limited networks. In contrast, there exists a positive optimal per-user rate that maximizes the aggregate throughput in noisy networks.

As an application of these general technical results, we study the performance of SIC in heterogeneous cellular networks (HCNs) in Chapter 5. Focusing on the coverage probability, *i.e.,* the probability of a typical user successfully connecting to at least one of the accessible BSs, Chapter 5 studies the performance of SIC (at the user equipment (UE) side) in the downlink of a $K$-tier interference-limited HCN with *accessible* and *non-accessible* BSs[2]. We characterize how the coverage probability behaves as a function of many system parameters including path loss exponent, coding rate, fading distributions and BS accessibilities and densities. This characterization is elegantly carried out by using a *marked path loss process with fading* (PLPF)-based framework and by calculating the *equivalent access probability* (EAP).

Our analysis suggests that for contemporary OFDM-based HCNs, infinite SIC capability is often unnecessary. In fact, under typical system parameters, most of the gain of SIC comes from the ability of canceling only a single non-accessible BS.

Parts of the results above appear in [73, 75–81].

---

[2] The non-accessible BSs can be interpreted as overloaded/biased BSs [29], femtocells with closed-access configuration, or simply interferers outside the cellular system.

# CHAPTER 2

# RANDOM POWER CONTROL IN NOISE-LIMITED NETWORKS

## 2.1 Motivation and Main Contribution

Consider a fading wireless link, where the transmitter keeps sending the same packet. The *delay till success* (DTS) is the mean number of transmissions needed, averaged over the fading, until this packet is successfully received (decoded) at the receiver. Assuming that the fading is iid and that the transmitter is allowed to vary only the transmit power, the DTS is a function of the fading statistics and the power control policy. The DTS can be interpreted as the service time of the head-of-line packet, if the transmit buffer and the link are viewed as a queueing system.

This chapter shows that under a mean and a peak transmit power constraint, memoryless random power control can significantly reduce the DTS compared to deterministic power control. In particular, we derive the optimal (DTS-minimizing) power control policies for different fading statistics. It turns out that for almost all popular fading distributions (Rayleigh, Nakagami-$m$, Rician, lognormal) the optimal power control policy is a random on-off policy.

Although this chapter exclusively considers noise-limited networks, we will see in Chapter 3 that the theorems proved in this chapter are some of the key building blocks for their counterparts in interference-limited networks.

## 2.2 Related Work

Recently, [9, 32, 36–38, 40, 82] introduced the notion of the *local delay*, which is a fundamental source of delay in wireless networks and a sensitive metric for interference correlation. It is the mean time until a node successfully transmits to its nearest neighbor in a wireless network whose node locations are governed by a point process, averaged over fading, channel access, and the point process. In [37], the author shows that power control can significantly reduce the local delay, but the optimum power control policy is not derived. The DTS can be viewed as the *conditional local delay*, *i.e.,* the local delay conditioned on the link distance (see Section 2.5.2 for details).

Besides its use in reducing the local delay, power control can benefit both point-to-point wireless communication and wireless networks in many different ways (see [48, 52, 57, 59] and the references therein). In the context of point-to-point communication, typical power control policies include water-filling, dynamic programming, channel inversion, etc. Water-filling is typically used to maximize the throughput[16, 30, 31, 49, 65]. Power control policies based on dynamic programming is useful in reducing the queueing delay under power constraints, or, conversely, reducing energy consumption under queueing delay constraints[13, 19, 28, 51, 59]. All the above power control policies require instantaneous channel state information (CSI) at the transmitter, while no such assumption is made in this thesis.

In wireless networks, power control is often considered as a tool of interference management, see, *e.g.,* [57] and the references therein. While this use of power control will be discussed in more detail in Chapter 3, this chapter consider the noise-limited case, with an explicit focus on delay-optimality.

## 2.3 Applications to Wireless Networks

The optimal power control schemes devised in this chapter have two direct applications in the context of noise-limited wireless networks: the minimization of the *local delay*[9, 36, 37]; and the minimization of the *local anycast delay*. The local delay is the DTS averaged over the random distances in an ensemble of links. The local anycast delay is the mean time until a packet is successfully received (decoded) in *any* of a set of the desired receivers. Since the DTS-minimizing power control policies (where the link distance is fixed) are also delay-optimal for random link distances if they are known at the transmitter, this work is the first to provide and prove the optimal power control schemes in terms of reducing the local delay.

For almost all fading distributions, the delay-optimal power control policy derived in this chapter is a random on-off policy, which coincides with the key feature of the ALOHA channel access (MAC) scheme [1]. While ALOHA is generally considered to be inefficient as a MAC scheme, our results show that it may in fact be optimum as a power control scheme.

## 2.4 Chapter Organization

The rest of this chapter is organized as follows: Section 2.5 introduces the system model and defines the DTS (or conditional local delay), local delay and local anycast delay. In Section 2.6, we provide and prove the optimal power control policy for Rayleigh fading, while Section 2.7 extends the results to general fading distributions. Concluding remarks are provided in Section 2.8.

## 2.5 Problem Formulation

### 2.5.1 Reception Model

The chapter considers a noise-limited network, where the received power at each link can be written as

$$P_{\mathrm{r}} = PHr^{-\alpha},$$

where $P$ is the transmit power, $H$ is the iid (power) fading coefficient, $r$ is the link distance, and $\alpha$ is the path loss exponent. We use an SNR condition to define whether a transmission is successful. A transmission is regarded successful if $P_{\mathrm{r}} > \theta$, where $\theta$ incorporates both the SNR threshold and the noise power. Then, we can write the success probability of a single transmission as a (deterministic) function of $r$ as

$$p_s(r) = \mathbb{P}(PHr^{-\alpha} > \theta).$$

While the distance $r$ is considered constant over time and can be learned by the transmitter, the fading coefficient $H$ is assumed iid over time and is unknown to the transmitter. So, $P$ can be a (stochastic) function of $r$.

### 2.5.2 Delay Definitions

DTS and Local Delay The *delay till success* (DTS) is defined as the mean number of time slots that the receiver needs to successfully receive (decode) the message over a link of distance $r$. With iid fading and iid transmit power $P$ (or constant transmit power), it is given by

$$D_r = \frac{1}{p_s(r)}\,, \tag{2.1}$$

which is simply the mean of a geometric random variable with parameter $p_s(r)$. If the link distance is a random variable $R$, which is constant over time, the *local delay*

[9, 36, 37] is the ensemble average of the DTS, *i.e.,*

$$D = \mathbb{E}_R[D_R] = \mathbb{E}_R\left[\frac{1}{p_s(R)}\right]. \tag{2.2}$$

Such a situation arises when considering a noise-limited static random wireless network, which can be modeled as a collection of links with random but fixed distances (Fig. 2.1). Hence the DTS can also be interpreted as the local delay conditioned on the link distance, and we may use the two terms DTS and conditional local delay interchangeably.

The Local Anycast Delay Consider the case where a transmitter wants to transmit the message to any one of the $n$ desired receivers (Fig. 2.2). Let $r_i$ be the distance from the transmitter to each receiver and $H_i$ be the fading coefficient from the transmitter to each receiver, where $i \in [n]$[1], and the $H_i$ are iid both over time and space. Then the local anycast delay, defined as the mean time until the message is successfully decoded at *any of the desired receivers*, is

$$\begin{aligned} D_a &= \frac{1}{1 - \mathbb{P}(PH_1 r_1^{-\alpha} \le \theta, PH_2 r_2^{-\alpha} \le \theta, \cdots, PH_n r_n^{-\alpha} \le \theta)} \\ &= \frac{1}{\mathbb{P}(P \max\{H_i r_i^{-\alpha}, i \in [n]\} > \theta)}. \end{aligned} \tag{2.3}$$

Comparing (2.3) with (2.1), it is obvious that $D_a$ is equivalent to the conditional local delay $D_1$, where the link distance $r = 1$ and the fading subject to the distribution of $\max\{H_i r_i^{-\alpha}, i \in [n]\} > \theta$. Since $H_i$ is iid over space, this fading distribution can be completely characterized by $\mathbb{P}(\max\{H_i r_i^{-\alpha}, i \in [n]\} \le x) = \prod_{i=1}^{n} \mathbb{P}(H_i r_i^{-\alpha} \le x)$.

[1]We use $[n]$ to denote the set $\{1, 2, 3, \cdots, n\}$.

### 2.5.3 The Optimal Stationary Power Control Policy

We define the optimal stationary (or memoryless) power control policy to be the stationary power control policy that minimizes the conditional local delay (or, delay till success). Without loss of generality, we consider a unit mean power constraint and a peak power constraint $P_{\max}$, with $P_{\max} > 1$ (otherwise, the mean power constraint will always be loose), and call a policy to be *valid* if and only if it satisfies both the constraints. We concentrate on stationary power control policies, *i.e.,* the statistics of the transmit power $P$ in different time slots are the same. Therefore, the unit mean power constraint and the peak power constraint above can be expressed as $\mathbb{E}P = 1$ and $P \leq P_{\max}$, respectively, and $P$ is iid.

Let $\mathcal{P}$ be the class of probability density functions (pdf's) with support at most $[0, P_{\max}]$ and mean 1. The problem is to find the pdf $f^*_{P|r}$ of the transmit power $P(r)$, where

$$f^*_{P|r} \triangleq \arg\min_{f_{P|r}\in\mathcal{P}} D_r = \arg\max_{f_{P|r}\in\mathcal{P}} \mathbb{P}(P(r)Hr^{-\alpha} > \theta).$$

The expression above implies the optimal power control policy that maximizes the transmission success probability of a link of length $r$. Therefore, given a single-bit ARQ, the optimal policy, if exists, is also the policy that maximizes the long term throughput for the link. However, in this chapter, we focus on the conditional local delay and make no assumptions about the feedback[2].

Initial efforts to reduce the local (unicast) delay using power control are made in [37]. (2.2) shows that the power control policy minimizing $D_r$ for all $r$ is the power control policy that minimizes the local delay. Thus, an important application of the results on conditional local delay is the discovery of a local delay-minimizing power

[2]Meanwhile, as stated earlier, we do assume that the link distance is known at the transmitter. This is not necessarily obtained by a feedback. Even if so (as the case discussed in Section 2.6.2), such feedback is assumed to be carried out in a different time scale from that of an ARQ, *e.g.,* a distance update in every thousand of transmission attempts.

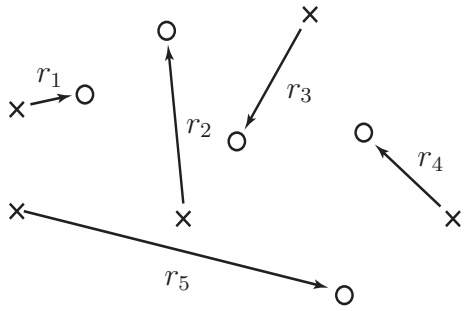


Figure 2.1. A collection of links with random distances. Transmitters are denoted by x and receivers are denoted by o. The distances $r_k, k \in [5]$ are iid drawn from some distribution $f_R(x)$.

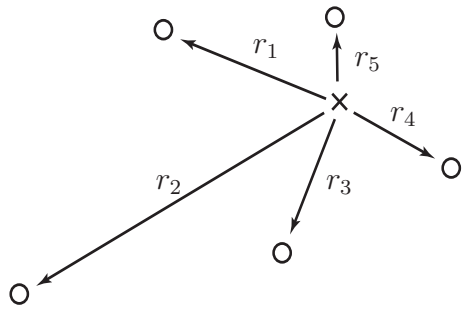


Figure 2.2. Broadcast in wireless network. Transmitters are denoted by x and receivers are denoted by o. The distances $r_k, k \in [5]$ are deterministic and known to the transmitter.

control policy.

For the local anycast delay, we observe from (2.3) that with the appropriate adjustment in the fading distribution, the optimal power control policy can also be used to minimize the local anycast delay.

## 2.6 Rayleigh Fading

### 2.6.1 ALOHA Is the Optimal Policy

In the iid fading case, the conditional local delay (or, delay till success) is simply the inverse of the success probability $\mathbb{P}(HPr^{-\alpha} > \theta)$. For Rayleigh fading,

$$\mathbb{P}(HPr^{-\alpha} > \theta) = \int_0^\infty \bar{F}_P\left(\frac{\theta r^\alpha}{h}\right) e^{-h} \mathrm{d}h = \theta r^\alpha \int_0^\infty \bar{F}_P(x^{-1}) e^{-\theta r^\alpha x} \mathrm{d}x,$$

where $\bar{F}_P(x)$ is the complementary cumulative distribution function (ccdf) of the randomly controlled power $P$. Thus it must be monotonically decreasing, $\bar{F}_P(x) = 0\ \forall x > P_{\max}$, and, by the mean power constraint $\int_0^\infty \bar{F}_P(x)dx \leq 1$.

To simplify the notation, we define the following function

$$F'(x) \triangleq \bar{F}_P(x^{-1}),\ \forall x > 0, \tag{2.4}$$

which is the cumulative distribution function (cdf) of $P^{-1}$. The constraints on $\bar{F}_P$ are mapped to the constraints that $F'(x)$ is monotonically increasing, $F'(x) = 0\ \forall x < P_{\max}^{-1}$, $\lim_{x\to\infty} F'(x) \leq 1$ and $\mathbb{E}P = \int_0^\infty x^{-2} F'(x) \mathrm{d}x \leq 1$.

Therefore, the problem now becomes to find the $F^*(x)$, defined as the optimal $F'(x)$ satisfying all the requirements above and maximizing $\int_0^\infty F'(x) e^{-\theta r^\alpha x} \mathrm{d}x$. Note that $\lim_{x\to\infty} F'(x)$ stands for $\mathbb{P}(P \leq 0)$ which is non-zero whenever there is a positive probability of the event $\{P = 0\}$. Since the distribution of $P$ is not necessarily continuous, in general, $\lim_{x\to\infty} F'(x)$ does not have to be 1[3].

**Lemma 1.** *The desired function $F^*(x)$ satisfies $F^*(x) = F^*(x_M),\ \forall x > x_M \triangleq \max\{P_{\max}^{-1}, \frac{1}{\theta r^\alpha}\}$.*

*Proof.* First, consider the case that $F^*(x)$ is a simple function. Since, $F^*(x)$ is mono-

[3]Rigorously speaking, $F'(x)$ needs to be defined on the extended real line $\overline{\mathbb{R}} = \mathbb{R} \cup \{-\infty, +\infty\}$. In this case, $F'(\infty) = 1$ by definition, but $\lim_{x\to\infty} F'(x)$ is not necessarily 1.

tonically increasing, we can write it as

$$F^*(x) = \sum_{i=0}^{N} a_i \mathbf{1}_{[b_i, b_{i+1})}(x), \tag{2.5}$$

where $0 = a_0 < a_1 < a_2 < \cdots < a_N \leq 1$ and $0 = b_0 < b_1 < b_2 < \cdots < b_{N+1} = \infty$. Suppose there exists a $x_0 > x_M$, such that $F^*(x_0) \neq F^*(x_M)$, *i.e.*, $F^*(x_0) > F^*(x_M)$, and assume $x_0 \in [b_j, b_{j+1})$, $x_M \in [b_l, b_{l+1})$, for some $l, j \in \mathbb{N}$ such that $0 < l < j$. Then, let

$$\tilde{F}(x) \triangleq F^*(x) - \sum_{n=l+1}^{j} (a_n - a_{n-1}) \mathbf{1}_{[b_n, \infty)}(x) + x_M \sum_{n=l+1}^{j} \frac{a_n - a_{n-1}}{b_n} \mathbf{1}_{[x_M, \infty)}(x). \tag{2.6}$$

It can be easily verified that $\int_0^\infty x^{-2} \tilde{F}(x) \mathrm{d}x = \int_0^\infty x^{-2} F^*(x) \mathrm{d}x$ and $\tilde{F}(x)$ satisfies all the requirements for a valid $F'(x)$ over $[0, \infty)$. Moreover,

$$\begin{aligned}
&\int_0^\infty e^{-\theta r^\alpha x} \tilde{F}(x) \mathrm{d}x - \int_0^\infty e^{-\theta r^\alpha x} F^*(x) \mathrm{d}x \\
&= \int_0^\infty e^{-\theta r^\alpha x} x_M \sum_{n=l+1}^{j} \frac{a_n - a_{n-1}}{b_n} \mathbf{1}_{[x_M, \infty)}(x) \mathrm{d}x - \int_0^\infty e^{-\theta r^\alpha x} \sum_{n=l+1}^{j} (a_n - a_{n-1}) \mathbf{1}_{[b_n, \infty)}(x) \mathrm{d}x \\
&= \sum_{n=l+1}^{j} \frac{a_n - a_{n-1}}{b_n \theta r^\alpha} \left( x_M e^{-\theta r^\alpha x_M} - b_n e^{-\theta r^\alpha b_n} \right),
\end{aligned}$$

which is strictly larger than zero because of the monotonicity of $x e^{-\theta r^\alpha x}$ at $[\frac{1}{\theta r^\alpha}, \infty)$ and the fact that $b_n > x_M \geq \frac{1}{\theta r^\alpha}$ $\forall n \geq l + 1$. This contradicts the assumption that $F^*(x)$ is the function which maximizes $\int_0^\infty F'(x) e^{-\theta r^\alpha x} \mathrm{d}x$ and satisfies all the constraints.

For general $F^*(x)$, consider a sequence of simple functions $(F_k^*)_1^\infty$ such that $F_i^* < F_j^* < F^*$, $\forall i < j$ and $\lim_{k \to \infty} F_k^* = F^*$. By the monotone convergence theorem, $\lim_{k \to \infty} \int_0^\infty x^{-2} F_k^*(x) \mathrm{d}x = \int_0^\infty x^{-2} F^*(x) \mathrm{d}x$ and $\lim_{k \to \infty} \int_0^\infty e^{-\theta r^\alpha x} F_k^*(x) \mathrm{d}x = \int_0^\infty e^{-\theta r^\alpha x} F^*(x) \mathrm{d}x$. Using the construction in the proof for the simple functions, we are

able to produce another sequence of simple functions $(\tilde{F}_k)_1^\infty$, such that $\int_0^\infty e^{-\theta r^\alpha x}\tilde{F}_k(x)\mathrm{d}x > \int_0^\infty e^{-\theta r^\alpha x}F_k^*(x)\mathrm{d}x, \forall k$. Meanwhile, $\lim_{k\to\infty}\tilde{F}_k \neq F^*$, since $\tilde{F}_k(x_0) = \tilde{F}_k(\frac{1}{\theta r^\alpha})$. Thus, the limiting function of $\tilde{F}_k(x)$ is a strictly better candidate for $F'(x)$ than $F^*(x)$. $\square$

Analogously, we have the following lemma.

**Lemma 2.** *If $1 \leq \theta r^\alpha \leq P_{\max}$, we have $F^*(x) = 0,\ \forall x < \frac{1}{\theta r^\alpha}$.*

*Proof.* The proof is essentially the same of that of the previous lemma. We start with the case where $F^*(x)$ is simple and then generalize to the case of all valid cdf's.

Consider the case where $F^*(x)$ is a simple function and write it as (2.5). Assuming $\frac{1}{\theta r^\alpha} \in [b_l, b_{l+1})$, we can construct

$$\tilde{F}(x) = F^*(x) - \sum_{n=1}^{l} a_n \mathbf{1}_{[b_n,\infty)}(x) + \sum_{n=1}^{l} \frac{a_n}{b_n\theta r^\alpha}\mathbf{1}_{[\frac{1}{\theta r^\alpha},\infty)}(x).$$

Suppose that $F^*(x_0) > 0$ for some $x_0 < \frac{1}{\theta r^\alpha}$, we know $\tilde{F}(x) \neq F^*(x)$, since $\tilde{F}(x) = 0,\ \forall x < \frac{1}{\theta r^\alpha}$. Meanwhile, it can be verified that $\int_0^\infty x^{-2}\tilde{F}(x)\mathrm{d}x = \int_0^\infty x^{-2}F^*(x)\mathrm{d}x$. By Lemma 1, $F^*(x) = F^*(\frac{1}{\theta r^\alpha}),\ \forall x > \frac{1}{\theta r^\alpha}$ and thus $\tilde{F}(x) \leq 1$ (because $\int_1^\infty x^{-2}\mathrm{d}x = 1$). All other constraints over $\tilde{F}(x)$ to be a valid candidate for $F'(x)$ are automatically satisfied. Also,

$$\begin{aligned}\int_0^\infty e^{-\theta r^\alpha x}\tilde{F}(x)\mathrm{d}x - \int_0^\infty e^{-\theta r^\alpha x}F^*(x)\mathrm{d}x &= \sum_{n=1}^{l}\int_0^\infty \left(\frac{a_n}{b_n\theta r^\alpha}\mathbf{1}_{[\frac{1}{\theta r^\alpha},\infty)} - a_n\mathbf{1}_{[b_n,\infty)}\right)e^{-\theta r^\alpha x}\mathrm{d}x \\ &= \sum_{n=1}^{l}\frac{a_n}{b_n\theta r^\alpha}\left(\frac{1}{\theta r^\alpha}e^{-\theta r^\alpha\frac{1}{\theta r^\alpha}} - b_n e^{-\theta r^\alpha b_n}\mathrm{d}x\right),\end{aligned}$$

which is strictly larger than zero due to the fact that $b_n \leq \frac{1}{\theta r^\alpha},\ \forall n \leq l$ by assumption and the monotonicity of $xe^{-\theta r^\alpha x}$ in $[0, \frac{1}{\theta r^\alpha}]$. Therefore, we found $\tilde{F}(x)$ as a strictly better candidate than $F^*(x)$, contradicting the assumption that it is the desired function. The generalization from simple function to general functions are the same as in the proof of Lemma 1. $\square$

Similarly, it can be shown that:

**Lemma 3.** *If $\theta r^\alpha < 1$, we have $F^*(x) = 0,\ \forall x < 1$.*

Although special care must be taken to make sure that $\tilde{F}(x) \leq 1$, the proof of Lemma 3 directly follows from that of Lemma 2 and is therefore omitted.

Combining Lemmas 1, 2, 3 and the requirements we have for a valid $F'(x)$, we conclude that $F^*(x)$ is of the form:

$$F^*(x) = \begin{cases} \mathsf{1}_{[1,\infty)}(x), & \theta r^\alpha \leq 1 \\ \frac{1}{\theta r^\alpha}\mathsf{1}_{[\frac{1}{\theta r^\alpha},\infty)}(x), & 1 < \theta r^\alpha \leq P_{\max} \\ P_{\max}^{-1}\mathsf{1}_{[P_{\max}^{-1},\infty)}(x), & \theta r^\alpha > P_{\max}. \end{cases}$$

As stated earlier, there is a one to one mapping between $F'(x)$ and $\bar{F}_P(x)$ (and thus $F_P(x)$). Hence, the result above directly leads to the following theorem.

**Theorem 1.** *For Rayleigh fading, given a link distance $r$, the optimal distribution of the transmit power $P$ that minimizes the local delay is*

$$F_P(x) = \begin{cases} \mathsf{1}_{[1,\infty)}(x), & \theta r^\alpha \leq 1 \\ (1 - \frac{1}{\theta r^\alpha})\mathsf{1}_{[0,\theta r^\alpha)}(x) + \mathsf{1}_{[\theta r^\alpha,\infty)}(x), & 1 < \theta r^\alpha \leq P_{\max} \\ (1 - P_{\max}^{-1})\mathsf{1}_{[0,P_{\max})}(x) + \mathsf{1}_{[P_{\max},\infty)}(x), & \theta r^\alpha > P_{\max}. \end{cases}$$

More concisely, we can define $\xi \triangleq \max\{1, \min\{P_{\max}, \theta r^\alpha\}\}$. Then Theorem 1 says: the optimal random power control strategy is an ALOHA-type random on-off policy with transmit probability $\xi^{-1}$ and transmit power $\xi$.

**Definition 1.** *A link is said to be in the peak-power-limited regime if the optimal power control policy is to transmit at power $P_{\max}$ with probability $P_{\max}^{-1}$.*

**Definition 2.** *A link is said to be in the mean-power-limited regime if constant power transmission ($P \equiv 1$) is the optimal power control policy.*

Interestingly, the optimal strategy *maximizes* the variance of the transmit power in the peak-power-limited regime, while *minimizing* this variance in the mean-power-limited regime.

Theorem 1 also indicates that in order to apply the optimal power control policy, the transmitter needs to know either $r$ and $\alpha$ or $r^\alpha$. Since $\mathbb{E}H = 1$, $r^\alpha$ can be easily obtained by simply taking the average of the received power.

**Corollary 1.** *Without peak power constraint, but with the mean power limited to* $\mathbb{E}P = 1$*, the optimal random power control policy is*

$$F_P(x) = \begin{cases} \mathsf{1}_{[1,\infty)}(x), & \theta r^\alpha \le 1 \\ (1 - \frac{1}{\theta r^\alpha})\mathsf{1}_{[0,\theta r^\alpha)}(x) + \mathsf{1}_{[\theta r^\alpha,\infty)}(x), & \theta r^\alpha > 1. \end{cases}$$

The exact value of the local delay depends on the distribution of the link distance $R$. An important case is the Rayleigh distribution, since it is the distribution of the nearest-neighbor distance in a 2-dimensional network, whose nodes are distributed as a Poisson point process (PPP)[34]. It is shown in [37] that with such a distribution of $R$, the local delay is unbounded if Rayleigh fading is considered and no power control is applied (except for the case of $\alpha \le 2$). The natural question is whether random power control can make the local delay finite in the same scenario. In the case where only a mean power constraint is imposed, applying the result in Corollary 1, we have

$$\begin{aligned} D = \mathbb{E}\left[\frac{1}{p_{s|R}}\right] &= 2\pi\lambda \int_0^{\theta^{-\frac{1}{\alpha}}} r e^{\theta r^\alpha - \lambda\pi r^2} \mathrm{d}r + 2\pi\lambda\theta e \int_{\theta^{-\frac{1}{\alpha}}}^{\infty} r^{\alpha+1} e^{-\lambda\pi r^2} \mathrm{d}r \\ &\le e(1 - e^{-\lambda\pi\theta^{-\frac{2}{\alpha}}}) + \theta e(\lambda\pi)^{-\frac{\alpha}{2}} \Gamma(\frac{\alpha}{2} + 1, \lambda\pi\theta^{-\frac{2}{\alpha}}) < \infty, \end{aligned}$$

where $\Gamma(\cdot,\cdot)$ is the upper incomplete gamma function. In other words, power control can keep the local delay finite while keeping the mean transmit power at each node limited even if the link distance is Rayleigh distributed.

**Proposition 1.** *With a peak power constraint, power control cannot reduce the local delay to a finite value when the link distance is Rayleigh distributed and* $\alpha > 2$.

*Proof.* With only a peak power constraint, the minimum local delay is achieved when the transmit power is $P_{\max}$ at each link in each time slot. Then the proposition trivially follows from the fact that any constant power in is not sufficient to keep the local delay finite when the link distance is Rayleigh distributed and $\alpha > 2$ [37]. □

A direct consequence of Proposition 1 is that the optimal policy in Theorem 1 cannot reduce the local delay to a finite value when the link distance is Rayleigh distributed and $\alpha > 2$.

### 2.6.2 Comparison of Random Power Control Schemes

In this subsection, we compare the DTS performance (in the presence of Rayleigh fading) of several power control policies, defined as follows:

**Definition 3.** *The optimal power control (OPC) policy is the power control policy defined in Theorem 1.*

**Definition 4.** *The peak power control (PPC) policy transmits at power* $P_{\max}$ *with probability* $P_{\max}^{-1}$ *and does not transmit with probability* $1 - P_{\max}^{-1}$*, regardless of the value of* $r$.

**Definition 5.** *The uniform power control (UPC) policy transmits at power* $P$ *each time with* $P$ *uniformly distributed in* $[1-\Delta, 1+\Delta]$. *Here,* $\Delta \triangleq \min\{1, P_{\max} - 1\}$.

**Definition 6.** *The hybrid uniform power control (HUPC) policy transmits with probability* $\frac{2}{P_{\max}+1}$. *If transmitting, the transmit power is uniformly distributed between* 1 *and* $P_{\max}$.

**Definition 7.** *The 1-bit power control (1BPC) policy transmits at constant power* $(P = 1)$ *when* $\theta r^{\alpha} \leq \frac{\log P_{\max}}{1-P_{\max}^{-1}}$. *When* $\theta r^{\alpha} > \frac{\log P_{\max}}{1-P_{\max}^{-1}}$*, the policy transmits at power* $P_{\max}$ *with probability* $P_{\max}^{-1}$ *and does not transmit with probability* $1 - P_{\max}^{-1}$.

While the peak power control (PPC) policy, the uniform power control (UPC) policy, and the hybrid uniform power control (HUPC) policy are all suboptimal, their complexity is lower than OPC's. In particular, they do not require the link distance information $R$. Meanwhile, their constructions are inspired by Theorem 1 in different ways. For example, in the peak-power-limited regime PPC is as good as OPC. The intuition behind HUPC is that Theorem 1 implies that for all realizations of $R$ it is not optimal to transmit with power in $(0, 1)$.

The 1-bit power control (1BPC) policy is proposed as a trade-off between OPC and other kinds of power control policies that do not utilize the link distance information. In practice, although the link distance can always be measured, its precise value might be difficult to acquire, *e.g.*, it may take too long to accurately measure. In such occasions, the performance of OPC becomes difficult to realize. Meanwhile, 1BPC turns out to be more suitable, since it only requires 1 bit of information regarding the link distance, and its performance is identical to OPC's in both the peak-power-limited regime and the mean-power-limited regime.

It is not difficult to find that if the link distance $r$ is known and OPC is applied, the conditional local delay is

$$D_r = \begin{cases} P_{\max} e^{\frac{\theta r^\alpha}{P_{\max}}}, & \theta r^\alpha \geq P_{\max} \\ \theta r^\alpha e, & 1 < \theta r^\alpha < P_{\max} \\ e^{\theta r^\alpha}, & \theta r^\alpha \leq 1. \end{cases}$$

In comparison, we can see that with constant power transmission, the conditional local delay is always equal to $\exp(\theta r^\alpha)$. When $P_{\max} \geq 2$, the transmit power of UPC is uniformly distributed in $[0, 2]$. Its conditional local delay can be calculated as $\left(\exp(-\frac{1}{2}\theta r^\alpha) - \frac{1}{2}\theta r^\alpha \int_{\frac{1}{2}\theta r^\alpha}^{\infty} \frac{\exp(-x)}{x} \mathrm{d}x\right)^{-1}$. Straightforward (but tedious) manipulation

reveals the conditional local delay for HUPC to be

$$\frac{P_{\max}^2-1}{2}\left(P_{\max}e^{-\frac{\theta r^\alpha}{P_{\max}}}-e^{-\theta r^\alpha}-\theta r^\alpha\int_{\frac{\theta r^\alpha}{P_{\max}}}^{\theta r^\alpha}\frac{e^{-x}}{x}\mathrm{d}x\right)^{-1}.$$

The calculation of the conditional local delay for 1BPC is similar to that of OPC.

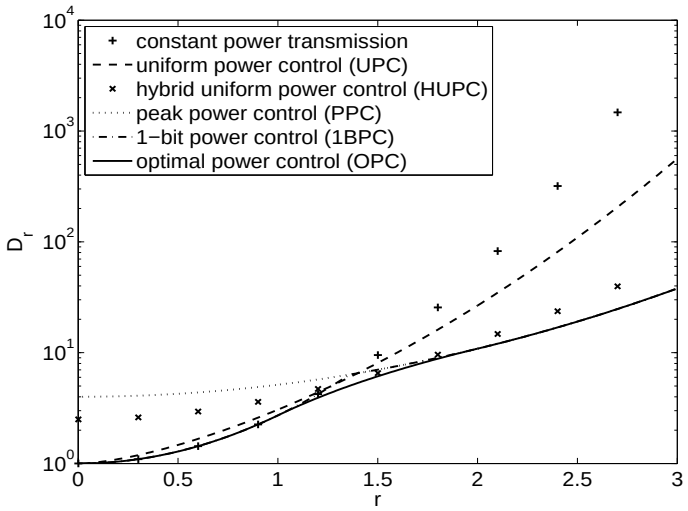


Figure 2.3. Comparison of the conditional local delay for different power control schemes. Here, $P_{\max}=4$, $\theta=1$, $\alpha=2$.

Figs. 2.3 compares all the power control policies defined above along with constant power transmission ($P\equiv 1$) in different scales. Fig. 2.3 shows that in the peak-power-limited regime (large $r$) the conditional local delay grows exponentially with $r$ for all power control policies. This is mainly due to the peak power constraint. However, for different power control schemes the exponent is quite different, which results in many orders of difference in conditional local delay. As expected, in this regime, OPC, PPC and 1BPC perform the best among all schemes, and constant power transmission is

the worst. Both UPC and HUPC appears to be trade-offs between the best and the worst.

In the mean-power-limited regime (small $r$), the difference in the conditional local delay between the different schemes can be at most by a factor of 4 (Fig. 2.3). Still, UPC and HUPC perform between the two extremes. Fig. 2.3 also shows that 1BPC is not considerably inferior to OPC even in its suboptimal regime ($1 < \theta r^{\alpha} < P_{\max}$), and thus appears to be a good substitute for OPC in many cases.

## 2.7 General Fading Distributions

### 2.7.1 The Optimality of ALOHA

Results in Section 2.6 raise a more general question: Is ALOHA (random on-off policy) still optimal in reducing the (conditional) local delay if the fading is not Rayleigh? To answer this question, this subsection derives more general sufficient conditions for the optimality of ALOHA. We use $g(x)$ to denote the pdf of the fading random variable $H$.

**Lemma 4.** *For given $r$, if there exists a constant $\vartheta < \infty$ such that $x\int_x^{\infty} g(\theta r^{\alpha} y)\mathrm{d}y$ is strictly monotonically decreasing for all $x > \vartheta$, we have*

$$F^*(x) = F^*(x_M),\ \forall x > x_M,$$

*where $F^*(x)$ is the desired function as defined before, and $x_M \triangleq \max\{P_{\max}^{-1}, \vartheta\}$.*

*Proof.* Using the definition of $\bar{F}_p(x)$ and $F'(x)$ as before, we have for general fading with pdf $g(x)$

$$\mathbb{P}(HPr^{-\alpha} > \theta) = \int_0^{\infty} \bar{F}_p\left(\frac{\theta r^{\alpha}}{h}\right) g(h)\mathrm{d}h = \theta r^{\alpha}\int_0^{\infty} F'(x) g(\theta r^{\alpha} x)\mathrm{d}x.$$

As in the proof of Lemma 1, we prove Lemma 4 by contradiction. Starting with simple

functions, we write $F^*(x)$ as in (2.5) and construct $\tilde{F}(x)$ as (2.6). Straightforward manipulation shows

$$\begin{aligned}&\int_0^\infty \tilde{F}(x)g(\theta r^\alpha x)\mathrm{d}x - \int_0^\infty F^*(x)g(\theta r^\alpha x)\mathrm{d}x \\ &= \sum_{n=l+1}^{j} \frac{a_n - a_{n-1}}{b_n}\left(x_M \int_{x_M}^\infty g(\theta r^\alpha x)\mathrm{d}x - b_n \int_{b_n}^\infty g(\theta r^\alpha x)\mathrm{d}x\right), \end{aligned} \tag{2.7}$$

which is strictly larger than zero by the monotonicity of $x\int_x^\infty g(\theta r^\alpha y)\mathrm{d}y$. Therefore, the lemma is proved for simple functions. The generalization to non-simple functions is just as in Lemma 1. □

A simple sanity check would be to consider the Rayleigh fading case, where $g(x) = \exp(-x)$. Then, $x\int_x^\infty g(\theta r^\alpha y)\mathrm{d}y = \frac{x}{\theta r^\alpha}\exp(-\theta r^\alpha)$, which is strictly monotonically decreasing for $x \geq \frac{1}{\theta r^\alpha}$. This retrieves Lemma 1. Similarly, Lemmas 2 and 3 can be generalized as follows:

**Lemma 5.** *For given $r$, let $\varsigma$ be any constant such that $x\int_x^\infty g(\theta r^\alpha y)\mathrm{d}y$ is strictly monotonically increasing for all $0 \leq x < \varsigma$. Then, the desired function $F^*(x)$ must have*

$$F^*(x) = 0,\ \forall x < x_m,$$

*where $x_m \triangleq \min\{1, \varsigma\}$.*

The proof is analogous to that of Lemma 4. For Rayleigh fading, $x\int_x^\infty g(\theta r^\alpha y)\mathrm{d}y$ is strictly increasing for all $0 \leq x \leq \frac{1}{\theta r^\alpha}$.

**Theorem 2.** *Let $\bar{G}(x)$ denote the ccdf of $H$. If there exists some $x_0 > 0$, such that $x\bar{G}(\theta r^\alpha x)$ is strictly increasing on $[0, x_0)$ and strictly decreasing on $(x_0, \infty)$, the optimal power control policy is an ALOHA-type random on-off policy with transmit power $\xi$ and transmit probability $\xi^{-1}$, where $\xi \triangleq \max\{1, \min\{P_{\max}, x_0^{-1}\}\}$.*

Theorem 2 is simply a combination of Lemmas 4 and 5.

Let $K(x) = x\Gamma(m, m\theta r^\alpha x)$. The following lemma helps us to show that Nakagami-$m$ fading satisfies the condition in Theorem 2.

**Lemma 6.** *There exists a unique $x_0 \in (0, \frac{m+1}{m\theta r^\alpha})$, such that $\frac{\mathrm{d}}{\mathrm{d}x}K(x) \mid_{x=x_0} = 0$. $K(x)$ is strictly increasing on $(0, x_0)$ and strictly decreasing on $(x_0, \infty)$.*

*Proof.* Since $K(x)$ is twice-differentiable, the monotonicity in the proposition can be shown by evaluating the derivatives of $K(x)$. To prove the first part of the proposition, we first notice that there must exists at least one $x_0 \in (0, \frac{m+1}{m\theta r^\alpha})$, such that $\frac{\mathrm{d}}{\mathrm{d}x}K(x) \mid_{x=x_0} = 0$. This is due to the continuity of $K(x)$ as well as the fact that $K(0) = \lim_{x\to\infty} K(x) = 0$ and $\frac{\mathrm{d}}{\mathrm{d}x}K(x) \mid_{x=0} = \Gamma(m) > 0$.

In the following, we prove the uniqueness of $x_0$ by contradiction. Assume there is another point $x_1 \neq x_0$ and $\frac{\mathrm{d}}{\mathrm{d}x}K(x) \mid_{x=x_1} = 0$. Without loss of generality, consider $x_1 > x_0$ (otherwise, we can exchange the subscript). Because $\lim_{t\to\infty} \frac{\mathrm{d}}{\mathrm{d}x}K(x) \mid_{x=t} = 0$ and

$$\frac{\mathrm{d}^2}{\mathrm{d}x^2}K(x) = (m\theta r^\alpha x)^m e^{-m\theta r^\alpha x}\left(m\theta r^\alpha - \frac{m+1}{x}\right), \tag{2.8}$$

which is strictly positive when $x > \frac{m+1}{m\theta r^\alpha}$, we must have $x_0 < x_1 < \frac{m+1}{m\theta r^\alpha}$. However, (2.8) also indicates $\frac{\mathrm{d}}{\mathrm{d}x}K(x)$ is strictly decreasing on $(0, \frac{m+1}{m\theta r^\alpha})$. Then, $\frac{\mathrm{d}}{\mathrm{d}x}K(x) \mid_{x=x_0} = \frac{\mathrm{d}}{\mathrm{d}x}K(x) \mid_{x=x_1} = 0$ implies $x_0 = x_1$, which contradicts the assumption that $x_1 \neq x_0$.

Since $K(x)$ is continuous and $K(0) = \lim_{t\to\infty} K(t) = 0$, the uniqueness of $x_0$ implies that there are at most two monotonic region of $K(x)$ over $[0, \infty)$. Combined with the fact that $\frac{\mathrm{d}}{\mathrm{d}x}K(x) \mid_{x=0} = \Gamma(m) > 0$, we conclude that $K(x)$ is strictly increasing on $[0, x_0)$ and strictly decreasing on $[x_0, \infty)$. □

Combining Theorem 2 and Lemma 6, we immediately obtain Corollary 2.

**Corollary 2.** *The optimal power control policy for Nakagami-m fading is an ALOHA-type random on-off policy.*

### 2.7.2 Peak-power-limited and Mean-power-limited Regimes

For a more general class of fading, the conditions in Theorem 2 may not be satisfied. The simplest example may be the (discrete) fading distribution with pdf

$$g(x) = q_1\delta(x - h_1) + q_2\delta(x - h_2), \tag{2.9}$$

where $0 \leq h_1 < h_2 < \infty$, $q_1h_1 + q_2h_2 = 1$, and $q_1 + q_2 = 1$. Then, $x\bar{G}(x) = x\mathbf{1}_{[0,h_1/\theta r^\alpha)}(x) + q_2 x\mathbf{1}_{[h_1/\theta r^\alpha, h_2/\theta r^\alpha)}$, which does not satisfy the conditions in Theorem 2 for two reasons: 1) there is no *strict* monotonicity for $x > \frac{h_2}{\theta r^\alpha}$; 2) even if we relax the strictness requirement, there is still no such $x_0$ that $x\bar{G}(x)$ is monotonically increasing on $[0, x_0)$ and decreasing on $(x_0, \infty)$, as long as $q_2 > 0$. Thus, results so far are not applicable in this case. However, some of the results can still be obtained in particular regimes of $r$ even when the conditions in Theorem 2 are not met.

**Theorem 3.** *For general fading distribution with ccdf $\bar{G}(x)$, fixed threshold $\theta$, and link distance $r_0$, if $x\bar{G}(\theta r_0^\alpha x)$ is monotonically decreasing for all $x > P_{\max}^{-1}$, the ALOHA-type random on-off peak power control policy with on power $P_{\max}$ achieves the minimum conditional local delay. Moreover, for all $r > r_0$, the same policy is still delay-optimal.*

*Proof.* When the monotonicity of $x\bar{G}(\theta r_0^\alpha x)$ is strict, the proof of the first part of Theorem 3 trivially follows from Lemma 4, since $F'(x) = 0\ \forall x < P_{\max}^{-1}$. In the non-strict case, Lemma 4 needs to be slightly generalized, *i.e.,* (2.7) is no longer strictly larger than zero. Yet, (2.7) is still no less than zero, which ensures that the constructed $\tilde{F}(x)$ produces a conditional local delay no larger than the minimum conditional local delay. Thus, the first part is of the theorem is proved.

For the second part, let $P_{\max}^{-1} < x_1 < x_2$ and $r > r_0$. Noting that $x\int_x^\infty g(\theta r_0^\alpha t)\mathrm{d}t =$

$\frac{x}{\theta r^\alpha}\int_{\theta r^\alpha x}^{\infty} g(t)\mathrm{d}t$ and using the monotonicity of $x\int_x^{\infty} g(\theta r_0^\alpha t)\mathrm{d}t$, we have

$$\begin{aligned}\frac{x_1}{\theta r^\alpha}\int_{\theta r^\alpha x_1}^{\infty} g(t)\mathrm{d}t &= \frac{\theta r_0^\alpha}{\theta r^\alpha}\left(\frac{r_0}{r}\right)^\alpha \frac{\left(\frac{r}{r_0}\right)^\alpha x_1}{\theta r_0^\alpha}\int_{\theta r_0^\alpha\left(\frac{r}{r_0}\right)^\alpha x_1}^{\infty} g(t)\mathrm{d}t \\ &> \frac{\theta r_0^\alpha}{\theta r^\alpha}\left(\frac{r_0}{r}\right)^\alpha \frac{\left(\frac{r}{r_0}\right)^\alpha x_2}{\theta r_0^\alpha}\int_{\theta r_0^\alpha\left(\frac{r}{r_0}\right)^\alpha x_2}^{\infty} g(t)\mathrm{d}t = \frac{x_2}{\theta r^\alpha}\int_{\theta r^\alpha x_2}^{\infty} g(t)\mathrm{d}t.\end{aligned}$$

Thus, the monotonicity of $x\int_x^{\infty} g(\theta r^\alpha t)\mathrm{d}t$ is proved for all $r > r_0$. □

Note that Theorem 3 does not imply the fact that, for general fading, there must exist a peak-power-limited regime where the ALOHA-type on-off peak power control (PPC) is delay-optimal. To show this, one can consider a fading distribution with an oscillating tail in the pdf, where $x\bar{G}(\theta r^\alpha x)$ does not have a monotonic tail for all $0 < r < \infty$.

Likewise, we can deduce the following theorem:

**Theorem 4.** *Constant power transmission minimizes the conditional local delay, if $x\bar{G}(\theta r_0^\alpha x)$ is monotonically increasing for all $x < 1$. Moreover, the optimality still holds for all $r < r_0$.*

For the particular example we raised at the beginning of this subsection, where the fading coefficient has a pdf as in (2.9), Theorems 3 and 4 indicate: 1) when $P_{\max}h_2 < \theta r^\alpha$, ALOHA-type random on-off power control policy achieves minimum conditional local delay; 2) when $h_1 > \theta r^\alpha$, constant power transmission minimizes local delay. These two facts are intuitive in this example. Because, when $P_{\max}h_2 < \theta r^\alpha$, even full power transmission ($P = P_{\max}$) cannot achieve a successful transmission, and thus the conditional local delay is always $\infty$. When $h_1 > \theta r^\alpha$, constant-power transmission ($P = 1$) always succeeds. So, the minimum conditional local delay $D_r = 1$ is achieved by such policy.

Despite the simplicity of the example above, Theorems 3 and 4 are particularly

useful when the fading distribution has a very complicated shape, making $x\bar{G}(\theta r^{\alpha}x)$ non-unimodal.

### 2.7.3 Numerical Approach

**Theorem 5.** *If there is a finite number of transmit power levels $P \in \{w_0, w_1, \cdots, w_N\}$, where $0 = w_0 < w_1 < \cdots < w_N = P_{\max}$, and $\bar{G}(x)$ is the ccdf of the fading coefficient $H$, then the optimal power control policy is of the form*

$$F_P^*(x) = \sum_{k=0}^{N} p_k w_k, \tag{2.10}$$

*where $(p_0, p_1, \cdots, p_N) \in [0,1]^{N+1}$ is the solution of the following linear programing problem:*

$$\begin{aligned} \underset{\{p_k, 0\le k\le N\}}{\textit{maximize}} \quad & \sum_{k=0}^{N} p_k \bar{G}\left(\frac{\theta r^{\alpha}}{w_k}\right) \\ \textit{subject to} \quad & p_k \ge 0,\ k = 0, \ldots, N \\ & \sum_{k=0}^{N} p_k = 1,\ \sum_{k=0}^{N} p_k w_k = 1. \end{aligned}$$

### 2.7.4 Examples

Nakagami-$m$ Fading The optimality of ALOHA in the presence of Nakagami-$m$ fading is shown in Corollary 2. Then, the implementation of the optimal policy hinges on finding the corresponding $x_0$, which is the solution of $\Gamma(m, m\theta r^{\alpha}x) = (m\theta r^{\alpha}x)^m e^{-m\theta r^{\alpha}x}$. Numerically solving this equation yields the optimal policy as well as the minimum conditional local delay. Fig. 2.4 compares the minimum conditional local delay for different $m$ ($m = 1$ is the Rayleigh fading case). As expected, when $r$ is small, a larger $m$ yields a lower conditional local delay, since there is less chance for the channel to be in a bad condition. On the other hand, for large $r$, Nakagami fading with a larger $m$ has a larger conditional local delay, since the chance of a

particularly good condition is considerably smaller than in the Rayleigh fading case.

In particular, for any two curves in Fig. 2.4, there is a crossover point slightly larger than $r = 2$. Before this point, channel (fading) randomness increases the conditional local delay, *i.e.,* a larger $m$ results in a smaller delay. After this point, channel (fading) randomness helps reducing the conditional localy delay, *i.e.,* a larger $m$ results in a larger delay.

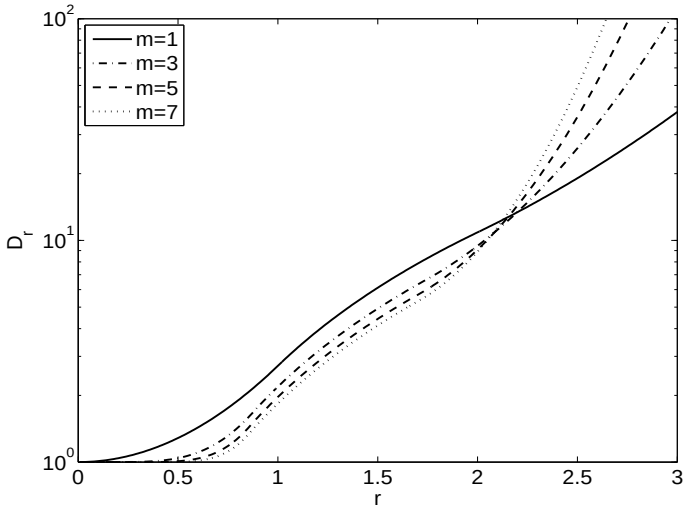


Figure 2.4. Minimum conditional local delay for Nakagami-$m$ fading, where $P_{\max} = 4$, $\theta = 1$, $\alpha = 2$.

Rician Fading and Lognormal Shadowing  The conditions in Theorem 3 are not restrictive. In fact, almost all practical continuous fading distributions satisfy them although it can be tedious to prove. In particular, apart from the Rayleigh fading and Nakagami-$m$ fading, two of the most common types of fading, Rician fading and lognormal shadowing, satisfy these conditions. In the following, we use the numerical

approach introduced above to verify the optimality of ALOHA.

The ccdf of the (power) Rician fading is $\bar{G}(x) = Q\left(\frac{s}{\sigma}, \frac{\sqrt{x}}{\sigma}\right)$, where $s^2$ is the line of sight (LOS) power component, $2\sigma^2$ is the non-LOS power component, and $Q(\cdot,\cdot)$ is the Marcum Q function. The mean power is the sum of these two power component. Let $K = s^2/2\sigma^2$, and fix the mean of $H$ to be one. The ccdf is written as

$$\bar{G}(x) = Q(\sqrt{2K}, \sqrt{2(K+1)x}). \tag{2.11}$$

If $H$ represents the effect of lognormal shadowing and $\mathbb{E}H = 1$, the ccdf of $H$ is

$$\bar{G}(x) = \frac{1}{2} - \frac{1}{2}\mathrm{erf}\left(\frac{\ln x + \sigma^2/2}{\sigma\sqrt{2}}\right), \tag{2.12}$$

where $\sigma^2$ is proportional to the variance of the received power in dB, and $\mathrm{erf}(\cdot)$ is the error function.

Fig. 2.5 and Fig. 2.6 show the cdf of the optimal power control policy for different link distances. For small link distances, *e.g.,* $r = 0.5$, constant power transmission is optimal. For large distances, *e.g.,* $r = 2$, peak power control (PPC) policy is optimal. Between these two regimes, *e.g.,* $r = 1.5$, the optimal policy is a random on-off power control policy with certain a transmit probability in $[P_{\max}^{-1}, 1]$. In any case, the optimal policy is ALOHA-type.

Local Anycast Delay As mentioned in Section 2.5.2, the optimal policy in this chapter can be directly applied as the optimal policy that minimizes the local anycast delay. In particular, we provide the following corollary.

**Corollary 3.** *When the desired receivers are located at the same distance to the transmitter and Rayleigh fading is considered, the optimal policy that minimizes the local anycast delay is an ALOHA random on-off policy.*

In the Rayleigh fading case, the distribution of fading coefficients $H_i$ is exponential

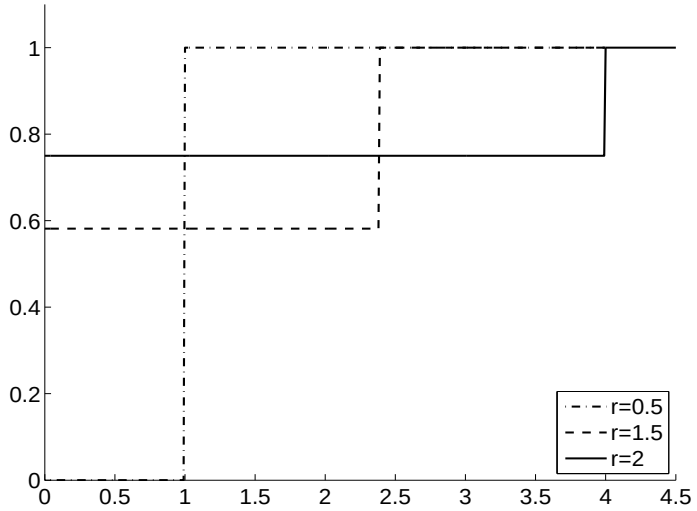


Figure 2.5. Numerically obtained $F_P^*(x)$ for Rician fading. $P_{\max} = 4$, $\theta = 1$, $\alpha = 2$, $K = 1$.

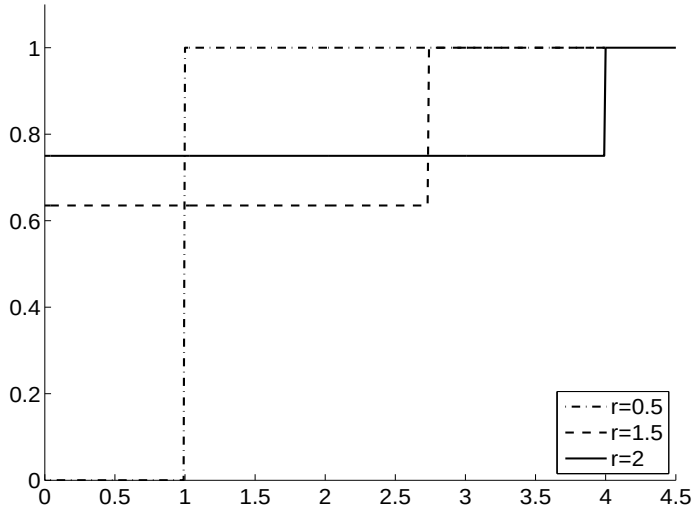


Figure 2.6. Numerically obtained $F_P^*(x)$ for lognormal fading. $P_{\max} = 4$, $\theta = 1$, $\alpha = 2$, $\sigma = 1$.

with unit mean. When the link distances to each of the $n$ desired receivers are the same, the cdf of $\max\{H_i r_i^{-\alpha}\}$ is $G(x) = (1 - e^{-r^\alpha x})^n$, where $r$ is the link distance. Therefore, Let $L(x) \triangleq x(1 - G(\theta x))$. Corollary 3 follows directly from Theorem 2 and Lemma 7 proved below.

**Lemma 7.** *There exists a unique $x_0$, such that $L(x)$ is monotonically increasing on $[0, x_0]$ and monotonically decreasing on $[x_0, \infty)$.*

*Proof.* Since $L(x)$ is differentiable on $[0, \infty)$ and its derivative is continuous, it suffices to show: there exists a unique $x_0$, such that $\frac{\mathrm{d}}{\mathrm{d}x}L(x) \mid_{x=x_0} = 0$, and $\frac{\mathrm{d}}{\mathrm{d}x}L(x)$ is positive on $[0, x_0]$ and negative on $[x_0, \infty)$. Observing that $\lim_{x\to 0+} \frac{\mathrm{d}}{\mathrm{d}x}L(x) > 0$ and that $\frac{\mathrm{d}}{\mathrm{d}x}L(x)$ approaches zero from below when $x \to \infty$, we can deduce the latter directly from the former. Thus, the key is to show $\frac{\mathrm{d}}{\mathrm{d}x}L(x) = 0$ has a unique solution on $[0, \infty)$.

This is proved in three steps: first, we show that there can be at most one solution of $\frac{\mathrm{d}}{\mathrm{d}x}L(x) = 0$ on $[0, \frac{1}{\theta r^\alpha}]$; second, we show there can be at most one solution of $\frac{\mathrm{d}}{\mathrm{d}x}L(x) = 0$ on $[\frac{1}{\theta r^\alpha}, \infty)$; third, we observe that cannot be two solutions of $\frac{\mathrm{d}}{\mathrm{d}x}L(x) = 0$ on $[0, \infty)$.

First, the derivative of $L(x)$ can be expanded as

$$\frac{\mathrm{d}}{\mathrm{d}x}L(x) = 1 - (1 - e^{-\theta r^\alpha x})^n - n\theta r^\alpha x e^{-\theta r^\alpha x}(1 - e^{\theta r^\alpha x})^{n-1}, \tag{2.13}$$

which is strictly decreasing on $[0, \frac{1}{\theta r^\alpha}]$ due to the monotonicity of $e^{-\theta r^\alpha x}$, the monotonicity of $xe^{-\theta r^\alpha x}$ on $[0, \frac{1}{\theta r^\alpha}]$. Thus there cannot be more than one solution of $\frac{\mathrm{d}}{\mathrm{d}x}L(x) = 0$ on $[0, \frac{1}{\theta r^\alpha}]$.

Second, $\frac{\mathrm{d}}{\mathrm{d}x}L(x) = 0$ can be rearranged as $1 - (1 - n\theta r^\alpha x)e^{-\theta r^\alpha x} = (1 - e^{-\theta r^\alpha x})^{1-n}$, where the left side is a strictly increasing function of $x$ for $x > \frac{n-1}{n\theta r^\alpha}$ and the right side is a decreasing function of $x$. Thus, there can be at most one solution of $\frac{\mathrm{d}}{\mathrm{d}x}L(x) = 0$ on $[\frac{1}{\theta r^\alpha}, \infty) \in (\frac{n-1}{n\theta r^\alpha}, \infty)$.

Third, there can be only an odd number of zero crossings of $\frac{\mathrm{d}}{\mathrm{d}x}L(x)$ on $[0,\infty)$ since $\frac{\mathrm{d}}{\mathrm{d}x}L(x)$ is continuous, $\lim_{x\to 0+}\frac{\mathrm{d}}{\mathrm{d}x}L(x) > 0$, and $\frac{\mathrm{d}}{\mathrm{d}x}L(x)$ approaches zero from below as $x \to \infty$. Combining with results above, we conclude there is a unique zero crossing of $\frac{\mathrm{d}}{\mathrm{d}x}L(x)$ on $[0,\infty)$. □

Similar to the Nakagami-$m$ fading case, in general, there is no closed form expression for the (optimal) transmit probability. However, this optimal configuration is implied by the solution of $\frac{\mathrm{d}}{\mathrm{d}x}L(x) = 0$.

Let $r$ be the common distance from the transmitter to the desired receivers, Table 2.1 compares the transmit power $\xi$ of the optimal (ALOHA) policy for different number of receivers. It shows that with a larger number of desired receivers, the optimal policy tends to reduce the transmit power of each transmission attempt while increasing the transmit probability $\xi^{-1}$. Fig. 2.7 shows that under an optimal policy, the local anycast delay decreases as more desired receivers are available. Both observations above are intuitive as anycast with more desired receiver can be interpreted as point-to-point communication with a more benign fading distribution. In both Table 2.1 and Fig. 2.7, the case $n = 1$ corresponds to the single link Rayleigh fading case.

## 2.8 Conclusions

This chapter provides a set of power control policies that minimize the conditional local delay (or, delay till success) for channels with different fading statistics. We show that an ALOHA-type random on-off power control is the delay-optimal policy for Rayleigh fading channels. We give a sufficient condition under which ALOHA-type policy is optimal and show that almost all common fading models satisfy these conditions, including Nakagami-$m$ fading, Rician fading and lognormal shadowing.

The result of this chapter directly leads to a solution for minimizing the local

TABLE 2.1

OPTIMAL TRANSMIT POWER $\xi$ FOR ANYCAST WITH RAYLEIGH FADING, WHERE $P_{\max} = 4$, $\alpha = 2$, $\theta = 1$.

| | $n = 1^4$ | $n = 2$ | $n = 3$ | $n = 4$ | $n = 5$ | $n = 6$ |
|---|---|---|---|---|---|---|
| $r = 0.5$ | 1.0000 | 1.0000 | 1.0000 | 1.0000 | 1.0000 | 1.0000 |
| $r = 1.5$ | 2.2500 | 1.8566 | 1.6352 | 1.4893 | 1.3841 | 1.3038 |
| $r = 2.5$ | 4.0000 | 4.0000 | 4.0000 | 4.0000 | 3.8448 | 3.6218 |
| $r = 3.5$ | 4.0000 | 4.0000 | 4.0000 | 4.0000 | 4.0000 | 4.0000 |

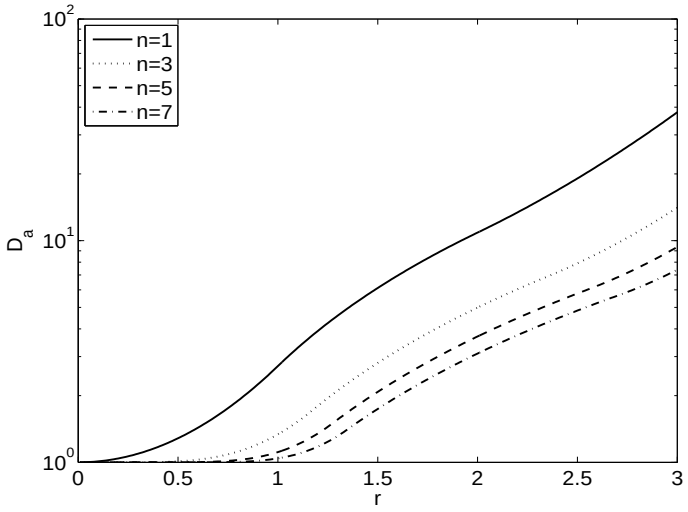


Figure 2.7. Minimum local anycast delay in the Rayleigh fading case. $P_{\max} = 4$, $\theta = 1$, $\alpha = 2$.

delay in random but fixed wireless networks, and also implies solutions for minimizing the local anycast delay. In the iid fading case, since the conditional local delay minimized by our policies is the inverse of the success probability of each transmission conditioned on the link distance, the delay-optimal policies are essentially throughput-maximizing policies in the random but fixed noise-limited wireless network if a single-bit ARQ is given to the transmitter. As in many cases the optimal policy concluded in this chapter is a 'peaky' scheme (ALOHA), our results bear interesting relations to some of the results also suggesting 'peaky' transmissions, *e.g.,* [55, 64, 66].

In a wireless network where interference is not negligible, our optimal scheme can be used as a lower-layer power control policy. When a specific link is activated by an upper layer interference-managing MAC scheme (*e.g.,* CSMA, LMAC [74], etc.), individual links can apply the policy in this chapter to minimize the conditional local delay, and thus the local delay.

# CHAPTER 3

# RANDOM POWER CONTROL IN INTERFERENCE-LIMITED NETWORKS

## 3.1 The SNOPC and NEPC Strategies

Chapter 2 considered a noise-limited network, which is essentially a collection of independent links. In this case, the individual optimum is the global optimum since there is no conflict of interests between links. However, in the interference-limited case, a higher throughput at a few links may result in a performance degradation of other links. Therefore, the best choice of the power control strategy of a link is a function of the power control strategy applied in other links.

In order to study this interaction among different users, we model power control as a non-cooperative game between transmitters and characterize two types of power control strategies: 1. Single-node optimal power control (SNOPC) strategies when only one node in the network uses power control; 2. Nash equilibrium power control (NEPC) strategies when all the nodes in the network use power control. SNOPC strategies maximize the expected throughput of the power-controllable link, whereas NEPC strategies ensure that no individual node of the network can achieve a higher expected throughput by unilaterally deviating from these strategies. In the discussion of each type of strategies, we consider three different levels of information available at the transmitters, which can be interpreted as corresponding to three levels of mobility of the network. It turns out that, in many cases, ALOHA-type random on-off power control policies are single-node optimal and constitute Nash equilibria.

## 3.2 Relation to Other Work

In the study of power control in wireless networks, two main approaches have been used to analyze and design sensible policies: the optimization approach [17, 27, 43, 44, 61] and the game theory approach [2, 3, 8, 25, 45, 53, 56, 62]. The former assumes inter-node cooperation and aims at finding the assignment of power that maximizes some global, while the latter provides a means to study the robust power control strategies such that malicious users cannot benefit from deviating from them.

Focusing on the case where any inter-node coordination is not allowed and the transmitters decide on their own power control strategies to maximize their own expected throughput, this chapter adopts a game theory framework.

Similar to Chapter 2, we allow the transmit power at each node to be a random variable with arbitrary distribution subject to a (unit) mean power and a peak power constraint. While most of the exiting power control literature considers deterministic power control strategies, this chapter shows that the additional randomness can potentially be highly beneficial.

Although this thesis is not the first one to demonstrate the benefits of randomly varying the transmit power in wireless networks with interference, only a very limited number of papers focus on it[26, 50]. While [26, 50] demonstrate the benefits of random power control in the presence of interference, both papers fail to justify their choice of random power control distribution (uniform distribution). Here, we show that there is a specific type of simple transmit power distribution (ALOHA-type random on-off) that not only maximizes a single user's throughput but also constitutes the network-wide Nash equilibrium.

Random power control schemes also naturally appear as mixed strategies in game-theoretic frameworks, *e.g.,* [6]. However, in this context, the combination of mean *and* peak power constraints is usually not considered. We show that these constraints have a significant impact on the strategies of interest. In particular, it turns out both

the SNOPC and the NEPC strategies are ALOHA-type random on-off policies.

Another important feature that contrasts the content of this chapter to other papers in the power control literature is the use of a stochastic point process to model the network and the explicit separation of channel uncertainty due to node location and fading. Although powerful tools from stochastic geometry have been introduced in the analysis of large wireless networks over the last decade [42], only a very small part of the power control literature considers the spatial distribution of wireless networks. Instead, most of the papers do not differentiate the path loss due to fading and path loss due to random location of the nodes. Such simplification does not matter when the (combined) channel state is known at the transmitters, *e.g.,* [27, 45], or stays fixed over time and thus can be learned gradually through channel feedback, *e.g.,* [6, 8, 25]. Yet, it prohibits the discovery of efficient power control schemes when the network has limited capability to acquire perfect channel state information. In this chapter, we explicitly account for these two sources of randomness.

## 3.3 Chapter Organization

The rest of the chapter is organized as follows: Section 3.4 introduces the system model and specifies three cases of interest (with different levels of information available at the transmitters). Sections 3.5, 3.6 and 3.7 analyze the SNOPC and NEPC strategies in three cases. The performance of these strategies is evaluated in Section 3.8. Section 3.9 concludes the chapter.

## 3.4 System Model

### 3.4.1 Network Model

The network topology is represented as a marked Poisson point process (PPP) $\hat{\Phi} = \{(x_i, y_{x_i})\} \subset \mathbb{R}^2 \times \mathbb{R}^2$, where $\Phi = \{x_i\}$ is a homogeneous PPP with intensity $\lambda$ and denotes the location of the transmitters and the mark $y_x$ denotes the location of a dedicated receiver of transmitter $x$. The link distances $R_x \triangleq \|x - y_x\|$ are iid with distribution $f_R$.

We consider the following SIR model, where a transmission attempt from $z$ to $y_z$ is considered successful iff

$$\mathrm{SIR}_z \triangleq \frac{S_z}{I_z} > \theta,$$

where $S_z = P_z h_z \|z - y_z\|^{-\alpha}$, $I_z = \sum_{x \in \Phi \setminus \{z\}} P_x h_{xz} \|x - y_z\|^{-\alpha}$, $P_x$ is the transmit power at node $x \in \Phi$, $\alpha > 2$ is the path-loss exponent, $\theta$ is the SIR threshold, and $h_z$ and $h_{xz}$ are (power) fading coefficients from the desired transmitter and the interferer $x$ to $z$ respectively. We focus on the iid Rayleigh fading case, thus $h_z$ and the sequence $(h_{xz})$ are iid exponentially distributed with unit mean. In the following, we use $I$ for $I_z$ for simplicity.

### 3.4.2 Game-Theoretic Formulation

The players in the game are all the transmitters in the network $x \in \Phi$. Each player can select a strategy $s_x$ from a common set of stationary strategies $\mathcal{S}$. Here, $\mathcal{S}$ is the set of distributions with (at most) unit mean and with support (at most) $[0, P_{\max}]$, where $P_{\max} > 1$ (otherwise, the mean power constraint would always be loose).

The strategy each node chooses is based on its knowledge about the network. We use $\mathcal{K}_x$ to denote this knowledge available at node $x$ and split our discussion into three cases: case 1: $\mathcal{K}_x = \{f_R\}$, case 2: $\mathcal{K}_x = \{\lambda, R_x, f_R\}$, and case 3: $\mathcal{K}_x = \{\hat{\Phi}\}$.

These three cases represent different levels of information in ascending order. Case 1 and case 2 are more suitable models for high-mobility networks, where only very limited network information can be acquired at each node. Case 3 applies to static networks, where the complete network topology information can be either provided off-line or learned gradually by each link.

The pay-off of node $x \in \Phi$ is its own expected throughput (success probability) averaged over all the randomness in the rest of the network, *i.e.,* $\pi_x(s_x) = p_{s|\mathcal{K}_x}(s_x) = \mathbb{P}(\frac{S_x}{I_x} > \theta \mid \mathcal{K}_x, s_x(\mathcal{K}_x))$. The single-node optimal power control (SNOPC) strategy of node $x$ maximizes $\pi_x(\cdot)$ if all the other transmitters in the network transmit with unit power (no power control). If all the transmitters in the network use power control, we say that a strategy set $\{s_x(\mathcal{K}_x), x \in \Phi\}$ is a *Nash equilibrium* and $s_x(\mathcal{K}_x)$ is the Nash equilibrium power control (NEPC) strategy if none of the transmitters is willing to unilaterally deviate from its current strategy as that cannot increase its pay-off (expected throughput).

In addition to the game-theoretic framework above, we study the global impact of SNOPC and NEPC by evaluating the spatially averaged throughput, (or, simply spatial throughput), defined as the throughput (success probability) of a typical node in the network, which can be expressed as

$$p_s = \mathbb{E}^{!x}[\pi_x(s_x)],$$

where $\mathbb{E}^{!x}$ is the expectation with respect to the reduced Palm measure. Loosely speaking, it is the expectation conditioned on the existence of a point at $x$ but not counting it. More details about the Palm measure and its applications in wireless networks can be found in [39, 42] and the references therein. In the case of a PPP, by Slivnyak's theorem, $\mathbb{E}^{!x} = \mathbb{E}$, *i.e.,* having a node at location $x$ does not change the distribution of the point process[39].

## 3.5 Case 1: Unknown Link Distances

We first consider the case of $\mathcal{K}_x = \{f_R\}$, *i.e.,* only the distribution of $R_x$ is known at the nodes with power control capability. In particular, we consider the case where the link distances $R_x$ are Rayleigh distributed with mean $1/2\sqrt{\lambda_r}$, *i.e.,* $f_R(x) = 2\lambda_r \pi x \exp(-\lambda_r \pi x^2)$. This distribution is of interest because $f_R$ is the distribution of the link distances when each node of $\Phi$ tries to connect to its nearest neighbor in an independent homogeneous PPP of intensity $\lambda_r$[34].

**Proposition 2.** *If only the node $z \in \Phi$ can use power control but all other transmitters transmit with unit power and $R$ is Rayleigh distributed, the SNOPC strategy at $z$ is constant power transmission (no power control).*

*Proof.* Since $\Phi$ is motion-invariant, without loss of generality, place the desired receiver at origin, *i.e.,* $y_z = o$. Then, if we let $h_x$ be the iid fading coefficient from $x$ to $o$, the Laplace transform of the interference $I$ can be expressed as

$$\mathcal{L}_I(s) = \mathbb{E}\Big[\prod_{y\in\Phi\setminus\{z\}} e^{sh_y\|y\|^{-\alpha}} \mid z \in \Phi\Big]$$
$$\stackrel{(a)}{=} \mathbb{E}^{!z}\Big[\prod_{y\in\Phi\setminus\{z\}} e^{sh_y\|y\|^{-\alpha}}\Big] \stackrel{(b)}{=} \mathbb{E}\Big[\prod_{y\in\Phi} e^{sh_y\|x\|^{-\alpha}}\Big] \stackrel{(c)}{=} e^{-\lambda\pi s^{\delta}\frac{\pi\delta}{\sin(\pi\delta)}},$$

where (a) is due to the definition of Palm distribution (b) is due to Slivnyak's theorem, (c) is shown in [41] and $\delta = 2/\alpha$. It is assumed that $\alpha > 2$ (otherwise the interference is infinite almost surely), so $\delta < 1$.

Thus, for an arbitrary power control policy characterized by random variable $P$,

the success probability can be written as

$$\begin{aligned}\mathbb{P}(PhR^{-\alpha} > \theta I) &= \mathbb{E}_{P,R}[\mathbb{P}(PhR^{-\alpha} > \theta I) \mid P, R] = \mathbb{E}_P \mathbb{E}_R[\mathcal{L}_I(s)|_{s=\frac{\theta R^\alpha}{P}}] \\ &= \mathbb{E}_P\left[\int_0^\infty 2\lambda_r \pi r \exp\left(-\lambda\pi \frac{\pi\delta}{\sin\pi\delta}\left(\frac{\theta r^\alpha}{P}\right)^\delta\right)\exp(-\lambda_r \pi r^2)\mathrm{d}r\right] \\ &= \mathbb{E}_P\left[\frac{b}{a\left(\frac{\theta}{P}\right)^\delta + b}\right],\end{aligned}$$

where $a = \lambda\pi\frac{\pi\delta}{\sin\pi\delta}$ and $b = \lambda_r\pi$. Since $\frac{b}{a(\theta/x)^\delta+b}$ is concave for $a, b, \theta > 0$ and $0 < \delta < 1$, by Jensen's inequality, the throughput is maximized when choosing $P \equiv \mathbb{E}P = 1$. $\square$

Proposition 2 shows that if $R$ is Rayleigh distributed and the rest of the network uses constant power transmission, the best strategy at node $z$ is constant power transmission, regardless of the values of $\lambda$ and $\lambda_r$. Since $z$ is arbitrarily chosen, this immediately implies that constant power transmission at all nodes is a Nash equilibrium. However, in order to find out whether there are other Nash equilibria, we need to study the interference distribution when the rest of the network uses power control.

**Lemma 8.** *If the interferers are distributed as a homogeneous Poisson point process $\Phi$ with intensity $\lambda$ and the transmit power at each transmitter is drawn iid from the same distribution $f_P$, the interference observed at any receiver $y_z$ with $z \in \Phi$ has the Laplace transform*

$$\mathcal{L}_I(s) = \exp(-\lambda c_d \mathbb{E}[P^\delta]\mathbb{E}[h^\delta]\Gamma(1-\delta)s^\delta).$$

*Proof.* First, by Slivnyak's theorem, $\mathcal{L}_I(s) = \mathbb{E}[\prod_{x\in\Phi} e^{-sP_x h_x \|x\|^{-\alpha}}]$, where $P_x$ is the transmit power at $x$. Second, since $(P_x)$, $x \in \Phi$, is iid, $P_x h_x$ can be considered as a new fading coefficient $\tilde{h}_y$. The proof is then completed by the Laplace transform of the interference distribution for arbitrary iid fading with finite $\delta$-th moment [41, Sec.

3.2]. □

**Proposition 3.** *If all nodes are capable of power control, constant power transmission is the unique NEPC policy in Poisson networks with Rayleigh distributed unknown link distances.*

*Proof.* By Proposition 2, the fact that constant power transmission is a NEPC strategy is evident. To show its uniqueness, we start by noting that the information available at each individual node $\mathcal{K}_x = \{f_R\}$ is the same. Thus, given that all the nodes are completely selfish and sufficiently and equally smart, at any Nash equilibrium, their choice of power control strategy must be the same. Assume the common choice of power control strategy (of the rest of the network) is characterized by the random variable $\tilde{P}$ with pdf $f_{\tilde{P}} \in \mathcal{S}$, and let the interference observed at arbitrary receiver $y_z$ under this power control policy be $\tilde{I}$. Then, Lemma 8 gives the Laplace transform of the $\tilde{I}$. Straightforward manipulation shows

$$\mathbb{P}(PhR^{-\alpha} > \theta\tilde{I}) = \mathbb{E}_P\left[\frac{b}{\tilde{a}\left(\frac{\theta}{P}\right)^{\delta} + b}\right], \tag{3.1}$$

where $\tilde{a} = \lambda\pi\frac{\pi\delta}{\sin\pi\delta}\mathbb{E}[\tilde{P}^{\delta}]$, $b = \lambda_r\pi$, and $P$ is the transmit power at $z$. As in the proof of Proposition 2, we can show that $P \equiv 1$ maximizes (3.1) under the unit mean power constraint. Since $z$ is arbitrarily chosen, we have $P = \tilde{P} \equiv 1$. □

**Corollary 4.** *If the transmitters and receivers are distributed as two independent homogeneous Poisson point processes $\Phi, \Phi_r \subset \mathbb{R}^2$ and all the transmitters in $\Phi$ try to connect to their nearest neighbor in $\Phi_r$, constant power transmission is the NEPC strategy.*

This corollary is a straightforward extension of Proposition 3. However, this result hinges critically on the special form of Nash equilibrium (constant power transmission), in Proposition 3. A similar result cannot be obtained in the two cases discussed in the next two sections.

## 3.6 Case 2: Known Link Distance

In this section, we consider the case where $\mathcal{K}_x = \{\lambda, R_x, f_R\}$, *i.e.,* the nodes with power control capability know the network density, the distances to their own dedicated receivers and the distribution of the link distance of the whole network. We first derive the form of the SNOPC and NEPC strategies for general $f_R$. Then, we take the Poisson bipolar network, *i.e.,* $f_R(x) = \delta(x - r)$, as an example to further illustrate the NEPC strategy.

### 3.6.1 General $f_R$

In this subsection, we start with the SNOPC strategy and then study the Nash equilibrium. First, we present a lemma:

**Lemma 9.** *Given a link of length $R = r$, if there exists $x_0 > 0$ such that $x\mathcal{L}_I(\theta r^\alpha x)$ is monotonically increasing for $x < x_0$ and monotonically decreasing for $x > x_0$, the power control strategy that maximizes the throughput at node $x$ is random on-off power control with transmit power $\gamma$ and transmit probability $\gamma^{-1}$ where $\gamma = \max\{1, \min\{P_{\max}, x_0^{-1}\}\}$.*

*Proof.* For interference-limited Rayleigh fading networks, the success probability of a transmission at power $P$ is $\mathcal{L}_I(s)|_{s=\frac{\theta r^\alpha}{P}}$. Thus, the success probability of any power control strategy characterized by the pdf $f_P$ of the random variable $P$ is

$$p_s = \mathbb{E}_P\left[\mathcal{L}_I(s)|_{s=\frac{\theta r^\alpha}{P}}\right] = \int_0^\infty \mathcal{L}_I\left(\frac{\theta r^\alpha}{x}\right) f_P(x)\mathrm{d}x. \tag{3.2}$$

It is easy to show that $\mathcal{L}_I(x)$ is a valid ccdf, *i.e.,* $\mathcal{L}_I(0) = 1$, $\lim_{x\to\infty} \mathcal{L}_I(x) = 0$, and $\mathcal{L}_I(x)$ is monotonically decreasing on $[0, \infty)$. So, instead, we can consider an interferenceless link of distance $r$ with another fading random variable $\tilde{h}$ whose ccdf

is $\bar{F}_{\tilde{h}}(x) = \mathcal{L}_I(x)$. The success probability is

$$\tilde{p}_s = \mathbb{P}(P\tilde{h}r^{-\alpha} > \theta) = \mathbb{E}_P\left[\bar{F}_{\tilde{h}}\left(\frac{\theta r^\alpha}{P}\right)\right] = \int_0^\infty \mathcal{L}_I\left(\frac{\theta r^\alpha}{x}\right) f_P(x)\mathrm{d}x. \tag{3.3}$$

Comparing (3.2) and (3.3), we find that finding the SNOPC strategy that maximizes $p_s$ and finding the one for $\tilde{p}_s$ are two identical problems. The latter problem has already been solved in Chapter 2. In particular, Theorem 2 shows that if there exists a $x_0$ as in the statement of the lemma, subject to the constraints $\mathbb{E}P \leq 1$ and $P \leq P_{\max}$, $\tilde{p}_s$ is maximized when $f_P(x) = (1-\gamma^{-1})\delta(x) + \gamma^{-1}\delta(x-\gamma)$, where $\gamma = \max\{1, \min\{P_{\max}, x_0^{-1}\}\}$. □

**Corollary 5.** *If the Laplace transform of the interference $I$ has the form $\mathcal{L}_I(s) = \exp(-as^\delta)$, where $\delta = 2/\alpha$ and $a > 0$, the throughput-maximizing power control strategy at any transmitter $z \in \Phi$ with $R_z = r$ is a random on-off power control strategy with transmit power $\gamma$ and transmit probability $\gamma^{-1}$, where*

$$\gamma = \max\{1, \min\{P_{\max}, (a\delta)^{1/\delta}\theta r^\alpha\}\}.$$

Corollary 5 is proved by simply verifying that the form of the Laplace transform of the interference satisfies the conditions in Lemma 9.

**Proposition 4.** *If only one node $z \in \Phi$ with $R_z = r$ uses power control and all other nodes $\Phi\backslash\{z\}$ transmit at unit power, the SNOPC strategy of $z$ is an ALOHA-type random on-off power control strategy with transmit power $\gamma$ and transmit probability $\gamma^{-1}$, where $\gamma = \max\{1, \min\{P_{\max}, \left(\lambda\frac{\pi^2\delta^2}{\sin\pi\delta}\right)^{1/\delta}\theta r^\alpha\}\}$.*

*Proof.* The proposition follows directly from Lemma 8 ($P \equiv 1$) and Corollary 5. □

Moreover, since the transmit power at each node $x \in \Phi$ is a (stochastic) function of the link distances $R_x = r$, where the $R_x$ are spatially iid, Lemma 8 shows that

the interference always has a Laplace transform in the form $\exp(-as^\delta)$, regardless of what kind of power control strategy is applied at each node. Then, the proposition below follows.

**Proposition 5.** *ALOHA-type random on-off power control is the unique NEPC strategy in a wireless network where the transmitters are distributed as a homogeneous Poisson point process* $\Phi$ *and* $\mathcal{K}_x = \{\lambda, R_x, f_R\}$*, for all* $x \in \Phi$*.*

*Proof.* The fact that ALOHA-type random on-off power control at each node is a Nash equilibrium can be deduced directly from Lemma 8 and Corollary 5. In particular, we can write $\mathbb{E}[P^\delta]$ in terms of the throughput-maximizing random on-off strategy at each link, which yields

$$\begin{aligned}\mathbb{E}[P^\delta] &= \mathbb{E}_R[P_R^\delta] = \mathbb{E}_R[\gamma_R^{-1}\gamma_R^\delta] \\ &= \mathbb{E}_R\left[\min\left\{1, \max\left\{P_{\max}^{\delta-1}, \left(\frac{\lambda\pi^2\delta^2}{\sin(\pi\delta)}\mathbb{E}[P^\delta]\right)^{1-1/\delta}(\theta R^\alpha)^{\delta-1}\right\}\right\}\right]. \qquad (3.4)\end{aligned}$$

Note that the RHS of (3.4) is a monotonically decreasing function of $\mathbb{E}[P^\delta]$ (since $1 - 1/\delta < 0$), and when $\mathbb{E}[P^\delta] = 0$, its value is $P_{\max}^{\delta-1} > 0$. Thus, there is a unique $\mathbb{E}[P^\delta] > 0$ satisfying (3.4). Once this value is found, the optimal power control strategy at $x$ is simply an ALOHA policy with transmit power $\gamma$ and transmit probability $\gamma^{-1}$, where $\gamma = \max\{1, \min\{P_{\max}, \left(\lambda\mathbb{E}[P^\delta]\frac{\pi^2\delta^2}{\sin\pi\delta}\right)^{1/\delta}\theta R_x^\alpha\}\}$.

Moreover, Lemma 8 also says that no matter what kind of power control policy is applied in the rest of the network, the interference distribution observed at an arbitrary receiver has a Laplace transform of the form $\mathcal{L}_I(s) = \exp(-as^\delta)$. Thus, Corollary 5 also indicates the uniqueness. □

### 3.6.2 Bipolar Networks

In general, analytically solving for the Nash equilibrium in (3.4) is difficult. As a special case, when all the link distances are known and constant, the network model

becomes a Poisson bipolar model[10], for which we have the following result:

**Corollary 6.** *If all the link distances are $r$, the NEPC strategy is an ALOHA-type random on-off policy with transmit power $\gamma$ and transmit probability $\gamma^{-1}$ where $\gamma = \max\{1, \min\{P_{\max}, \lambda\frac{\pi^2\delta^2}{\sin\pi\delta}\theta^\delta r^2\}\}$, $\lambda$ is the density of the transmitters and $\delta = 2/\alpha$.*

*Proof.* For Rayleigh fading, $h$ is exponentially distributed with mean 1, and thus $\mathbb{E}[h^\delta] = \Gamma(1+\delta)$. Then, when the link distances are the same, (3.4) becomes

$$\mathbb{E}[P^\delta] = \left(\max\left\{1, \min\left\{P_{\max}, \left(\lambda\mathbb{E}[P^\delta]\frac{\pi^2\delta^2}{\sin\pi\delta}\right)^{1/\delta}\theta r^\alpha\right\}\right\}\right)^{\delta-1}. \tag{3.5}$$

Solving this equation for $\mathbb{E}[P^\delta]$ and applying to $\max\{1, \min\{P_{\max}, (\lambda\mathbb{E}[P^\delta]\frac{\pi^2\delta^2}{\sin\pi\delta})^{1/\delta}\theta r^\alpha\}\}$ yields the desired result. □

Corollary 6 says that in any case, an ALOHA-type random on-off policy is the NEPC policy in a Poisson bipolar network. For ALOHA-type random on-off strategies with transmit power $\gamma$ and transmit probability $\gamma^{-1}$, we define the following regimes to facilitate our illustration.

**Definition 8.** *A random on-off power control strategy is said to be in its ALOHA-peak-power-limited regime if $\gamma = P_{\max}$.*

**Definition 9.** *A random on-off power control strategy is said to be in its ALOHA-bandwidth-limited regime if $\gamma = 1$.*

As a MAC scheme, ALOHA in Poisson bipolar networks is well studied in the literature. In particular, [10] derived the ALOHA scheme that maximizes the spatial throughput in Poisson bipolar networks, which we call the globally optimal (GOPT) ALOHA scheme. GOPT ALOHA maximizes the spatial throughput by properly choosing transmit probability, and when only the SIR is considered, the absolute transmit power does not affects its optimality. However, in order to make a fair

comparison with the NEPC strategy, we interpret GOPT as a power control scheme and always choose the maximum transmit power for GOPT under the mean and peak power constraints. Then, it can be shown that the transmit probability of GOPT is $p_{\mathrm{GOPT}} = \min\{1, \left(\lambda \frac{\pi^2\delta}{\sin \pi\delta} \theta^\delta r^2\right)^{-1}\}$, and the transmit power is $P_{\mathrm{GOPT}} = \min\{p_{\mathrm{GOPT}}^{-1}, P_{\max}\}$. For the same set of parameters, we always have $P_{\mathrm{GOPT}} \geq \gamma$ and $p_{\mathrm{GOPT}} \leq \gamma^{-1}$, where $\gamma$ is the transmit power of the Nash equilibrium power control strategy. In other words, GOPT achieves higher spatial throughput by forcing each transmitter to back off on their transmit probability.

However, GOPT is unstable in the sense that any selfish link can apply another power control strategy and thus obtain a performance far better than anyone else. It is not difficult to see (by slight variation to Proposition 4) that the best response of any individual link in a Poisson bipolar network applying GOPT is an ALOHA policy with transmit power $\gamma_{\mathrm{BR}}$ and transmit probability $\gamma_{\mathrm{BR}}^{-1}$, where the subscript BR stands for best response and

$$\gamma_{\mathrm{BR}} = \max\left\{1, \min\left\{P_{\max}, \left(\lambda p_{\mathrm{GOPT}} P_{\mathrm{GOPT}}^{\delta} \frac{\pi^2\delta^2}{\sin \pi\delta}\right)^{1/\delta} \theta r^{\alpha}\right\}\right\} = \max\{1, P_{\mathrm{GOPT}}\delta^{\delta}\}.$$

Here, $\gamma_{\mathrm{BR}}^{-1} \geq p_{\mathrm{GOPT}}$, and the equality holds only when $\gamma_{\mathrm{BR}}^{-1} = p_{\mathrm{GOPT}} = 1$, *i.e.,* both strategies operate in the ALOHA-bandwidth-limited regime.

Fig. 3.1 compares the spatial throughput of 4 strategies: constant-power transmission (no power control), NEPC strategy, the globally optimal (GOPT) ALOHA, and the best response to GOPT in Poisson bipolar networks. We can see from the figure that the Nash equilibrium power control policy has a better performance than constant power transmission. As expected, outside the ALOHA-bandwidth-limited regime of both GOPT and NEPC, NEPC has a spatial throughput strictly smaller than GOPT. However, the performance gain of GOPT over NEPC mostly comes from forcing each transmitter in the network to reduce its mean transmit power and thus

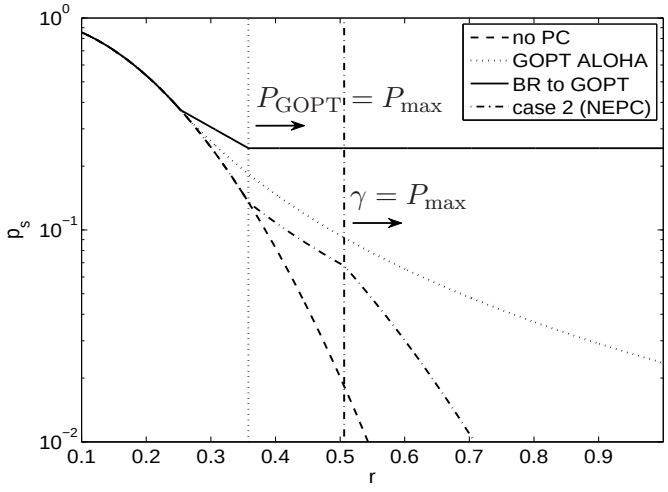


Figure 3.1. Comparison of throughput using 1) constant power transmission (no power control) 2) GOPT ALOHA 3) the best response to the GOPT ALOHA and 4) NEPC strategy. Here, $\lambda = 1$, $P_{\max} = 2$, $\alpha = 2$, $\theta = 10$. To the right of the two vertical lines, the transmit power of the GOPT and NEPC strategies hits their corresponding peak power limits.

manage the interference, *i.e.,* for large $r$, $p_{\mathrm{GOPT}} P_{\mathrm{GOPT}} < 1$. Fig. 3.1 shows that in such cases, if any node cheats by using another power control strategy, in particular, the best response to GOPT, its expected throughput gain is significant. Such gain can be a strong incentive for individual links to cheat.

## 3.7 Case 3: Static Network

This section considers the case where $\mathcal{K}_x = \{\hat{\Phi}\}$. This assumption is particularly interesting in a static network, where the topology of the network can be acquired either directly off-line or gradually by observing the interference from the rest of the network. In fact, in this context, the assumption on the spatial distribution of the network becomes unimportant. We are in fact considering an arbitrary realization of the random network. Results in this section thus also apply to deterministic networks.

First, we provide a lemma to explicitly address the case where $x\mathcal{L}_I(\theta r^\alpha x)$ is mono-

tonically increasing for all $x > 0$. This lemma complements Lemma 9 as it is essentially considering the case where $x_0 = \infty$.

**Lemma 10.** *If the Laplace transform of the interference $I$ is $\mathcal{L}_I(s)$ and $x\mathcal{L}_I(\theta r^\alpha x)$ is monotonically increasing for all $x > 0$, the optimal power control strategy is constant power transmission,* i.e., $P \equiv 1$.

*Proof.* Construct another random variable $\tilde{I}$ with Laplace transform

$$\mathcal{L}_{\tilde{I}}(s) = \mathcal{L}_I(s)1_{[0,\theta r^\alpha]}(s) + \frac{1}{s^2}\mathcal{L}_I(\theta r^\alpha)1_{(\theta r^\alpha,\infty)}(s),$$

for all $s > 0$. Since $x\mathcal{L}_I(\theta r^\alpha x)$ is monotonically increasing, it can be verified that $x\mathcal{L}_{\tilde{I}}(\theta r^\alpha x)$ is monotonically increasing on $[0, 1]$ and strictly decreasing on $(1, \infty)$. Applying Lemma 9, we know that

$$\max_{f_P \in \mathcal{S}} \int_0^\infty \mathcal{L}_{\tilde{I}}\left(\frac{\theta r^\alpha}{x}\right) f_P(x)\mathrm{d}x = \mathcal{L}_{\tilde{I}}(\theta r^\alpha) = \mathcal{L}_I(\theta r^\alpha),$$

where the maximum is achieved when $P \equiv 1$.

Let $f_P^*$ be the distribution of the optimal power control policy for interference $I$. With the help of Lemma 5, it is straightforward to show that $f_P^*(x) = 0,\ \forall x \in (0, 1)$. Therefore,

$$\begin{aligned}\max_{f_P \in \mathcal{S}} \int_0^\infty \mathcal{L}_I\left(\frac{\theta r^\alpha}{x}\right) f_P(x)\mathrm{d}x &= \max_{f_P \in \mathcal{S}} \int_1^\infty \mathcal{L}_I\left(\frac{\theta r^\alpha}{x}\right) f_P(x)\mathrm{d}x \\ &\overset{\text{(a)}}{=} \max_{f_P \in \mathcal{S}} \int_1^\infty \mathcal{L}_{\tilde{I}}\left(\frac{\theta r^\alpha}{x}\right) f_P(x)\mathrm{d}x \\ &\overset{\text{(b)}}{=} \max_{f_P \in \mathcal{S}} \int_0^\infty \mathcal{L}_{\tilde{I}}\left(\frac{\theta r^\alpha}{x}\right) f_P(x)\mathrm{d}x = \mathcal{L}_I(\theta r^\alpha),\end{aligned}$$

where (a) is due to the definition of $\tilde{I}$ and (b) is due to the fact that SNOPC policy for $\tilde{I}$ is constant power transmission. The lemma then follows the fact that when $P \equiv 1$, $\int_0^\infty \mathcal{L}_I(\frac{\theta r^\alpha}{x}) f_P(x)\mathrm{d}x = \mathcal{L}_I(\theta r^\alpha)$, *i.e.,* the maximum success probability is

achieved. □

**Proposition 6.** *If only one transmitter at $z \in \Phi$ uses power control and the transmitter knows the positions of all interferers, the SNOPC strategy at this link is an ALOHA-type power control policy.*

*Proof.* Assume the desired receiver is located at $o$ and the positions of all interferers are $\phi_z$, *i.e.,* $\phi_z$ is one realization of $\Phi\backslash\{z\}$. Then, the Laplace transform of the interference $I \mid \phi_z = \sum_{x\in\phi_z} h_x \|x\|^{-\alpha}$ is

$$\mathcal{L}_{I|\phi_z}(s) = \prod_{x\in\phi_z} \frac{1}{\|x\|^{-\alpha}s + 1}.$$

In order to simplify the notation and eliminate ambiguity, in the following we use $l = \|x\|$ to be the label of each interferer. $\{l\}$ forms another PPP on $\mathbb{R}^+$[34]. Thanks to the fact that $\{l\}$ is a simple point process, there will be no ambiguity introduced by this change of labeling[1]. With a slight abuse of notation, we let $l = \|x\| \in \phi$ iff $x \in \phi$.

Then, the variable $x$ can be reserved for examining the condition in Lemma 9. Since $\log(\cdot)$ preserves the monotonicity, once the (monotonicity) conditions are proved for $\log(x\mathcal{L}_I(\theta r^\alpha x))$, they are proved for $x\mathcal{L}_I(\theta r^\alpha x)$. Thanks to the continuity of $\log(x\mathcal{L}_I(\theta r^\alpha x))$, we examine the monotonicity of $\log(x\mathcal{L}_I(\theta r^\alpha x))$ by calculating its derivative

$$\frac{\mathrm{d}}{\mathrm{d}x}\log(x\mathcal{L}_I(\theta r^\alpha x)) = \frac{1}{x} - \sum_{l\in\phi_z} \frac{1}{x + l^\alpha/\theta r^\alpha}. \tag{3.6}$$

We rearrange the equation $\frac{\mathrm{d}}{\mathrm{d}x}\log(x\mathcal{L}_I(\theta r^\alpha x)) = 0$ as

$$\sum_{l\in\phi_z} \frac{1}{1 + l^\alpha/\theta r^\alpha x} = 1, \tag{3.7}$$

[1]Even in a deterministic network where $\|x_1\| = \|x_2\|$ may exist, one can still avoid ambiguity by simply denoting $l_1 = \|x_1\|$ and $l_2 = l_1 + \epsilon = \|x_2\|$ for $\epsilon$ sufficiently small.

where the LHS is a (strict) monotonically increasing function of $x$. Thus, there is at most one positive zero-crossing for $\log(x\mathcal{L}_I(\theta r^\alpha x))$. Moreover, it can be shown that $\lim_{x\downarrow 0} \frac{\mathrm{d}}{\mathrm{d}x} \log(x\mathcal{L}_I(\theta r^\alpha x)) = +\infty$. Therefore, $\log(x\mathcal{L}_I(\theta r^\alpha x))$ is either monotonically increasing on $(0,\infty)$ or has a unique $x_0 \in (0,\infty)$, such that $x\mathcal{L}_I(\theta r^\alpha x)$ is monotonically increasing for $x < x_0$ and monotonically decreasing for $x > x_0$. Applying Lemma 10 in the former case and applying Lemma 9 in the latter case yields the desired result. □

In addition to finding the SNOPC policy, Proposition 6 provides the NEPC policy for a network of two links. Interestingly, no matter what kind of topology these two pairs of transmitter and receiver form, the NEPC strategy for this network is always constant power transmission at both transmitters. To see this, we can first assume one of the two transmitters is transmitting with constant power. For the other transmitter, (3.7) becomes

$$\frac{1}{1 + l/\theta r^\alpha x} = 1,$$

where $l$ is the distance between the desired the receiver and the interferer. This equation does not have a solution on the positive axis and thus by applying Lemma 10, constant power transmission is single-node optimal. The same analysis applies to the other node. Thus, constant power transmission is a NEPC strategy in two-link networks. However, for networks of more than two links, the NEPC strategy is in general not constant power control, as is shown in the following proposition.

**Proposition 7.** *ALOHA random on-off power control is a NEPC strategy for Rayleigh fading wireless networks, where the positions of the nodes of the whole network (both the transmitters and the receivers) are available at each transmitter.*

*Proof.* We first focus on the power control strategy of an arbitrary transmitter $z \in \phi$ and assume the rest of the network uses certain ALOHA random on-off power control

policies which are known at $z$. We show that in such scenario the best response power control strategy for $z$ is ALOHA.

The proof is analogous to that of Proposition 6. Again, we let $y_z = o$ without loss of generality and denote $\phi \backslash \{z\}$ by $\phi_z$. We assume that the transmit probability of node with label $l = \|x\| \in \mathbb{R}^+$ is $\gamma_l^{-1}$ and its transmit power is $\gamma_l$. Then, the Laplace transform of the interference is

$$\mathcal{L}_{I|\phi}(s) = \prod_{l \in \phi_z} \left( \frac{\gamma_l^{-1}}{\gamma_l l^{-\alpha} s + 1} + 1 - \gamma_l^{-1} \right). \tag{3.8}$$

Again, we use the logarithm to change the product to a sum and examine the derivative of $\log(x\mathcal{L}_I(\theta r^\alpha x))$, which can be written as

$$\frac{\mathrm{d}}{\mathrm{d}x} \log(x\mathcal{L}_I(\theta r^\alpha x)) = \frac{1}{x} - \sum_{l \in \phi_z} \left( \frac{1}{x + l^\alpha/\theta r^\alpha \gamma_l} - \frac{1}{x + l^\alpha/\theta r^\alpha (\gamma_l - 1)} \right),$$

where $\gamma_l > 0,\ \forall l$. Then, $\frac{\mathrm{d}}{\mathrm{d}x} \log(x\mathcal{L}_I(\theta r^\alpha x)) = 0$ can be rearranged as

$$\sum_{l \in \phi_z} \left( \frac{1}{1 + l^\alpha/\theta r^\alpha \gamma_l x} - \frac{1}{1 + l^\alpha/\theta r^\alpha (\gamma_l - 1)x} \right) = 1,$$

where the LHS is a (strict) monotonically increasing function of $x$. Thus, there is at most one positive zero crossing for $\log(x\mathcal{L}_I(\theta r^\alpha x))$. Moreover, it can be shown that $\lim_{x \downarrow 0} \frac{\mathrm{d}}{\mathrm{d}x} \log(x\mathcal{L}_I(\theta r^\alpha x)) = +\infty$. The rest of the proof follows the one of Proposition 6.

Since $z$ is an arbitrary transmitter in the network, a Nash equilibrium is established. The assumption that each node knows the power control policy of the rest of the network is justified by the fact that each node has the same knowledge when deciding its own power control policy. Therefore, if a particular node can calculate its optimal power control policy, all the other nodes can do that as well. □

While Proposition 7 shows that a set of random on-off power control strategies is a Nash equilibrium, the exact equilibrium point, *i.e.* the transmit power $\gamma_l$, $\forall l \in \phi$, is typically difficult to determine. In general, for a finite network of $n$ transmitter-receiver pairs, let $l_{ij}$ be the distance from the transmitter $i$ to the receiver $j$, and $r_k$ be the distance of the transmitter-receiver pair $k$, $i, j, k \in [n]$[2]. We have the following $2n$ equations

$$\begin{cases} \frac{1}{x_j} - \sum_{i\in[n]\setminus\{j\}} \left( \frac{1}{x_j + l_{ij}^{\alpha}/\theta r_j^{\alpha}\gamma_i} - \frac{1}{x_j + l_{ij}^{\alpha}/\theta r_j^{\alpha}(\gamma_i - 1)} \right) = 0, & \forall j \in [n] \\ \gamma_j = 1/\min\{1, \max\{P_{\max}^{-1}, x_j\}\}, & \forall j \in [n], \end{cases} \tag{3.9}$$

where $\gamma_j, x_j, j \in [n]$ are $2n$ unknowns. Although the value of $x_j$ does not often have any physical meaning, it helps solve for the power level $\gamma_j$ at each node $j$. Also, Proposition 7 implies that there is at least one solution of (3.9), despite the fact that finding it analytically is almost hopeless. In the following, we use numerically found solutions to evaluate this Nash equilibrium. Fig. 3.2 shows an example of the NEPC policy as well as its throughput for a realization of a Poisson bipolar network.

## 3.8 Performance Evaluation

### 3.8.1 The Single-node Optimal Power Control (SNOPC) Strategies

When all the interferers are transmitting with unit power, the interference distribution does not dependent on the distribution of the link distance. Thus, if the throughput conditioned on the link distance $r$ is $p_s(r)$, the mean throughput is just $\mathbb{E}_R[p_s(R)]$. For this reason, in this subsection, we only focus on $p_s(r)$.

If no power control is applied, the throughput can be expressed in terms of the

[2]We use $[n]$ to denote the set $\{1, 2, 3, \cdots, n\}$.

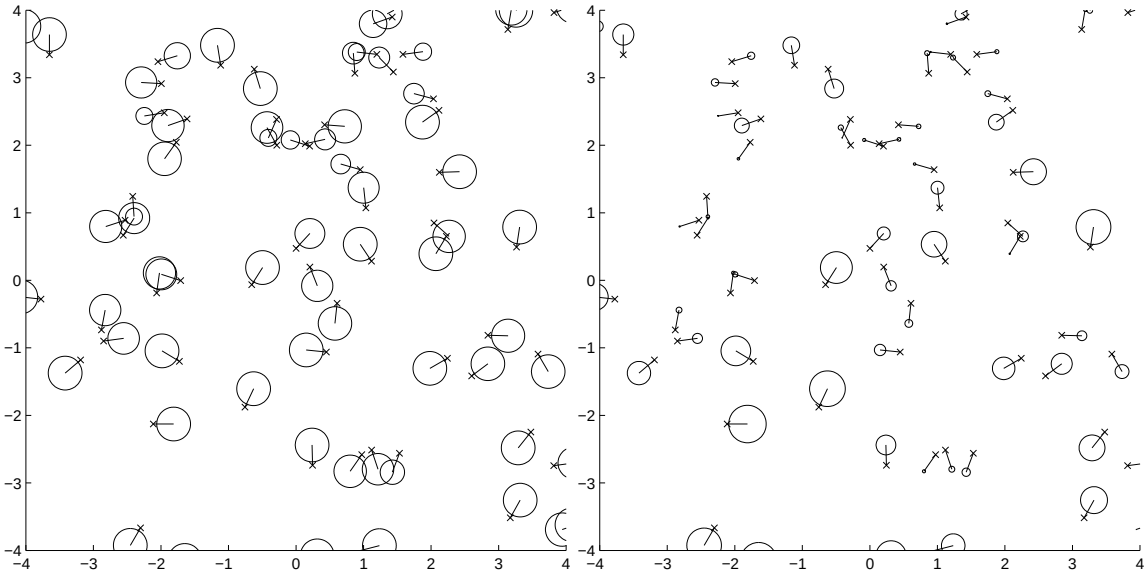

(a) transmit probability (b) throughput

Figure 3.2. The NEPC in a Poisson bipolar network in case 3. Each transmitter-receiver pair is linked by a line, where a circle is centered at the transmitter and the receiver is labeled by ×. The radius of each circle is proportional to the Nash equilibrium transmit probability (Fig. 3.2a) or the throughput (Fig. 3.2b) at the corresponding link. Here, $\lambda = 1$, $r \equiv 0.3$, $P_{\max} = 2$, $\theta = 10$.

Laplace transform of the interference distribution; it is given by [41]

$$p_s(r) = \exp\left(-\frac{\lambda\pi^2\delta}{\sin(\pi\delta)}\theta^\delta r^2\right).$$

The optimal power control policy for the case where only the link distance is available at the transmitter is given by Proposition 4. The throughput conditioned on the link distance $r$ is

$$p_s(r) = \begin{cases} \exp\left(-\lambda\pi(\theta r^\alpha)^\delta \frac{\pi\delta}{\sin\pi\delta}\right), & r < \theta^{-1/\alpha}\sqrt{\frac{\sin\pi\delta}{\lambda\pi^2\delta^2}} \\ \frac{\exp(-1/\delta)}{\theta r^\alpha}\left(\frac{\sin\pi\delta}{\lambda\pi^2\delta^2}\right)^{1/\delta}, & \theta^{-1/\alpha}\sqrt{\frac{\sin\pi\delta}{\lambda\pi^2\delta^2}} < r < \left(\frac{P_{\max}}{\theta}\right)^{1/\alpha}\sqrt{\frac{\sin\pi\delta}{\lambda\pi^2\delta^2}} \\ P_{\max}^{-1}\exp\left(-\lambda\pi\left(\frac{\theta r^\alpha}{P_{\max}}\right)^\delta \frac{\pi\delta}{\sin\pi\delta}\right), & r > \left(\frac{P_{\max}}{\theta}\right)^{1/\alpha}\sqrt{\frac{\sin\pi\delta}{\lambda\pi^2\delta^2}}. \end{cases}$$

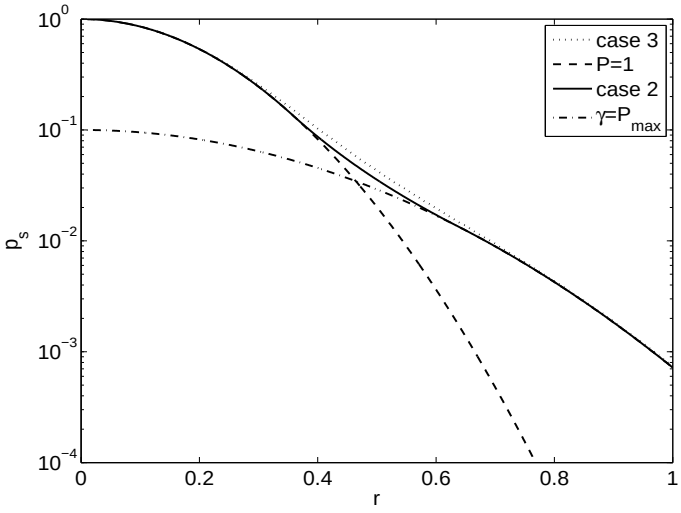


Figure 3.3. Comparison of throughput using three different SNOPC strategies. Here, $\lambda = 1$, $P_{\max} = 10$, $\alpha = 4$, $\theta = 10$. The throughput of case 3 is averaged over 10,000 realizations of the PPP.

When the complete network topology $\Phi = \phi$ is available at the central node (case 3), the optimal performance can be achieved by applying the policy suggested by the proof of Proposition 7. However, analytically characterizing the spatial throughput of such power control strategy requires a closed form expression for $\max_{1\le\gamma\le P_{\max}} \gamma^{-1} \prod_{l\in\phi} \frac{1}{1+\theta r^\alpha/l^\alpha\gamma}$, which seems hopeless. Therefore, we first solve for the single node optimal transmit power $\gamma(\phi)$ and transmit probability $1/\gamma(\phi)$. The expected throughput is given by $\gamma^{-1} \prod_{l\in\phi} \frac{1}{\theta r^\alpha/l^\alpha\gamma+1}$. We can then use simulation to average over a large number of realizations of $\Phi$ and compare the result with other two cases.

Fig. 3.3 compares the three SNOPC strategies for different levels of information. As expected, the SNOPC strategies with more information does strictly better than the SNOPC strategies based on less information. However, while the gain of knowing the link distance is significant especially when the link distance is large, the gain of knowing the complete network topology is marginal.

### 3.8.2 Nash Equilibrium Power Control (NEPC) Strategies

In contrast to SNOPC, it is not clear whether more information results in a higher throughput for NEPC. In this subsection, we evaluate the spatial throughput for different NEPC strategies.

Bipolar Networks When the link distance is the same and constant throughout the network, the NEPC strategy for case 2 is the one described in Corollary 6, and the expected throughput at each link is

$$p_s(r) = \gamma^{-1} \exp\left(-\lambda\gamma^{-1}\frac{\pi^2\delta}{\sin\pi\delta}\theta^\delta r^2\right),$$

where $\gamma = \max\{1, \min\{P_{\max}, \lambda\pi r^2 \frac{\pi\delta^2}{\sin\pi\delta}\theta^\delta\}\}$.

Evaluating the performance of NEPC for complete network topology information (case 3) involves solving (3.9). Once $(\gamma_l)$ is (numerically) found, the throughput can be determined by making use of the Laplace transform in (3.8).

Fig. 3.4 compares the spatial throughput of NEPC strategies in the bipolar network and the throughput of SNOPC. The case where all nodes in the network transmit with power $P_{\max}$ and probability $P_{\max}^{-1}$ is also plotted for reference. We see for case 2 when the link distance is larger than 0.5, the NEPC strategy enters its ALOHA-peak-power-limited regime.

A key observation of Fig. 3.4 is that by allowing all the transmitters in the network selfishly to use power control, the spatial throughput of the network can be improved (although not necessarily maximized) in comparison with the case where all the transmitters transmit with unit power. In particular, the comparison between the performance of SNOPC and NEPC strategy in case 2 shows that the throughput gain of a smart user is larger when all the other users are also smart. This result is somewhat surprising, since it is natural to conjecture that a smart user should

be able to take more advantage of others if they are all dumb. The root of this counter-intuitive phenomenon lies in the special form of the Nash-equilibrium, *i.e.,* each node transmits with (the same) power $\gamma \geq 1$ and probability $\gamma^{-1}$. At this equilibrium, the interference $I_\gamma$ observed at any receiver has the Laplace transform $\mathcal{L}_{I_\gamma}(s) = \exp(-\lambda\pi\gamma^{\delta-1}\frac{\pi\delta}{\sin(\pi\delta)}s^\delta)$, which is larger than the Laplace transform of the interference without power control $\mathcal{L}_I(s) = \exp(-\lambda\pi\frac{\pi\delta}{\sin(\pi\delta)}s^\delta)$ for all $s > 0$. Due to the relation between success probability and Laplace transform, this implies that any power control strategy achieves a higher expected throughput when the network operates at a certain the Nash equilibrium than when all other nodes transmit with constant power. Moreover, the NEPC strategy, by definition, maximizes the (individual) throughput at the Nash equilibrium, and thus the spatial throughput of NEPC is always higher than what SNOPC can achieve if the rest of the network does not use power control.

The fact that $\mathcal{L}_{I_\gamma}(s) > \mathcal{L}_I(s),\ \forall s > 0$ in case 2 suggests that by selfishly choosing its power control strategy, each node is essentially *reducing* its interference to other nodes. Therefore, the spatial throughput of NEPC is always larger than without power control (this is also confirmed in Fig. 3.4).

However, as is shown in Section 3.6.2, NEPC does *not* maximize the spatial throughput, which interestingly is also due to the special form of the NEPC strategy, which always ensures that $\mathbb{E}[P] = 1$. In contrast, if we replace the mean power constraint $\mathbb{E}[P] \leq 1$ with the constraint $\mathbb{E}[P^\delta] \leq 1$, it can be shown that the resulting NEPC policy coincides with GOPT ALOHA, *i.e.,* the spatial throughput is maximized at the Nash equilibrium. This can be interpreted as follows: A (smart) selfish power control strategy always has $\mathbb{E}[P^\delta] = 1$, since otherwise it is easy to construct another random variable (as a function of $P$) which statistically dominates $P$ but still satisfies both power constraints. This, by Lemma 8, ensures that the power control strategy does not affect the interference distribution. Then, by adjusting the power

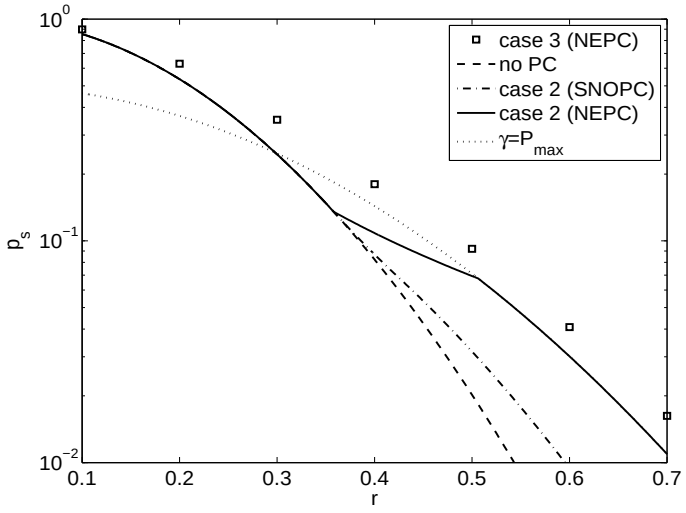


Figure 3.4. Comparison of throughput in bipolar network using constant power transmission, NEPC strategies in case 2 and case 3, the case where all nodes transmit with power $P_{\max}$ and probability $P_{\max}^{-1}$ ($\gamma = P_{\max}$), and SNOPC strategy in case 2. Here, $\lambda = 1$, $P_{\max} = 2$, $\alpha = 4$, $\theta = 10$.

control strategy, each node only maximizes its own throughput without inflicting more or less interference on others.

The comparison between the two NEPC strategies in Fig. 3.4 also indicates that the more information is available at each transmitter, the higher the throughput. This phenomenon is also observed in the scenario of variable link distances which is discussed in the next subsection.

Networks with Variable Link Distances  Here, we focus on the case where the link distance $R$ is Rayleigh distributed with mean $1/2\sqrt{\lambda_r}$. As discussed earlier, in case 1, the NEPC strategy is constant power transmission, and the resulting throughput is

$$\mathbb{E}_R\left[p_s(R)\right] = \frac{\lambda_r}{\lambda_r + \lambda \frac{\pi\delta}{\sin(\pi\delta)}\theta^{\delta}}.$$

For case 2, the NEPC strategy hinges on solving for $\mathbb{E}[P^{\delta}]$ in (3.4). A closed-form

solution is not available in this case, but a numerical solution is easy to obtain. Given $\mathbb{E}[P^\delta]$, the spatial throughput can be calculated by averaging over the distribution of $R$, which yields

$$\mathbb{E}_R[p_s(R)] = \frac{\lambda_r}{\lambda_r + a\theta^\delta}\left(1 - e^{-(\lambda_r\pi + a\pi\theta^\delta)R_1^2}\right) + \frac{\lambda_r/P_{\max}}{\lambda_r + \frac{a\theta^\delta}{P_{\max}^\delta}}\left(1 - e^{-(\lambda_r\pi + \frac{a\pi\theta^\delta}{P_{\max}^\delta})R_m^2}\right) + (\lambda_r a\pi^2\delta e)^{-1/\delta}\left(\Gamma(1+1/\delta, \lambda_r\pi R_1^2) - \Gamma(1+1/\delta, \lambda_r\pi R_m^2)\right),$$

where $a = \frac{\lambda\pi\delta}{\sin\pi\delta}\mathbb{E}[P^\delta]$, $R_1 = \theta^{-\delta/2}(a\pi\delta)^{-1/2}$, $R_m = (\theta/P_{\max})^{-\delta/2}(a\pi\delta)^{-1/2}$ and $\Gamma(\cdot,\cdot)$ is the upper incomplete Gamma function.

Fig. 3.5 compares the Nash equilibrium power control strategies in three cases, where the throughput of case 3 is calculated by simulation, averaged over 10,000 network topologies (realizations of the PPP). Again, we see that the more information available at each node, the higher the spatial throughput will be, even if each node acts selfishly.

Although this chapter focuses on Rayleigh distributed links, the results are applicable to general link distributions. More specifically, for case 3, the link distance distribution does not matter since the complete network topology is assumed to be available at the transmitters. For cases 1 and 2, as long as the link distance is iid, the transmit power at each individual transmitter is iid. Therefore, the link distance distribution enters the interference distribution only by the $\delta$-th moment of the transmit power. In case 2, this means the interference distribution property required by Lemma 9 always holds, and thus results for Rayleigh-distributed link distance hold for arbitrary link distance distribution. In case 1, this means all the proofs in Section 3.5 can stay the same as long as the concavity of $\mathbb{E}_R[\mathcal{L}_I(s)|_{s=\frac{\theta R^\alpha}{P}}]$ (w.r.t. $P$) holds.

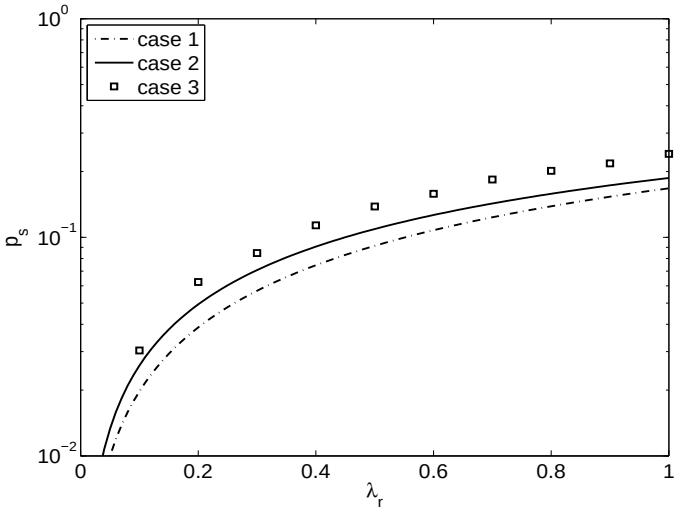


Figure 3.5. Comparison of the spatial throughput under NEPC when link distance are Rayleigh distributed with mean $1/2\sqrt{\lambda_r}$ in three cases. Here, $\lambda = \lambda_r = 1$, $P_{\max} = 2$, $\alpha = 4$, $\theta = 10$. The throughput in case 3 is averaged over 10,000 PPP realizations.

## 3.9 Conclusions

This chapter considers the single-node optimal power control (SNOPC) strategies and the Nash equilibrium power control (NEPC) strategies in wireless networks whose node distribution is governed by a Poisson point process (PPP). The SNOPC strategies maximize one link's expected throughput given that the rest of the network uses constant power transmission. When all the nodes in the network can use power control, the NEPC strategies are the stable strategies in the sense that no individual link would deviate from these strategies as that cannot increase the expected throughput at this link.

With the basic assumption that the channel fading state is unobservable at each node, we analytically characterize SNOPC and NEPC strategies in three cases of different levels of knowledge at each node. We show that in all cases the optimal and Nash equilibrium power control strategies are ALOHA-type random on-off strategies

whose transmit power level and transmit probability are functions of the knowledge at each transmitter. While ALOHA is generally considered to be inefficient as a MAC scheme, our results show that, as a power control scheme, it constitutes a natural Nash equilibrium in interference-limited Poisson networks[3].

In bipolar networks (fixed link distance), the performance comparison between the NEPC strategy and the globally optimal (GOPT) power control strategy reveals the inefficiency of the NEPC strategy. However, it is also shown that in such a scenario the NEPC strategy achieves a spatial throughput larger than without power control. Since nodes in a real network are likely to cooperate to some degree, the performance of the NEPC strategy provides a worst case scenario for wireless networks with random power control capability. In this sense, this chapter demonstrates the potential benefits of random power control in wireless networks.

Numerical results suggest, just like SNOPC, under NEPC, the more information is available, the higher the spatial throughput. In other words, spreading network topology information over all nodes can increase the spatial throughput even if all the nodes are selfish. Thus, there exists a trade-off between the gain in spatial throughput and the overhead of acquiring topology information, which can be quantified by the tools provided in this chapter.

[3]Nevertheless, there is a subtle but important distinction between the random on-off power control strategy and the conventional ALOHA MAC scheme: the optimal random on-off strategy allows each transmitter to use a different transmit power and probability while the conventional ALOHA often assumes that all the users have the same access probability.

# CHAPTER 4

# THE PERFORMANCE OF SUCCESSIVE INTERFERENCE CANCELLATION

## 4.1 Successive Interference Cancellation and Related Work

Chapter 3 assumed each receiver has only one dedicated transmitter and used the signal-to-interference-ratio (SIR) to this transmitter as the indicator for the channel quality. Such modeling is often referred to treating interference as background noise. It is the most classic approach to model the relation among concurrent transmissions in wireless networks and complies with the contemporary implementation of wireless systems.

However, as contemporary wireless systems are becoming increasingly interference-limited, there is an ascending interest in using advanced interference mitigation techniques to improve the network performance in addition to this conventional approach of treating interference as background noise [12, 14, 15, 20, 46, 47, 58, 71]. One important approach is successive interference cancellation (SIC). First introduced in [21], the idea of SIC is to decode different users sequentially, *i.e.,* the interference due to the decoded users is subtracted before decoding other users. Although SIC is not always the optimal multiple access scheme in wireless networks [12, 14], it is especially amenable to implementation [4, 68] and does attain boundaries of the capacity regions in multiuser systems in many cases[12, 22, 60].

Conventional performance analyses of SIC do not take into account the spatial distribution of the users. The transmitters are either assumed to reside at given locations with deterministic path loss, see, *e.g.,* [72] and references therein, or assumed

subject to centralized power control which to a large extent compensates for the channel randomness [5, 70]. To establish advanced models that take into account the spatial distribution of the users, recent papers attempt to analyze the performance of SIC using tools from stochastic geometry [39, 42]. In this context, a *guard-zone* based approximation is often used to model the effect of interference cancellation due to the well-acknowledged difficulty in tackling the problem directly [71]. Despite many interesting results obtained by this approximation, it does not provide enough insights on the effect of received power ordering from different transmitters, which is essential for successive decoding[70]. Therefore, this approach provides a good approximation only for one or at most two interferers. Furthermore, most of the work in this line of research considers Rayleigh fading and/or uniformly distributed networks. In contrast, this chapter uses an exact approach to tackle the problem directly for a more general type (non-uniform) of networks with arbitrary fading distribution.

Besides SIC, there are many other techniques that can potentially significantly mitigate the interference in wireless networks including interference alignment [15] and dirty paper coding [20]. Despite the huge promise in terms of performance gain, these techniques typically rely heavily on accurate channel state information at the transmitters (CSIT) and thus are less likely to impact practical wireless systems in the near future [46, 58]. Also, many recent works study interference cancellation based on MIMO techniques in the context of random wireless networks, *e.g.,* [46, 69] and references therein. These interference cancellation techniques should not be considered as successive interference cancellation (SIC), although they can be combined with SIC to achieve (even) better performance[67].

## 4.2 Contributions and Organization

This chapter considers SIC as a pure receiver end technique[1], which does not require any modifications to the conventional transmitter architecture. We focus on a $d$-dimensional Poisson network where all the nodes are transmitting at the same rate. The main contributions of this chapter can be summarized as follows:

- We show that fading does not affect the performance of successively decoding in a large class of interference-limited networks, including uniform networks as a special case. However, in noisy networks, fading always reduces the decoding probability.
- We provide a set of closed-form upper and lower bounds on the probability of successively decoding at least $k$ users. These bounds are based on different ideas and are reasonably tight in different regimes.
- In interference-limited networks, when the per-user information rate goes to 0, we show that the aggregate throughput at the receiver is upper bounded by $\frac{1}{\beta} - 1$, where $\beta$ is a simple function of the path loss exponent and network density. A Laplace transform-based approximation is also found for the aggregate throughput at the receiver for general per user information rate.
- We observe that in interference-limited network the aggregate throughput at a typical receiver is a monotonically decreasing function of the per user information rate, while in noisy networks, there exists an optimal positive per-user rate that maximizes the aggregate throughput.

The rest of the chapter is organized as follows: Section 4.3 describes the system models and the metrics we are using in this chapter. Section 4.4 introduces the path loss process with fading (PLPF)-based framework which facilitates the analysis in the rest of the chapter. In Section 4.5, we provide a set of bounds on the probability of decoding at least $k$ users in system. These bounds directly lead to bounds on the expected gain of SIC presented in Section 4.6. We discuss the effect of noise in Section 4.7. The chapter is concluded in Section 4.8.

[1]In general, SIC can be combined with (centralized) power control, which can significantly boost its usefulness. However, this places extra overhead in transmitter coordination and is beyond the discussion of this thesis.

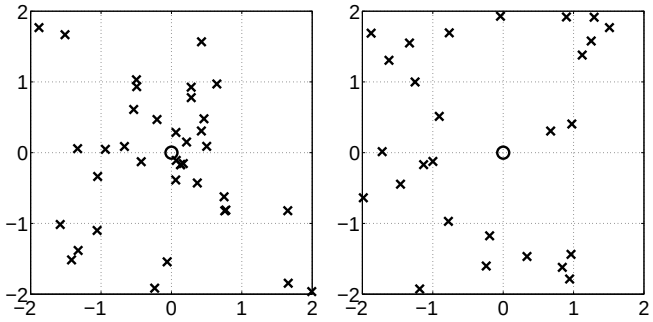

(a) $b = -1$ (b) $b = 1$

Figure 4.1. Realizations of two non-uniform PPP with intensity function $\lambda(x) = 3\|x\|^b$ with different $b$, where x denotes an active transmitter and o denotes the receiver at the origin.

## 4.3 System Model and Metrics

### 4.3.1 The Power-law Poisson Network with Fading (PPNF)

Let the receiver be at the origin $o$ and the active transmitters be represented by a marked Poisson point process (PPP) $\hat{\Phi} = \{(x_i, h_{x_i})\} \subset \mathbb{R}^d \times \mathbb{R}^+$, where $x$ is the location of a user, $h_x$ is the iid (power) fading coefficient associated with the link from $x$ to $o$, and $d$ is the number of dimensions of the space. When the density function of the ground process $\Phi \subset \mathbb{R}^d$ is $\lambda(x) = a\|x\|^b,\ a > 0,\ b \in (-d, \alpha - d)$, where $\|x\|$ is the distance from $x \in \mathbb{R}^d$ to the origin and $\alpha$ is the path-loss exponent, we refer this network as a *power-law Poisson network with fading (PPNF)*. The condition $b \in (-d, \alpha - d)$ is needed in order to maintain a finite total received power at $o$ and will be revisited later.

Fig. 4.1 shows realizations of two 2-d PPNFs with different $b$; Fig. 4.1-(a) represents a network clustered around $o$ whereas the network in Fig. 4.1-(b) is sparse around the receiver at $o$. In general, the smaller $b$, the more clustered the network is at the origin, and $b = 0$ refers to uniform networks.

### 4.3.2 SIC Model and Metrics

Consider the case where all the nodes (users) transmit with unit power. Then, with an SIR model, a particular user at $x \in \Phi$ can be successfully decoded (without SIC) iff

$$\mathrm{SIR}_x = \frac{h_x \|x\|^{-\alpha}}{\sum_{y \in \Phi \setminus \{x\}} h_y \|y\|^{-\alpha}} > \theta,$$

where $h_x\|x\|^{-\alpha}$ is the received signal power from $x$, $\sum_{y\in\Phi\setminus\{x\}} h_y\|y\|^{-\alpha}$ is the aggregate interference from the other active transmitters, and $\theta$ is the SIR decoding threshold[2].

Similarly, in the case of perfect interference cancellation, once a user is successfully decoded, its signal component can be completely subtracted from the received signal. Assuming the decoding order is always from the stronger users to the weaker users[3], we can generalize the SIR model above to the case with SIC, where a user $x$ can be decoded if all the users in $\mathcal{I}_c = \{y \in \Phi : h_y\|y\|^{-\alpha} > h_x\|x\|^{-\alpha}\}$ are successfully decoded and

$$\frac{h_x \|x\|^{-\alpha}}{\sum_{y \in \Phi \setminus \{x\} \setminus \mathcal{I}_c} h_y \|y\|^{-\alpha}} > \theta.$$

Consequently, consider the ordering of all nodes in $\Phi$ such that $h_{x_i}\|x_i\|^{-\alpha} > h_{x_j}\|x_j\|^{-\alpha},\ \forall i < j$. The number of users that can be successively decoded is $N$ iff $h_{x_i}\|x_i\|^{-\alpha} > \theta \sum_{j=i+1}^{\infty} h_{x_j}\|x_j\|^{-\alpha},\ \forall j \le N$ and $h_{x_{N+1}}\|x_{N+1}\|^{-\alpha} \le \theta \sum_{j=N+2}^{\infty} h_{x_j}\|x_j\|^{-\alpha}$. One of the goals of this chapter is to evaluate $\mathbb{E}[N]$, *i.e.,* the mean number of users that can be successively decoded, with respect to different system parameters, and the distribution of $N$ in the form

$$p_k \triangleq \mathbb{P}(N \ge k),$$

[2]This model will be generalized in Section 4.7 to include noise.

[3]It is straightforward to show that this stronger-to-weaker decoding order maximizes the number of decodable users and thus the aggregate throughput (defined later) despite the fact that it is not necessarily the *only* optimal decoding order.

*i.e.,* the probability of successively decoding at least $k$ users at the origin. To make the dependence on the point process explicit, we sometimes use $p_k(\hat{\Phi})$.

Since SIC is inherently a multiple packet reception (MPR) scheme [72], we can further define the aggregate throughput (or, sum rate) to be the total information rate received at the receiver $o$. Since all the users in the system transmit at the same rate $\log(1+\theta)$, the sum rate is

$$R = \mathbb{E}[\log(1+\theta)N] = \log(1+\theta)\mathbb{E}[N]. \tag{4.1}$$

Another important goal of this chapter is to evaluate $R$ as a function of different system parameters.

## 4.4 The Path Loss Process with Fading (PLPF)

We use the unified framework introduced in [35] to jointly address the randomness from fading and the random node locations. We define the path loss process with fading (PLPF) as $\Xi \triangleq \{\xi_i = \frac{\|x_i\|^\alpha}{h_{x_i}}\}$, where the index $i$ is introduced in the way such that $\xi_i < \xi_j$ for all $i < j$. Then, we have the following lemma, which follows from the mapping theorem [39, Theorem 2.34].

**Lemma 11.** *The PLPF* $\Xi = \{\frac{\|x_i\|^\alpha}{h_{x_i}}\}$, *where* $\{(x_i, h_{x_i})\}$ *is a PPNF, is a one-dimensional PPP on* $\mathbb{R}^+$ *with intensity measure* $\Lambda([0,r]) = a\delta c_d r^\beta \mathbb{E}[h^\beta]/\beta$, *where* $\delta \triangleq d/\alpha$, $\beta \triangleq \delta + b/\alpha \in (0,1)$ *and* $h$ *is a fading coefficient.*

In Lemma 11, the condition $\beta \in (0,1)$ corresponds to the condition $b \in (-d, \alpha - d)$ in the definition of the PPNF; it is necessary since otherwise the aggregate received power at $o$ is infinite almost surely. More specifically, when $b > \alpha - d$ the intensity measure of the transmitter process grows faster than the path loss with respect to the network size, which results in infinite received power at origin, (*i.e.,* far users contribute infinite power); when $b < -d$, the PLPF is not locally finite (with singularity

at $o$), and thus the number of transmitters that contribute to the received power *more* than any arbitrary value is infinite almost surely, (*i.e.,* near users contribute infinite power).

Since for all $\xi_i \in \Xi \subset \mathbb{R}^+$, $\xi_i^{-1}$ can be considered as the $i$th strongest received power component (at $o$) from the users in $\Phi$, when studying the effect of SIC, it suffices to just consider the PLPF $\Xi$. For a PLPF $\Xi$ mapped from $\hat{\Phi}$, if we let $p_k(\Xi)$ be the probability of successively decoding at least $k$ users in the network $\hat{\Phi}$, we have the following proposition.

**Proposition 8** (Scale-invariance)**.** *If $\Xi$ and $\bar{\Xi}$ are two PLPFs with intensity measures $\Lambda([0,r]) = r^\beta$ and $\mu([0,r]) = Cr^\beta$, respectively, where $C$ is any positive constant, then $p_k(\Xi) = p_k(\bar{\Xi}),\ \forall k \in \mathbb{N}$.*

*Proof.* Consider the mapping $f(x) = C^{-1/\beta}x$. Then $f(\Xi)$ is a PPP on $\mathbb{R}^+$ with intensity measure $Cx^\beta$ of the set $[0,x]$. Let $\mathcal{N}$ be the sample space of $\Xi$, *i.e.,* the family of all countable subsets of $\mathbb{R}^+$. Then, we can define a sequence of indicator functions $\chi_k : \mathcal{N} \to \{0,1\},\ k \in \mathbb{N}$, such that

$$\chi_k(\phi) = \begin{cases} 1, & \text{if } \xi_i^{-1} > \theta I_i,\ \forall i \leq k \\ 0, & \text{otherwise,} \end{cases} \tag{4.2}$$

where $I_i = \sum_{j=i+1}^{\infty} \xi_j^{-1}$, $\phi = \{\xi_i\}$ and $\xi_i < \xi_j,\ \forall i < j$. Note that $\chi_k(\cdot)$ is scale-invariant, *i.e.,* $\chi_k(\{\xi_i\}) = \chi_k(\{C'\xi_i\}),\ \forall C' > 0$. Then, we have

$$p_k(\Xi) = \mathsf{P}_\Xi(Y_k) = \mathbb{E}[\chi_k(\Xi)] \overset{\text{(a)}}{=} \mathbb{E}[\chi_k(f(\Xi))] \overset{\text{(b)}}{=} \mathbb{E}[\chi_k(\bar{\Xi})] = \mathsf{P}_{\bar{\Xi}}(Y_k) = p_k(\bar{\Xi}),$$

where $Y_k = \{\phi \in \mathcal{N} : \xi_i^{-1} > \theta I_i,\ \forall i \leq k\}$, $\mathsf{P}_\Xi$ is the probability measure on $\mathcal{N}$ with respect to the distribution of $\Xi$, (a) is due to the scale-invariance property of $\chi_k(\cdot)$ and (b) is because both $f(\Xi)$ and $\bar{\Xi}$ are PPPs on $\mathbb{R}^+$ with intensity measure $\mu([0,r]) = Cr^\beta$.

Proposition 8 shows that the absolute value of the density is not relevant as long as we restrict our analysis to the power-law density case. Combining it with Lemma 11, where it is shown that, in terms of the PLPF, the only difference introduced by different fading distributions is a constant factor in the density function, we immediately obtain the following corollary.

**Corollary 7** (Fading-invariance)**.** *In an interference-limited PPNF, the probability of successively decoding $k$ users (at the origin) does not depend on the fading distribution as long as $\mathbb{E}[h^\beta] < \infty$.*

Futhermore, we can define a standard PLPF as follows:

**Definition 10.** *A* standard PLPF (SPLPF) $\Xi_\beta$ *is a one-dimensional PPP on $\mathbb{R}^+$ with intensity measure $\Lambda([0, r]) = r^\beta$, where $\beta \in (0, 1)$.*

Based on Proposition 8 and Corollary 7, we have the following fact which significantly simplifies the analysis in the rest of the chapter.

**Fact 1.** *The statistics of $N$ in a PPNF is identical to those of $N$ in $\Xi_\beta$ for any fading distribution and any values of $a$, $b$, $d$, $\alpha$, with $\beta = \delta + b/\alpha = (d + b)/\alpha$.*

## 4.5 Bounds on the Probability of Successive Decoding

Despite the unified framework introduced in Section 4.4, analytically evaluating $p_k$ requires the joint distribution of the received powers from the $k$ strongest users and the aggregate interference from the rest of the network, which is daunting even for the simplest case (one-dimensional homogeneous PPP). In this section, we derive bounds on $p_k$. These bounds provide us with insights on how $p_k$ depends on different system parameters.

### 4.5.1 Basic Bounds

The following lemma introduces basic upper and lower bounds on $p_k$ in terms of the probability of decoding the $k$th strongest user assuming the $k-1$ strongest users do not exist. Although not being bounds in closed-form, the bounds form the basis for the bounds introduced later.

**Lemma 12.** *In a PPNF, the probability of successively decoding $k$ users is bounded as follows:*

- $p_k \geq (1+\theta)^{-\frac{\beta k(k-1)}{2}} \mathbb{P}(\xi_k^{-1} > \theta I_k)$
- $p_k \leq \theta^{-\frac{\beta k(k-1)}{2}} \mathbb{P}(\xi_k^{-1} > \theta I_k)$

*where $\Xi_\beta = \{\xi_i\}$ is the corresponding SPLPF and $I_k \triangleq \sum_{j=k+1}^{\infty} \xi_j^{-1}$.*

*Proof.* By Fact 1, $p_k$ can be evaluated by considering $\Xi_\beta$. In particular, if we define $A_i = \{\xi_i^{-1} > \theta I_i\}$, the probability of successively decoding at least $k$ users can be written as $p_k = \mathbb{P}(\bigcap_{i=1}^{k} A_i)$.

Let $B_i = \{\xi_i^{-1} > (1+\theta)\xi_{i+1}^{-1}\}$ and consider an arbitrary sample (realization) $\omega \in \bigcap_{i=1}^{k-1} B_i \cap A_k$. Assuming (again) the increasing ordering of all $\xi_i(\omega) \in \Xi(\omega),\ \forall i \in \mathbb{N}$, we have

$$\xi_i^{-1}(\omega) \overset{\text{(a)}}{>} \xi_{i+1}^{-1}(\omega) + \theta\xi_{i+1}^{-1}(\omega) \overset{\text{(b)}}{>} \theta I_{i+1}(\omega) + \theta\xi_{i+1}^{-1}(\omega) = \theta I_i(\omega),\ \forall i \in [k-1]$$

where (a) is due to $\omega \in B_i$, and (b) is due to $\omega \in B_{i+1}$ (if $i < k$) and $\omega \in A_k$ (if $i = k$). Therefore, $\omega \in \bigcap_{i=1}^{k} A_i$. Since $\omega$ is arbitrarily chosen, we have $\left(\bigcap_{i=1}^{k-1} B_i \cap A_k\right) \subset \bigcap_{i=1}^{k} A_i$, and thus

$$\begin{aligned} p_k &\geq \mathbb{P}\left(\bigcap_{i=1}^{k-1} B_i \cap A_k\right) = \mathbb{E}_{\xi_k}\left[\mathbb{P}\left(\bigcap_{i=1}^{k-1} B_i \cap A_k \mid \xi_k\right)\right] \\ &= \mathbb{E}_{\xi_k}\left[\mathbb{P}\left(\bigcap_{i=1}^{k-1} B_i\right)\mathbb{P}\left(A_k\right) \mid \xi_k\right], \end{aligned} \tag{4.3}$$

where the last equality is because of the conditional independence between $B_i,\ \forall i \in [k-1]$ and $A_k$ given $\xi_k$. Here, by definition, $\mathbb{P}\left(\bigcap_{i=1}^{k-1} B_i\right) = \mathbb{P}\left(\frac{\xi_i}{\xi_{i+1}} < (1+\theta)^{-1}, \forall i < k\right)$.

Conditioned on $\xi_k,\ k \geq 2$, we have $\frac{\xi_i}{\xi_k} \stackrel{\mathrm{d}}{=} X_{i:k-1},\ \forall 1 \leq i \leq k-1$, where $\stackrel{\mathrm{d}}{=}$ means equality in distribution, $X$ is a random variable with cdf $F(x) = x^\beta \mathbf{1}_{[0,1]}(x)$, and $X_{i:k-1}$ is the $i$th order statistics of $k-1$ iid random variables with the distribution of $X$, *i.e.,* the $i$th smallest one among $k-1$ iid random variables with the distribution of $X$.

Since $X^\beta \sim \text{Uniform}(0,1)$, we can apply the results from the order statistics of uniform random variables [7]. In particular, if $U \sim \text{Uniform}(0,1)$, then $\left(\frac{U_{i:k-1}}{U_{i+1:k-1}}\right)^i \sim \text{Uniform}(0,1)$ and $\left(\frac{U_{i:k-1}}{U_{i+1:k-1}}\right)^i$ is iid for all $1 \leq i \leq k-2$. Therefore,

$$\mathbb{P}\left(\frac{\xi_i}{\xi_{i+1}} < (1+\theta)^{-1}, \forall i < k \mid \xi_k\right) = \prod_{i=1}^{k-1} \mathbb{P}(U < (1+\theta)^{-i\beta}) = (1+\theta)^{-\frac{\beta}{2}k(k-1)}, \tag{4.4}$$

where the last inequality is due to $\left(\frac{X_{i:k-1}}{X_{i+1:k-1}}\right)^{i\beta} \stackrel{\mathrm{d}}{=} U,\ \forall i \in [k-2]$. The lower bound is thus proved by combining (4.3) and (4.4).

Defining $\hat{B}_i = \{\xi_i^{-1} > \theta \xi_{i+1}^{-1}\}$ in the place of $B_i$, we can derive the upper bound in a very similar way.

### 4.5.2 The Lower Bounds

#### 4.5.2.1 High-rate lower bound

Lemma 12 provides bounds on $p_k$ as a function of $\mathbb{P}(\xi_k^{-1} > \theta I_k)$. In the following, we give the high-rate lower bounds[4] by lower bounding $\mathbb{P}(\xi_k^{-1} > \theta I_k)$.

---

[4]The high-rate lower bound also holds in the low-rate case, *i.e.,* $\theta$ is small. The bound is named as such since in the low-rate case we will provide another (tighter) bound.

**Lemma 13.** *The kth smallest element in $\Xi_\beta$, $\xi_k$, has pdf*

$$f_{\xi_k}(x) = \frac{\beta x^{k\beta-1}}{\Gamma(k)} \exp(-x^\beta).$$

The proof of Lemma 13 is analogous to the one of [34, Theorem 1].

**Lemma 14.** *For $\Xi_\beta = \{\xi_i\}$, $\mathbb{P}(\xi_k^{-1} > \theta I_k)$ is lower bounded by*

$$\Delta_1(k) \triangleq \frac{1}{\Gamma(k)} \left( \gamma\left(k, \frac{1-\beta}{\theta\beta}\right) - \frac{\theta\beta}{1-\beta} \gamma\left(k+1, \frac{1-\beta}{\theta\beta}\right) \right),$$

*where $\gamma(\cdot,\cdot)$ is the* lower *incomplete gamma function.*

*Proof.* In order to establish the lower bound, we first calculate the mean of the interference $I_k$ conditioned on $\xi_k = \rho$, and then derive the bound based on the Markov inequality. Denoting $I_k \mid \{\xi_k = \rho\}$ as $I_\rho$, we can calculate the conditional mean interference by Campbell's Theorem [39]

$$\mathbb{E}[I_\rho] = \mathbb{E}\left[ \sum_{x \in \Xi \cap [\rho,\infty)} x^{-1} \right] = \int_\rho^\infty x^{-1} \Lambda(\mathrm{d}x) = \frac{a\beta}{1-\beta} \rho^{\beta-1}.$$

Thus, by the Markov inequality,

$$\mathbb{P}(\xi_k^{-1} > \theta I_k \mid \xi_k = \rho) = \mathbb{P}(\rho^{-1} > \theta I_\rho) \geq 1 - \theta\rho\mathbb{E}[I_\rho].$$

The lower bound can be refined as $[1 - \theta\rho\mathbb{E}[I_\rho]]^+$, where $[\cdot]^+ = \max\{0, \cdot\}$. Deconditioning over the distribution of $\xi_k$ (given by Lemma 13) yields the stated lower bound.

In principle, one could use methods similar to the one in the proof of Lemma 14 to find the higher-order moments of $I_\rho$ and thus obtain tighter bounds by applying inequalities involving these moments, *e.g.,* the Chebyshev inequality. However, these bounds cannot be expressed in closed-form, and the improvements are marginal.

Combining Lemmas 12 and 14, we immediately obtain the following proposition.

**Proposition 9** (High-rate lower bound)**.** *In the PPNF,* $p_k \geq (1+\theta)^{-\frac{\beta k(k-1)}{2}} \Delta_1(k)$.

Since $\Delta_1(k)$ is monotonically decreasing with $k$, the lower bound in Proposition 9 decays super-exponentially with $k^2$.

#### 4.5.2.2 Low-rate lower bound

The lower bound in Proposition 9 is tight for large $\theta$. However, it becomes loose when $\theta \to 0$. This is because Proposition 9 estimates $p_k$ by approximating the relation between $\xi_i$ and $I_i$ with the relation between $\xi_i$ and $\xi_{i+1}$. This approximation is accurate when $\xi_{i+1}^{-1} \approx \theta I_{i+1}$. But, when $\theta \to 0$, $\xi_{i+1}^{-1} \gg \theta I_{i+1}$ happens frequently, making the bound loose. The following proposition provides an alternative lower bound particularly tailored for the small $\theta$ regime.

**Proposition 10** (Low-rate lower bound)**.** *In the PPNF, for* $k < 1/\theta + 1$, $p_k$ *is lower bounded by*

$$\underline{p}_k^{\mathrm{LR}} \triangleq \frac{1}{\Gamma(k)} \left( \gamma\left(k, \frac{1-\beta}{\tilde{\theta}\beta}\right) - \frac{\tilde{\theta}\beta}{1-\beta} \gamma\left(k+1, \frac{1-\beta}{\tilde{\theta}\beta}\right) \right),$$

*where* LR *means* low-rate *and* $\tilde{\theta} \triangleq \frac{\theta}{1-(k-1)\theta}$.

*Proof.* Using Fact 1, we work with $\Xi_\beta = \{\xi_i\}$. For all $n \in [k-1],\ k < 1/\theta + 1$, we have

$$\begin{aligned}
&\mathbb{P}\left( \left\{ \xi_n^{-1} > \frac{\theta I_n}{1-(n-1)\theta} \right\} \cap \{\xi_i > \theta I_i,\ n < i \leq k\} \right) \\
&\overset{\text{(a)}}{\geq} \mathbb{P}\left( \left\{ \xi_{n+1}^{-1} > \frac{\theta I_n}{1-(n-1)\theta} \right\} \cap \{\xi_i > \theta I_i,\ n < i \leq k\} \right) \\
&\overset{\text{(b)}}{=} \mathbb{P}\left( \left\{ \xi_{n+1}^{-1} > \frac{\theta I_{n+1}}{1-n\theta} \right\} \cap \{\xi_i > \theta I_i,\ n < i \leq k\} \right) \\
&\overset{\text{(c)}}{=} \mathbb{P}\left( \left\{ \xi_{n+1}^{-1} > \frac{\theta I_{n+1}}{1-n\theta} \right\} \cap \{\xi_i > \theta I_i,\ n+1 < i \leq k\} \right),
\end{aligned}$$

where (a) is because of the ordering of $\Xi$, (b) is due to $I_n = \xi_{n+1}^{-1} + I_{n+1}$, and (c) is due to the fact that $\left\{\xi_{n+1}^{-1} > \frac{\theta I_{n+1}}{1-n\theta}\right\} \subset \left\{\xi_{n+1}^{-1} > \theta I_{n+1}\right\}$. Using the inequality above sequentially for $n = 1, 2, \cdots, k-1$ yields

$$p_k \geq \mathbb{P}\left(\xi_k^{-1} > \frac{\theta I_k}{1-(k-1)\theta}\right),$$

where a lower bound for the RHS is given by Lemma 14 (substituting $\theta$ with $\tilde{\theta}$).

The bound in Proposition 10 is only constructed for $k < 1/\theta + 1$. However, as will be shown in Section 4.6, when $\theta \to 0$, this bound behaves much better than the one in Proposition 9.

### 4.5.3 The Upper Bound

Similar to the high-rate lower bound, we derive an upper bound by upper bounding $\mathbb{P}(\xi_k^{-1} > \theta I_k)$.

**Lemma 15.** *For $\Xi_\beta = \{\xi_i\}$, $\mathbb{P}(\xi_k^{-1} > \theta I_k)$ is upper bounded by*

$$\Delta_2(k) \triangleq \bar{\gamma}(k, 1/c) + \frac{e}{(1+c)^k}\bar{\Gamma}(k, 1+1/c),$$

*where $c = \theta^\beta \gamma(1-\beta, \theta) - 1 + e^{-\theta}$, $\bar{\gamma}(z,x) = \frac{\gamma(z,x)}{\Gamma(z)}$ and $\bar{\Gamma}(z,x) = \frac{\Gamma(z,x)}{\Gamma(z)}$ are the* normalized lower *and* upper *incomplete gamma function, and $\Gamma(\cdot,\cdot)$ is the* upper *incomplete gamma function.*

*Proof.* For a non-fading 1-d network, the Laplace transform of the aggregate interference from $[\rho, \infty)$ can be calculated by the probability generating functional (PGFL) of the PPP [41]. Similarly, the Laplace transform of $I_\rho \triangleq I_k \mid \{\xi_k = \rho\}$ is

$$\begin{aligned}\mathcal{L}_{I_\rho}(s) &= \exp\left(-\int_\rho^\infty (1-e^{-sr^{-1}})\Lambda(\mathrm{d}r)\right) \\ &= \exp\left(-\Big(s^\beta \int_0^{s\rho^{-1}} r^{-\beta} e^r \mathrm{d}r - \rho^\beta(1-e^{-s\rho^{-1}})\Big)\right),\end{aligned} \tag{4.5}$$

where $\Lambda(\cdot)$ is the intensity measure of the SPLPF $\Xi_\beta$ (see Definition 10).

Let $H$ be an exponential random variable with unit mean and independent of PLPF $\Xi$. We can relate $\mathbb{P}(\xi_k^{-1} > \theta I_k)$ with $\mathcal{L}_{I_k}(s)$ as

$$\begin{aligned}
\mathbb{P}(\xi_k^{-1} > \theta I_k) &= e\mathbb{P}(H > 1)\mathbb{P}(\xi_k^{-1} > \theta I_k) \\
&\overset{\text{(a)}}{=} e\mathbb{P}(\xi_k^{-1} > \theta I_k, H > 1) \\
&\leq e\mathbb{P}(H\xi_k^{-1} > \theta I_k) \\
&\overset{\text{(b)}}{=} e\mathbb{E}_{\xi_k}[\mathcal{L}_{I_k|\xi_k}(s)|_{s=\theta\xi_k}] \\
&\overset{\text{(c)}}{=} \mathbb{E}_{\xi_k}\left[\exp\left(-[c\xi_k^\beta - 1]^+\right)\right],
\end{aligned}$$

where (a) is due to the independence between $H$ and $\Xi$, (b) is due to the well-known relation between the Laplace transform of the interference and the success probability over a link subject to Rayleigh fading [41], (c) makes use of the PGFL in (4.5), taking into account the fact that $\mathbb{P}(\xi_k^{-1} > \theta I_k) \leq 1$. With the distribution of $\xi_k$ given by Lemma 13, the proposition is then proved by straightforward but tedious manipulation. Combining Lemmas 15 and 12 yields the following proposition.

**Proposition 11** (Combined upper bound)**.** *In the PPNF, we have* $p_k \leq \overline{p}_k \triangleq \bar{\theta}^{-\frac{\beta}{2}k(k-1)}\Delta_2(k)$*, where* $\bar{\theta} = \max\{\theta, 1\}$.

For $\theta > 1$, similar to the high-rate lower bound in Proposition 9, the upper bound in Proposition 11 decays super-exponentially with $k^2$, *i.e.,* $-\log \overline{p}_k \propto k^2$, which suggests that, in this regime, the marginal gain of adding SIC capability (*i.e.,* the ability of successively cancelling more users) diminishes very fast.

### 4.5.4 The Sequential Multi-user Decoding (SMUD) Bounds

The bounds derived in Sections 4.5.2 and 4.5.3 applies to all $\theta > 0$. This subsection provides an alternative set of bounds constructed based on a different idea. These

bounds are typically much tighter than the previous bounds in the sequential multi-user decoding regime defined as follows.

**Definition 11.** *A receiver with SIC capability is in the sequential multi-user decoding (SMUD) regime if the decoding threshold* $\theta \geq 1$.

It can be observed that in the SMUD regime multiple packet reception (MPR) can be only carried out with the help of SIC, whereas outside this regime, *i.e.,* $\theta < 1$, MPR is possible without SIC, *i.e.,* by parallel decoding. The necessity of SIC for MPR in the SMUD regime can be easily deduced by the following lemma.

**Lemma 16.** *Consider an arbitrary* $k$*-element index set* $\mathcal{K} \subset \mathbb{N}$ *and an increasingly ordered PLPF* $\Xi = \{\xi_i\}$. $\xi_i^{-1} > \theta \sum_{j \notin \mathcal{K}} \xi_j^{-1}$ *always implies* $\xi_i^{-1} > \theta \sum_{j>k} \xi_j^{-1},\ \forall i \leq k$. *Moreover, if* $\theta \geq 1$ *and* $\xi_i^{-1} > \theta \sum_{j \notin \mathcal{K}} \xi_j^{-1}$, *then* $\mathcal{K} = [k]$.

*Proof.* The first part of the lemma is obviously true when $\mathcal{K} = [k]$. If not, for any $l \in \mathcal{K} \backslash [k]$, we have $\xi_i^{-1} > \xi_l,\ \forall i \in [k]$ by the ordering of $\Xi$. For the same reason, we have $\sum_{j \notin \mathcal{K}} \xi_j^{-1} > \sum_{j \notin [k]} \xi_j^{-1}$. As $\xi_l^{-1} > \theta \sum_{j \notin \mathcal{K}} \xi_j^{-1}$, we have $\xi_i^{-1} > \sum_{j \notin [k]} \xi_j^{-1},\ \forall i \in [k]$.

To show the second part, consider an arbitrary $l \in \mathcal{K}$. Since all elements in $\Xi$ are positive and $\theta \geq 1$, $\xi_l^{-1} > \theta \sum_{j \notin \mathcal{K}} \xi_j^{-1}$ implies $\xi_l < \xi_j,\ \forall j \notin \mathcal{K}$, and consequently $\mathcal{K} = [k]$.

Consider the case of $k = 1$. The second part of Lemma 16 shows that if $\theta \geq 1$, there is at most one user ($\xi_1$) that can be decoded without the help of SIC. In other words, MPR is not feasible through parallel decoding. This is exactly the reason why $\theta \geq 1$ is defined as sequential multi-user decoding (SMUD) regime.

Lemma 16 also helps us to show following theorem which gives a closed-form expression for $\mathbb{P}(\xi_k^{-1} > \theta I_k)$.

**Theorem 6.** *For* $\theta \geq 1$,

$$\mathbb{P}(\xi_k^{-1} > \theta I_k) = \frac{1}{\theta^{k\beta}\Gamma(1+k\beta)\big(\Gamma(1-\beta)\big)^k}, \tag{4.6}$$

*where $\Gamma(\cdot)$ is the gamma function. Moreover, the RHS of (4.6) is an upper bound on $\mathbb{P}(\xi_k^{-1} > \theta I_k)$ when $\theta < 1$.*

*Proof.* Consider a 1-d Poisson point process $\Phi \subset \mathbb{R}^+$ with intensity measure $\Lambda([0,r]) = r^\beta$. For each element $x \in \Phi$ we introduce a iid mark $h_x$ with exponential distribution with unit mean. In the following, we will refer this marked process as a path loss process with induced fading (PLPIF) $\hat{\Phi} \subset \mathbb{R}^+ \times \mathbb{R}^+$. Similar as before, based on $\hat{\Phi}$, we can construct a PLPF $\Xi(\hat{\Phi}) = \{\hat{\xi}_i\}$ by letting $\hat{\xi}_i = \frac{x_i}{h_{x_i}},\ \forall x \in \Phi$, where, without loss of generality, we assume the indices $i$ are introduced such that $\Xi(\hat{\Phi})$ is increasingly ordered.

By Corollary 7, we see that $p_k(\Xi(\hat{\Phi})) = p_k(\Xi_\beta)$. Using the same technique in the proof of Proposition 8, we can easily show that

$$\mathbb{P}(\xi_k > \theta I_k) = \mathbb{P}(\hat{\xi}_k > \theta \hat{I}_k),\ \forall k \in \mathbb{N}, \tag{4.7}$$

where $\hat{I}_k = \sum_{i=k+1}^{\infty} \hat{\xi}_i^{-1}$. Therefore, in the following, we focus on the PLPIF $\hat{\Phi}$.

First, considering a $k$-tuple of positive numbers $\mathbf{y} = (y_i)_{i=1}^k \in (\mathbb{R}^+)^k$, with a slight abuse of notation, we say $(y_i)_{i=1}^k \subset \Phi$ if and only if $y_i \in \Phi,\ \forall i \in [k]$. Conditioned on $\mathbf{y} \subset \Phi$, we denote the interference from the rest of the network $\sum_{x \in \Phi \setminus \mathbf{y}} h_x x^{-1}$ as $I^{!\mathbf{y}}$. Since $\{y_i,\ i \in [k]\}$ is a set of Lebesgue measure zero, by Slivnyak's theorem, we have $I^{!\mathbf{y}} \stackrel{\mathrm{d}}{=} I = \sum_{x \in \Phi} h_x x^{-1}$. Thus,

$$\begin{aligned}\mathcal{L}_I^{!\mathbf{y}}(s) &\triangleq \mathbb{E}[\exp(-sI^{!\mathbf{y}})] = \mathcal{L}_I(s) = \exp\left(-\mathbb{E}_h\left(\int_0^\infty \left(1 - \exp(-shr^{-1})dr^\beta\right)\right)\right) \\ &= \exp\left(-\frac{s^\beta}{\operatorname{sinc}\beta}\right),\end{aligned} \tag{4.8}$$

where the derivation exploits the fact that $h_x$ are iid exponential random variables with unit mean.

Second, let $\hat{\mathcal{N}}$ be the sample space of $\hat{\Phi}$ and consider the indicator function

$\bar{\chi}_k : (\mathbb{R}^+ \times \mathbb{R}^+)^k \times \hat{\mathcal{N}} \to \{0,1\}$ defined as follows

$$\bar{\chi}_k\big((x_i, h_{x_i})_{i=1}^k, \hat{\phi}\big) = \begin{cases} 1, & \text{if } h_{x_i} x_i^{-1} > \theta \sum_{y \in \phi \setminus \{x_j,\ j \in [k]\}} h_y y^{-1},\ \forall i \in [k] \\ 0, & \text{otherwise,} \end{cases}$$

where $\phi \subset \mathbb{R}^+$ is the ground pattern of the marked point pattern $\hat{\phi}$. In words, $\bar{\chi}_k\big((x_i, h_{x_i})_{i=1}^k, \hat{\phi}\big)$ is one iff $k$ of the users in the network $(x_i)_{i=1}^k$ all have received power larger than $\theta$ times the interference from the rest of the network. Then, for any $\hat{\phi}$ and $k \in \mathbb{N}$,

$$\mathsf{1}_{\{\hat{\xi}_k > \theta \hat{I}_k\}}(\hat{\phi}) = \mathsf{1}_{\{\hat{\xi}_i > \theta \hat{I}_k,\ \forall i \in [k]\}}(\hat{\phi}) \overset{\text{(a)}}{\leq} \frac{1}{k!} \sum_{x_1, \ldots, x_k \in \phi}^{\neq} \bar{\chi}_k\big((x_i, h_{x_i})_{i=1}^k, \hat{\phi}\big), \tag{4.9}$$

where $\neq$ means $x_i \neq x_j,\ \forall i \neq j$ and (a) is due to the first part of Lemma 16. Also, the second part of Lemma 16 shows that when $\theta \geq 1$ the equality in (a) holds.

Therefore, we have

$$\begin{aligned} \mathbb{P}(\hat{\xi_k}^{-1} > \theta \hat{I}_k) &= \mathbb{E}[\mathsf{1}_{\{\hat{\xi}_k > \theta \hat{I}_k\}}(\hat{\Phi})] \\ &\overset{\text{(b)}}{\leq} \frac{1}{k!} \mathbb{E}\left[ \sum_{x_1, \ldots, x_k \in \Phi}^{\neq} \bar{\chi}_k\big((x_i, h_{x_i})_{i=1}^k, \hat{\Phi}\big) \right] \\ &= \frac{1}{k!} \mathbb{E}_\Phi \left[ \sum_{x_1, \ldots, x_k \in \Phi}^{\neq} \mathbb{E}\left[ \bar{\chi}_k\big((x_i, h_{x_i})_{i=1}^k, \hat{\Phi}\big) \right] \right] \\ &\overset{\text{(c)}}{=} \frac{1}{k!} \mathbb{E}_\Phi \left[ \sum_{\mathbf{x}:\, x_1, \ldots, x_k \in \Phi}^{\neq} \mathcal{L}_I^{!\mathbf{x}}(\theta \sum_{i=1}^k x_i) \right] \\ &\overset{\text{(d)}}{=} \frac{1}{k!} \int_{(\mathbb{R}^+)^k} \mathcal{L}_I^{!\mathbf{x}}(\theta \sum_{i=1}^k x_i) \Lambda^{(k)}(\mathrm{d}\mathbf{x}), \end{aligned}$$

where (b) is due to (4.9) and the equality holds when $\theta \geq 1$, (c) holds since $h_y$ are iid exponentially distributed with unit mean for all $y \in \Phi$, and (d) is due to the definition of $\Lambda^{(k)}(\cdot)$, the $k$th factorial moment measure of $\Phi$ [39, Chapter 6]. Since

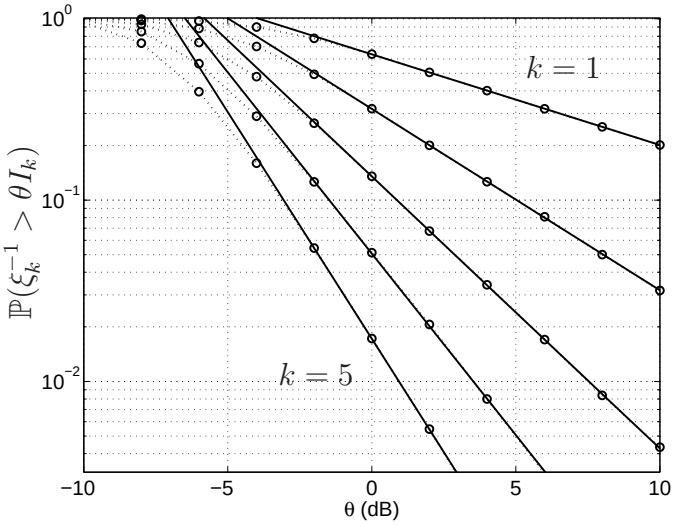


Figure 4.2. Comparison of $\mathbb{P}(\xi_k^{-1} > \theta I_k)$ between simulation and the analytical value according to Corollary 9 for $k = 1, 2, 3, 4, 5$.

$\Phi$ is a PPP with intensity function $\lambda([0, r]) = r^\beta$, we have $\Lambda^{(k)}(\mathrm{d}\mathbf{x}) = \prod_{i\in[k]} \mathrm{d}x_i^\beta$. Applying (4.7) and (4.8), we have

$$\mathbb{P}(\xi_k^{-1} > \theta I_k) \leq \frac{1}{k!} \int_{(\mathbb{R}^+)^k} \exp\left(-\frac{\theta^\beta}{\operatorname{sinc}\beta} \|\mathbf{x}\|_{\frac{1}{\beta}}\right) \mathrm{d}\mathbf{x}.$$

where $\|\cdot\|_p$ denotes the $L_p$ norm, and the equality holds when $\theta \geq 1$. The integral on the RHS can be further simplified into closed-form by using the general formulas in [33, eqn. 4.635], which completes the proof.

Combining Theorem 6 with Lemma 12, we obtain another set of bounds on $p_k$.

**Proposition 12** (SMUD bounds)**.** *For $\theta \geq 1$ and $\Xi_\beta = \{\xi_i\}$, we have*

$$p_k \geq \frac{1}{(1+\theta)^{\frac{\beta}{2}k(k-1)} \theta^{k\beta} \Gamma(1+k\beta) \big(\Gamma(1-\beta)\big)^k}$$

*and*

$$p_k \leq \frac{1}{\theta^{\frac{\beta}{2}k(k+1)}\Gamma(1+k\beta)\big(\Gamma(1-\beta)\big)^k}.$$

*More generally, for all $\theta > 0$, we have*

$$p_k \leq \frac{1}{\bar{\theta}^{\frac{\beta}{2}k(k-1)}\theta^{k\beta}\Gamma(1+k\beta)\big(\Gamma(1-\beta)\big)^k}, \tag{4.10}$$

*where $\bar{\theta} = \max\{\theta, 1\}$.*

Note that the SMUD upper bound in Proposition 12 is valid also for $\theta < 1$. The name of the bounds only suggests that these bounds are tightest in the SMUD regime.

### 4.5.5 Two General Outage Results

Taking $k = 1$, we obtain the following corollary of Theorem 6, which gives the exact probability of decoding the strongest user in a PPNF for $\theta > 1$ and a general upper bound of the probability of decoding the strongest user.

**Corollary 8.** *For $\theta \geq 1$, we have*

$$p_1 = \mathbb{P}(\xi_1^{-1} > \theta I_1) = \frac{\operatorname{sinc}\beta}{\theta^\beta}, \tag{4.11}$$

*and the RHS is an upper bound on $\mathbb{P}(\xi_1^{-1} > \theta I_1)$ when $\theta < 1$.*

It is worth noting that the closed-form expression in Corollary 8 has been discovered in several special cases. For example, [24] derived the equality part of (4.11) in the Rayleigh fading case, and [54] showed that the equality is true for arbitrary fading distribution. However, none of the exiting works derives the results in Corollary 8 in as much generality as here. More precisely, we proved that (4.11) holds for arbitrary fading (including the no-fading case) in $d$-dimensional PPNF (including non-uniform user distribution).

When $\beta = \frac{1}{2}$, (4.6) can be further simplified and we have the following corollary.

**Corollary 9.** *When $\beta = 1/2$,*

$$\mathbb{P}(\xi_k^{-1} > \theta I_k) = \frac{1}{(\pi\theta)^{\frac{k}{2}}\Gamma(\frac{k}{2}+1)}, \tag{4.12}$$

*and the RHS is an upper bound on $\mathbb{P}(\xi_k^{-1} > \theta I_k)$ when $\theta < 1$.*

Fig. 4.2 compares the (4.12) with simulation results for $k = 1, 2, 3, 4, 5$. We found that the estimate in Corollary 9 is not only exact for $\theta \geq 1$ but also quite accurate for $\theta > -4$dB, which is consistent with the observation in [24], where only the case $k = 1$ is studied. Moreover, we can see that with larger $k$, the regime where (4.12) is accurate extends to smaller $\theta$. This gives additional confidence in applying Theorem 6 to the analysis of SIC.

### 4.5.6 Numerical Results

Focusing on $k = 1, 2, 3$, Fig. 4.3 plots the combined upper bounds, high-rate lower bounds, SMUD upper bounds as a function of $\theta$. We see that $p_k$ decays very rapidly with $\theta$, especially when $k$ is large, which suggests that the benefit of decoding many users can be very small under high-rate codes.

Note that the combined upper bound behaves slightly differently for $\theta > 1$ and $\theta < 1$ when $k > 1$. This is because the combined upper bound in Proposition 11 becomes $\Delta_2(k)$ when $\theta < 1$. More precisely, the combined upper bound ignores the ordering among the $k$ strongest users and only considers $\mathbb{P}(\xi_k^{-1} > \theta I_k)$ when $\theta < 1$. Therefore, the combined upper bound is, in most cases, tighter when $\theta > 1$, with only one exception: for $k = 1$, $p_k = \mathbb{P}(\xi_k^{-1} > \theta I_k)$, which is upper bounded by $\Delta_2(1)$ irrespective to $\theta$.

As is shown in the figure, the SMUD bounds are generally tighter than the combined upper bound. However, these bounds a less informative when $\theta \ll 1$, where

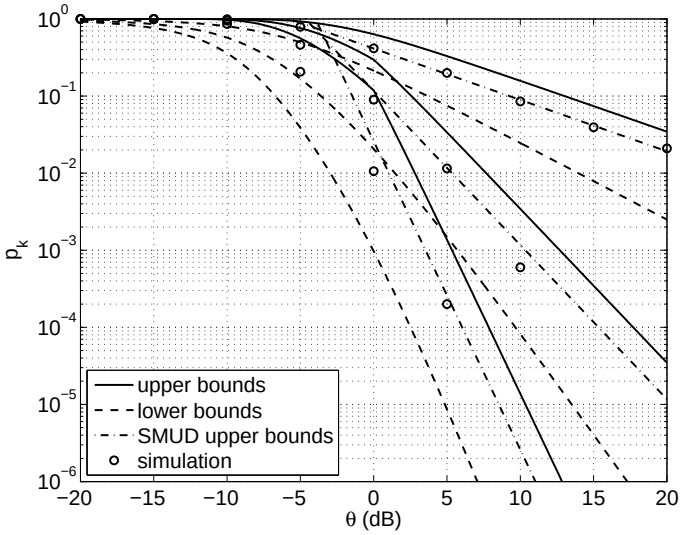


Figure 4.3. Combined upper bound (Proposition 11), high-rate lower bound (Proposition 9), and SMUD upper bound (Proposition 12) for $p_k$ ($k = 1, 2, 3$, from top to bottom) in a 2-d uniform network with path loss exponent $\alpha = 3$.

the upper bound blows above one at about $-5$dB.

The bounds derived above also provide a good method to study the impact of clustering on the effectiveness of SIC. Fig. 4.4 compares the bounds on probability of successively decoding 1, 2 and 3 users for different network clustering parameters $b$, using the upper and high-rate lower bounds derived in Sections 4.5.2 and 4.5.3. The corresponding SMUD bounds on the same quantities derived in Section 4.5.4 are plotted in Fig. 4.5, where the upper and lower bounds for the case $k = 1$ are both tight and overlapping.

By comparing Figs. 4.4 and 4.5, it is appearant that the SMUD bounds are much sharper than the other bounds. This is generally true for $\theta \geq 1$. Nevertheless, the SMUD lower bound is only defined for $\theta \geq 1$ and can be less informative than the combined and lower-rate upper bounds when $\theta < 1$.

Although the bounds in Figs. 4.4 and 4.5 are derived using rather different tech-

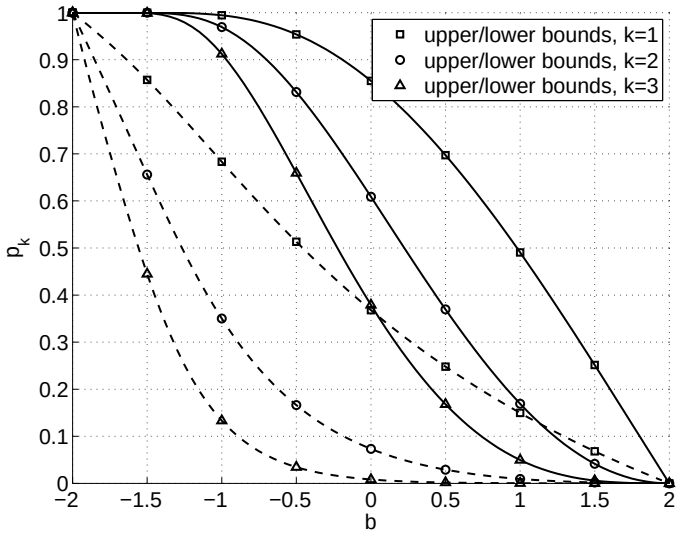


Figure 4.4. Upper and (high-rate) lower bounds (in Proposition 11 and 9, respectively) for $p_k$ $(k = 1, 2, 3)$ in a 2-d network with with path loss exponent $\alpha = 4$, $\theta = 1$ and density function $\lambda(x) = a\|x\|^b$. $b = 0$ is the uniform case.

niques and provide different levels of tightness for different values of $\theta$, both figures capture the important fact that *the more clustered the network, the more useful SIC.*

## 4.6 The Expected Gain of SIC

### 4.6.1 The Mean Number of Successively Decoded Users

With the bounds on $p_k$, we are able to derive bounds on $\mathbb{E}[N]$, the expected number of users that can be successively decoded in the system, since $\mathbb{E}[N] = \sum_{k=1}^{\infty} p_k$.

**Proposition 13.** *In the PPNF, we have* $\mathbb{E}[N] \geq \sum_{k=1}^{K}(1+\theta)^{-\frac{\beta}{2}k(k-1)}\Delta_1(k)$ *for all* $K \in \mathbb{N}$.

On the one hand, Proposition 13 follows directly from Proposition 9 when $K \to \infty$. On the other hand, since for large $\theta$, $p_k$ decays very fast with $k$, a tight approximation can be obtained for small integers $K$. In fact, the error term $\sum_{k=K+1}^{\infty}(1+$

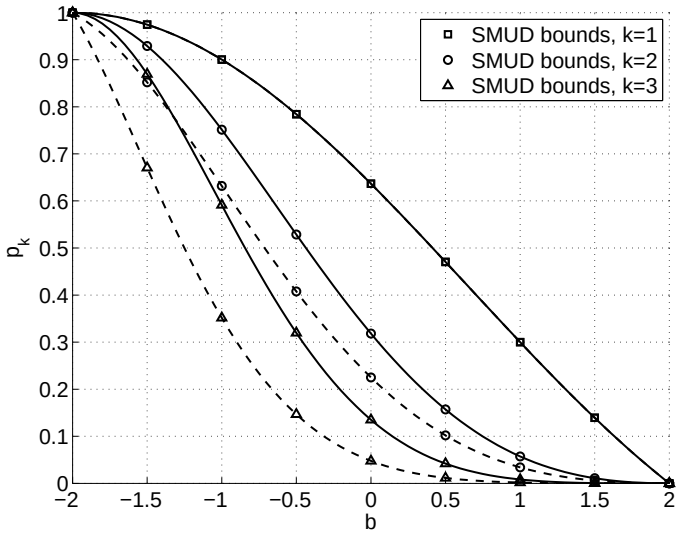


Figure 4.5. SMUD bounds (in Proposition 12) for $p_k$ $(k = 1, 2, 3)$ in a 2-d network with path loss exponent $\alpha = 4$, $\theta = 1$ and density function $\lambda(x) = a\|x\|^b$. $b = 0$ is the uniform case.

$\theta)^{-\frac{\beta}{2}k(k-1)}\Delta_1(k)$ can be upper bounded as

$$\begin{aligned}\sum_{k=K+1}^{\infty}(1+\theta)^{-\frac{\beta}{2}k(k-1)}\Delta_1(k) &\le \Delta_1(K)\sum_{k=K+1}^{\infty}(1+\theta)^{-\frac{\beta}{2}k(k-1)}\\ &\le \Delta_1(K)\int_K^{\infty}(1+\theta)^{-\frac{\beta}{2}x(x-1)}\mathrm{d}x\\ &= \frac{(1+\theta)^{\frac{\beta}{8}}\Delta_1(K)\sqrt{\pi}}{\sqrt{2\beta\log(1+\theta)}}\operatorname{erfc}\left((K-\frac{1}{2})\sqrt{\frac{\beta}{2}\log(1+\theta)}\right),\end{aligned} \tag{4.13}$$

where $\operatorname{erfc}(\cdot)$ is the complementary error function. By inverting (4.13), one can control the numerical error introduced by choosing an finite $K$. Due to the tail property of complementary error function and the monotonicity of $\Delta_1(k)$, it is easy to show that the error term decays super-exponentially with $K^2$ when $K \gg 1$ and thus a finite $K$ is a good approximation for the case $K \to \infty$ .

On the other hand,

$$\frac{(1+\theta)^{\frac{\beta}{8}}\Delta_1(K)\sqrt{\pi}}{\sqrt{2\beta\log(1+\theta)}}\operatorname{erfc}\left((K-\frac{1}{2})\sqrt{\frac{\beta}{2}\log(1+\theta)}\right) \sim \sqrt{\frac{\pi}{2\beta}}\theta^{-\frac{1}{2}}, \text{ as } \theta\to 0, \quad (4.14)$$

where we use the fact that $\lim_{\theta\to 0}\Delta_1(K)=1$ and $\lim_{x\to 0}\operatorname{erfc}(x)=1$. (4.14) suggests that when $\theta\to 0$, for any finite $K$, the error *may* blow up quickly, which is verified numerically. Therefore, in the small $\theta$ regime, we need another, tighter, bound, and this is where the low-rate lower bound in Proposition 10 helps.

**Proposition 14.** *In the PPNF, we have* $\mathbb{E}[N]\geq\sum_{k=1}^{\lfloor 1/\theta\rfloor}\underline{p}_k^{\mathrm{LR}}$.

A rigorous upper bound can be derived similarly but with more caution as we cannot simply discard a number of terms in the sum. The following lemma presents a bound based on Proposition 11.

**Proposition 15.** *In the PPNF,* $\mathbb{E}[N]$ *is upper bounded by*

$$\frac{e^{1+K}}{\sqrt{2\pi}}\frac{(cK)^{1-K}}{cK-1}+\frac{e}{c}(1+c)^{1-K}+\sum_{k=1}^{K-1}\bar{\theta}^{-\frac{\beta}{2}k(k-1)}\Delta_2(k),$$

*for all* $K\in\mathbb{N}\cap[e/c,\infty)$, *where* $\bar{\theta}=\max\{\theta,1\}$.

*Proof.* By Proposition 11, we have $\mathbb{E}[N]\leq\sum_{k=1}^{\infty}\Delta_2(k)$. The proposition then follows by summing up the first $K-1$ terms of the infinite series and upper bounding the residue part. Specifically, we have

$$\begin{aligned}\sum_{k=K}^{\infty}\frac{\gamma(k,1/c)}{\Gamma(k)} &= e^{-1/c}\sum_{k=K}^{\infty}\sum_{j=0}^{\infty}\frac{(1/c)^{j+k}}{(j+k)!}\\ &\overset{\text{(a)}}{\leq}\frac{\exp(-1/c)}{\sqrt{2\pi}}\sum_{k=K}^{\infty}\sum_{j=0}^{\infty}\frac{(e/c)^{j+k}}{(j+k)^{j+k+\frac{1}{2}}}\\ &\leq\frac{\exp(-1/c)}{\sqrt{2\pi}}\sum_{k=K}^{\infty}\frac{(e/c)^k}{K^k}\sum_{j=0}^{\infty}\frac{(e/c)^j}{(j+K)^{j+\frac{1}{2}}},\end{aligned}$$

where (a) uses Stirling's approximation for $n!$, *i.e.*, $\sqrt{2\pi}n^{n+1/2}e^{-n} \leq n! \leq en^{n+1/2}e^{-n}$. Moreover, $\sum_{j=0}^{\infty} \frac{(e/c)^j}{(j+K)^{j+\frac{1}{2}}} \leq e + \sum_{j=1}^{\infty} \frac{(e/c)^j}{j^{j+\frac{1}{2}}}$ since $K \geq 1$. Using Stirling's approximation again on $\sum_{j=0}^{\infty} \frac{(e/c)^j}{j^{j+\frac{1}{2}}}$ yields

$$\sum_{k=K}^{\infty} \frac{\gamma(k, 1/c)}{\Gamma(k)} \leq \frac{\exp(K+1)}{\sqrt{2\pi}} \frac{(cK)^{1-K}}{cK-1}.$$

Furthermore, we have

$$\sum_{k=K}^{\infty} \frac{e}{(1+c)^k} \frac{\Gamma(k, 1+1/c)}{\Gamma(k)} \leq \sum_{k=K}^{\infty} \frac{e}{(1+c)^k} = \frac{e}{c}(1+c)^{1-K},$$

which completes the proof.

Likewise, another upper bound can be derived based on the SMUD bounds on $p_k$ in Proposition 12 as follows:

**Proposition 16.** *The mean number of decodable users is upper bounded by*

$$\mathbb{E}N \leq \sum_{k=1}^{K-1} \left( \frac{C(k)}{\Gamma(1-\beta)} \right)^k \frac{1}{\Gamma(1+k\beta)} + \frac{1}{\Gamma(1+K\beta)} \left( \frac{C(K)}{\Gamma(1-\beta)} \right)^K \frac{\Gamma(1-\beta)}{\Gamma(1-\beta) - C(K)},$$

*where* $C(k) \triangleq \theta^{-\beta} \bar{\theta}^{-\frac{\beta}{2}(k-1)}$.

*Proof.* Since $\mathbb{E}N = \sum_{k=1}^{\infty} p_k$, an upper bound on $\mathbb{E}N$ can be obtained by summing the bound in (4.10). The proposition follows by summing the bound for $k < K$ and then upper bounding the terms for $k \geq K$.

Fig. 4.6 compares the bounds provided in Propositions 13, 14, 15 and 16 with simulation results in a uniform 2-d network with $\alpha = 4$. Although the low-rate lower bound can be calculated for all $\theta < 1$, it is only meaningful when $\theta$ is so small that the lower bound in Proposition 13 fails to capture the rate at which $\mathbb{E}N$ grows with decreasing $\theta$. Thus, we only plot the low-rate lower bound for $\theta < -5$dB.

As is shown in the figure, $\mathbb{E}N$ increases unboundedly with the decreasing of $\theta$,

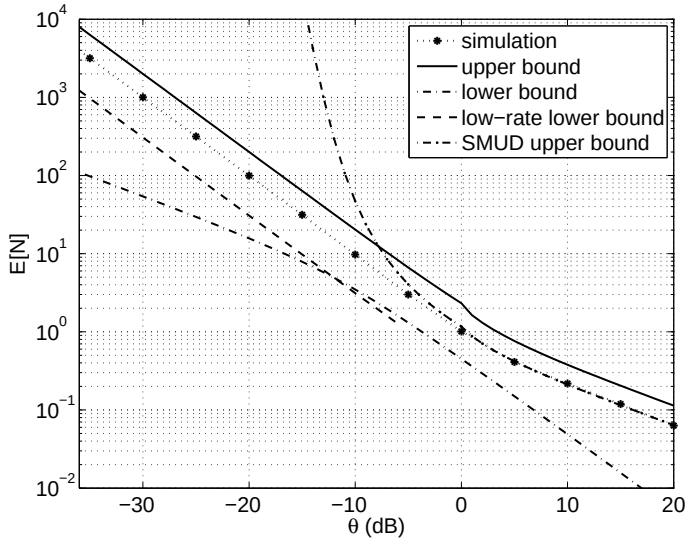


Figure 4.6. The mean number of users that can be successively decoded in a 2-d uniform network with path loss exponent $\alpha = 4$. Here, the upper bound, lower bound, low-rate lower bound, SMUD upper bound refer to the bounds in Proposition 13, 15, 14 and 16, respectively.

which further confirms that SIC is particularly beneficial for low-rate applications in wireless networks, such as node discovery, cell search, *etc.*

Fig. 4.6 also shows the different merits of the different closed-form bounds presented above. The bounds of Propositions 13 and 15 behave well in most of the regime where the practical systems operate. In the lower SIR regime, *i.e.,* when $\theta \to 0$, the low-rate lower bound outperforms the lower bound in Proposition 13 which does not capture the asymptotic behavior of $\mathbb{E}N$. The SMUD bound in Proposition 16 provides a tight alternative to the upper bound in Proposition 15 and is especially tight for $\theta > 1$.

### 4.6.2 The Aggregate Throughput

Although a smaller $\theta$ results in more effective successive interference cancellation, it also means the information rate at each transmitter is smaller. Thus, it

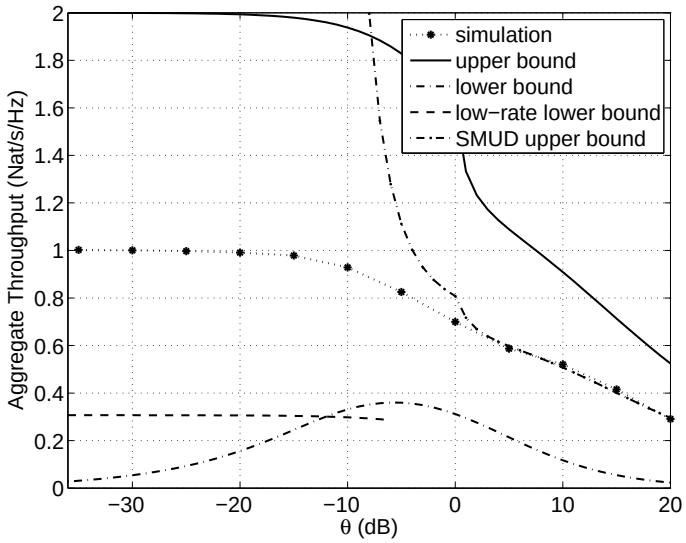


Figure 4.7. Aggregate throughput at $o$ in a 2-d uniform network with with path loss exponent $\alpha = 4$, *i.e.,* $\beta = \delta = 2/\alpha = 1/2$. The upper bound, lower bound, low-rate lower bound and SMUD upper bound come from Propositions 15, 13, 14 and 16 respectively.

is interesting to see how the aggregate throughput defined in (4.1) changes with respect to $\theta$. One way of estimate the aggregate throughput is by using Propositions 13, 14, 15 and 16.

Fig. 4.7 shows the total information rate as a function of $\theta$ with analytical bounds and simulation. Again, we only show the lower bounds for $\theta < -5$dB. In this case, we see that the lower bound of the aggregate throughput becomes a non-zero constant when $\theta \to 0$ just like the upper bound. Therefore, our results indicate that while the aggregate throughput diminishes when $\theta \to \infty$, it converges to a finite non-zero value when $\theta \to 0$. In particular, by using Proposition 15 and letting $\theta \to 0$, we can upper bound the asymptotic aggregate throughput by $\frac{2}{\beta} - 2$, which turns out to be a loose bound.

Nevertheless, it is possible to construct a better bound which improves (reduces) the bound by a factor of 2 and is numerically shown to be asymptotically tight. To

show this better bound, we need the following lemma.

**Lemma 17.** *The Laplace transform of $\xi_k I_k$ is*

$$\mathcal{L}_{\xi_k I_k}(s) = \frac{1}{(c(s)+1)^k}, \tag{4.15}$$

*where $c(s) = s^\beta \gamma(1-\beta, s) - 1 + e^{-s}$.*

*Proof.* As in the proof of Lemma 15, we consider $I_\rho \triangleq I_k \mid \{\xi_k = \rho\}$ and the Laplace transform of $I_\rho$ is given in (4.5). Then, considering another random variable $\rho I_\rho \triangleq \xi_k I_k \mid \{\xi_k = \rho\}$, we have

$$\mathcal{L}_{\rho I_\rho}(s) = \mathbb{E}[e^{-s\xi_k I_k} \mid \xi_k = \rho] = \mathcal{L}_{I_\rho}(s\rho) = \exp(-c(s)\rho^\beta), \tag{4.16}$$

where $c(s) = s^\beta \gamma(1-\beta, s) - 1 + e^{-s}$. Using the results in Lemma 13, we can calculate the Laplace transform of $\xi_k I_k$,

$$\begin{aligned}\mathcal{L}_{\xi_k I_k}(s) &= \mathbb{E}_{\xi_k}[\mathcal{L}_{\rho I_\rho}(s) \mid \xi_k = \rho] \\ &= \int_0^\infty \frac{\beta x^{k\beta-1}}{\Gamma(k)} e^{-(1+c(s))x^\beta} \mathrm{d}x = \frac{1}{(1+c(s))^k}.\end{aligned}$$

Then, we have the following asymptotic bound on the aggregate throughput, which is numerically verified to be tight.

**Proposition 17.** *The aggregate throughput $R = \log(1+\theta)\mathbb{E}[N]$ is (asymptotically) upper bounded by*

$$\lim_{\theta \to 0} R \leq \frac{1}{\beta} - 1. \tag{4.17}$$

*Proof.* First, obviously we have

$$\mathbb{E}[N] = \sum_{k=1}^{\infty} p_k \leq \sum_{k=1}^{\infty} \mathbb{P}(\xi_k I_k < 1/\theta) = \sum_{k=1}^{\infty} \int_0^{1/\theta} f_{\xi_k I_k}(x)\mathrm{d}x = \int_0^{1/\theta} \sum_{k=1}^{\infty} f_{\xi_k I_k}(x)\mathrm{d}x. \tag{4.18}$$

In general, the RHS of (4.18) is not available in closed-form since $f_{\xi_k I_k}$, the pdf of $\xi_k I_k$, is unknown. However, when $\theta \to 0$, this quantity can be evaluated in the Laplace domain. To see this, consider a sequence of functions $(f_n)_{n=1}^{\infty}$, where $f_n(x) = \frac{1}{n}\sum_{k=1}^{n} f_{\xi_k I_k}(x),\ \forall x > 0$ and, obviously, $\int_0^{\infty} f_n(x)\mathrm{d}x = 1$ for all $n$. Thus,

$$1 = \lim_{\theta\to 0} \frac{\int_0^{1/\theta} f_n(x)\mathrm{d}x}{\int_0^{\infty} e^{-\theta x} f_n(x)\mathrm{d}x} = \lim_{\theta\to 0} \frac{\int_0^{1/\theta} \sum_{k=1}^{\infty} f_{\xi_k I_k}(x)\mathrm{d}x}{\int_0^{\infty} e^{-\theta x} \sum_{k=1}^{\infty} f_{\xi_k I_k}(x)\mathrm{d}x},\ \forall n \in \mathbb{N} \tag{4.19}$$

where

$$\int_0^{\infty} e^{-\theta x} \sum_{k=1}^{\infty} f_{\xi_k I_k}(x)\mathrm{d}x = \sum_{k=1}^{\infty} \int_0^{\infty} e^{-\theta x} f_{\xi_k I_k}(x)\mathrm{d}x = \sum_{k=1}^{\infty} \mathcal{L}_{\xi_k I_k}(s)|_{s=\theta}.$$

Comparing (4.18) and (4.19) yields that

$$\lim_{\theta\to 0} \frac{\mathbb{E}[N]}{\sum_{k=1}^{\infty} \mathcal{L}_{\xi_k I_k}(s)|_{s=\theta}} \leq 1,$$

where $\mathcal{L}_{\xi_k I_k}(s)$ is given by Lemma 17. Therefore, we have

$$\lim_{\theta\to 0} \log(1+\theta)\mathbb{E}[N] \leq \lim_{\theta\to 0} \theta \sum_{k=1}^{\infty} \mathcal{L}_{\xi_k I_k}(s)|_{s=\theta} = \lim_{\theta\to 0} \frac{\theta}{c(s)|_{s=\theta}}.$$

The proof is completed by noticing that $\lim_{\theta\to 0} \frac{\theta}{c(\theta)} = \frac{1-\beta}{\beta}$.

In the example considered in Fig. 4.7, we see the bound in Proposition 17 matches the simulation results. Along with this example, we tested $\beta = 1/3$ and $\beta = 2/3$, and the bound is tight in both cases, which is not surprising. Because, in the proof of

Proposition 17, the only slackness introduced is due to replacing $p_k$ with $\mathbb{P}(\xi_k^{-1} > \theta I_k)$, and it is conceivable that, for every given $k$, this slackness diminishes in the limit, since $\lim_{\theta\to 0} \mathbb{P}(\xi_k^{-1} > \theta I_k) = \lim_{\theta\to 0} p_k = 1$. Thus, estimating $\mathbb{E}[N]$ by $\sum_{k=1}^{\infty} \mathbb{P}(\xi_k^{-1} > \theta I_k)$ is exact in the limit.

Many simulation results (including the one in Fig. 4.7) suggest that the aggregate throughput monotonically increases with decreasing $\theta$. Assuming this is true, Proposition 17 provides an upper bound on the aggregate throughput in the network for all $\theta$. We also conjecture that this bound is asymptotically tight and thus can be achieved by driving the code rate at every user to 0, which is also backed by simulations (*e.g.,* see Fig. 4.7).

Since the upper bound is a monotonically decreasing function of $\beta$ we can design system parameters to maximize the achievable aggregate throughput provided that we can manipulate $\beta$ to some extent. For example, since $\beta = \delta + b/\alpha$ and $\delta = d/\alpha$, one can try to reduce $b$ to increase the upper bound. Note that $b$ is a part of the density function of the *active* transmitters in the network and can be changed by independent thinning of the transmitter process [39], and a smaller $b$ means the active transmitters are more clustered around the receiver. This shows that a MAC scheme that introduces clustering has the potential to achieve higher aggregate throughput in the presence of SIC.

### 4.6.3 A Laplace Transform-based Approximation

Lemma 17 gives the Laplace transform of $\xi_k I_k$, which completely characterizes $\mathbb{P}(\xi_k^{-1} > \theta I_k)$, an important quantity in bounding $p_k$, $\mathbb{E}[N]$ and thus $R$. As analytically inverting (4.15) seems hopeless, a numerical inverse Laplace transform naturally becomes an interesting alternative to provide more accurate system performance estimates. However, the numerical inverse Laplace transform (numerical integration in complex domain) is generally difficult to interpret and offers limited insights into the

system performance.

On the other hand, $\mathcal{L}_{\xi_k I_k}(s)|_{s=\theta} = \mathbb{P}(H > \theta\xi_k I_k)$ for an unit-mean exponential random variable $H$. This suggests to use $\mathcal{L}_{\xi_k I_k}(s)|_{s=\theta}$ to approximate $\mathbb{P}(\xi_k^{-1} > \theta I_k)$. We would expect such an approximation to work for (at least) small $\theta$. Because, first, it is obvious that for each $k$, this approximation is exact as $\theta \to 0$ since in that case both the probabilities go to 1; second and more importantly, Proposition 17 shows that the approximated $R$ based on this idea is asymptotically exact.

According to such an approximation, we have

$$R \approx \frac{\log(1+\theta)}{c(\theta)} = \frac{\log(1+\theta)}{\theta^\beta \gamma(1-\beta,\theta) - 1 + e^{-\theta}}. \tag{4.20}$$

This approximation is compared with simulation results in Fig. 4.8, where we consider $\beta = \frac{1}{3}$, $\frac{1}{2}$ and $\frac{2}{3}$. As shown in the figure, the approximation performs quite well from -20dB to 20dB which covers the typical values of $\theta$. Also, as expected, the approximation is most accurate in the small $\theta$ regime[5], which is known to be the regime where SIC is most useful [14, 71, 75].

## 4.7 The Effect of Noise

In many wireless network outage analyses, the consideration of noise is neglected mainly due to the argument that most networks are interference-limited (without SIC). However, this is not necessarily the case for a receiver with SIC capability, especially when a large number of transmitters are expected to be successively decoded. Since the users to be decoded in the later stages have significantly weaker signal power than the users decoded earlier, even if for the first a few users interference dominates noise, after decoding a number of users, the effect of noise can no

[5]The fact that the approximation seems also accurate for very large $\theta$ is more of a coincidence, as the construction of the approximation ignores ordering requirement within the strongest (decodable) $k$ users and is expected to be fairly inaccurate when $\theta \to \infty$ (see Lemma 12).

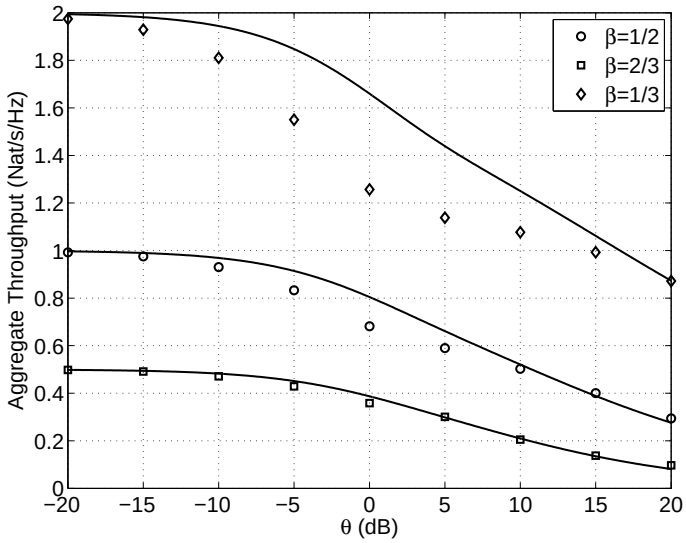


Figure 4.8. Simulated and approximated, by (4.20), aggregate throughput at $o$ in a 2-d uniform network.

longer be neglected.

Fortunately, most of the analytical bounds derived before can be adapted to the case where noise is considered. If we let $\tilde{N}$ be the number of users that can be successively decoded in the presence of noise of power $W$, we can define $p_k^W \triangleq \mathbb{P}(\tilde{N} \geq k)$ to be the probability of successively decoding at least $k$ users in the presence of noise. Considering the (ordered) PLPF $\Xi = \{\xi_i = \frac{\|x\|^\alpha}{h_x}\}$ as before, we can write $p_k^W$ as

$$p_k^W \triangleq \mathbb{P}\left(\xi_i^{-1} > \theta(I_i + W),\ \forall i \leq k\right),$$

and we have a set of analogous bounds as in the noiseless case.

**Lemma 18.** *In a noisy PPNF, the probability of successively decoding $k$ users is bounded as follows:*

- $p_k^W \geq (1+\theta)^{-\frac{\beta k(k-1)}{2}} \mathbb{P}(\xi_k^{-1} > \theta\,(I_k + W))$
- $p_k^W \leq \theta^{-\frac{\beta k(k-1)}{2}} \mathbb{P}(\xi_k^{-1} > \theta(I_k + W))$

*where* $\Xi_\beta = \{\xi_i\}$ *is the corresponding SPLPF and* $I_k \triangleq \sum_{j=k+1}^{\infty} \xi_j^{-1}$.

*Proof.* The proof is analogous to the proof of Lemma 12 with two major distinctions: First, we need to redefine the event $A_i$ to be $\{\xi_i^{-1} > \theta(I_i + W)\}$. Second, Fact 1 does not hold in the noisy case, and thus the original PLPF (instead of the normalized SPLPF) needs to be considered. However, fortunately, this does not introduce any difference on the order statistics of the first $k-1$ smallest elements in $\Xi$ conditioned on the $\xi_k$, and thus the proof can follow exactly the same as that of Lemma 12.

Thanks to Lemma 18, bounding $p_k^W$ reduces to bounding $\mathbb{P}(\xi_k^{-1} > \theta\,(I_k + W))$. Ideally, we can bound $\mathbb{P}(\xi_k^{-1} > \theta\,(I_k + W))$ by reusing the bounds we have on $\mathbb{P}(\xi_k^{-1} > \theta I_k)$. Yet, this method does not yield a closed-form expression. Thus, we turn to a very simple bound which can still illustrate the distinction between the noisy case and the noiseless case.

**Lemma 19.** *In a noisy PPNF, we have*

$$\mathbb{P}(\xi_k^{-1} > \theta\,(I_k + W)) \leq \bar{\gamma}(k, \frac{\bar{a}}{\theta^\beta W^\beta}), \tag{4.21}$$

*where* $\bar{a} = a\delta c_d \mathbb{E}[h^\beta]/\beta$, $\beta = \delta + b/\alpha$, *and* $\delta = d/\alpha$.

*Proof.* First, note that $\mathbb{P}(\xi_k^{-1} > \theta\,(I_k + W)) \leq \mathbb{P}(\xi_k < \frac{1}{\theta W})$ which equals the probability that there are no fewer than $k$ elements of the PLPF smaller than $1/\theta W$. By Lemma 11, the number of elements of the PLPF in $(0, 1/\theta W)$ is Poisson distributed with mean $\bar{a}/\theta^\beta W^\beta$, and the lemma follows.

Although being a very simple bound, Lemma 19 directly leads to the following proposition which contrasts what we observed in the noiseless network.

**Proposition 18.** *In a noisy PPNF, the aggregate throughput goes to 0 as* $\theta \to 0$.

*Proof.* Combining Lemma 18 and Lemma 19, we have

$$\mathbb{E}[N] = \sum_{k=1}^{\infty} p_k^W \leq \sum_{k=1}^{\infty} \mathbb{P}(\xi_k^{-1} > \theta\,(I_k + W)) \leq \sum_{k=1}^{\infty} \bar{\gamma}(k, \frac{\bar{a}}{\theta^\beta W^\beta}) = \bar{a}/\theta^\beta W^\beta.$$

In other words, $\mathbb{E}[N]$ is upper bounded by the mean number of elements of the PLPF in $(0, 1/\theta W)$. Then, it is straightforward to show that $\lim_{\theta\to 0} R \leq \lim_{\theta\to 0} \bar{a}\theta^{1-\beta}/W^\beta$, and the RHS equals zero since $\beta \in (0, 1)$.

Since it is obvious that $\lim_{\theta\to\infty} R = 0$, we immediately obtain the following corollary.

**Corollary 10.** *There exists at least one optimal $\theta > 0$ that maximizes the aggregate throughput in a noisy PPNF.*

As is shown in the proof of Proposition 18, $\bar{a}/\theta^\beta W^\beta$ is an upper bound on $\mathbb{E}[N]$. We can obtain an upper bound on the aggregate throughput by taking the minimum of $\log(1+\theta)\bar{a}/\theta^\beta W^\beta$ and the upper bound shown in Fig. 4.7. Fig. 4.9 compares the upper bounds with simulation results, considering different noise power levels. This figure shows that the noisy bound becomes tighter and the interference bound becomes looser as $\theta \to 0$. This is because as $\theta$ decreases the receiver is expected to successively decode a larger number of users. The large amount of interference canceled makes the residual interference (and thus the aggregate throughput) dominated by noise. In this sense, the optimal per-user rate mentioned in Corollary 10 provides the right *balance* between interference and noise in noisy networks.

Thanks to Lemma 19, we see that Proposition 8 clearly does not hold for noisy networks. Nevertheless, there is still a monotonicity property in noisy networks, analogous to the scale-invariance property in noiseless networks, as stated by the following proposition.

**Proposition 19** (Scale-monotonicity)**.** *For two PLPF $\Xi$ and $\bar{\Xi}$ with intensity measure $\Lambda([0, r]) = a_1 r^\beta$ and $\mu([0, r]) = a_2 r^\beta$, where $a_1$ and $a_2$ are positive real numbers*

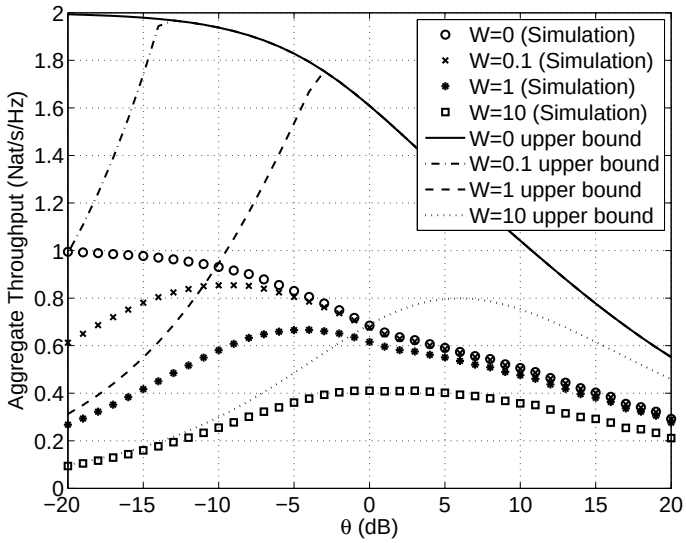


Figure 4.9. Aggregate throughput at $o$ in a 2-d uniform network with noise. Here, the path loss exponent $\alpha = 4$. Three levels of noise are considered: $W = 0.1$, $W = 1$ and $W = 10$.

*and* $a_1 \leq a_2$*, we have* $p_k^W(\Xi) \leq p_k^W(\bar{\Xi}),\ \forall k \in \mathbb{N}$.

*Proof.* The proof is similar to that of Proposition 8. Consider the mapping, $f(x) = (a_1/a_2)^{1/\beta} x^\beta$. Then, $f(\Xi)$ is a PPP on $\mathbb{R}^+$ with intensity measure $a_2 x^\beta$ over the set $[0, x]$ for all $x > 0$. As before, let $\mathcal{N}$ be the sample space of $\Xi$, *i.e.,* the family of all countable subset of $\mathbb{R}^+$. Consider an indicator function $\chi_k^W(\phi) : \mathcal{N} \to \{0, 1\},\ k \in \mathbb{N}$ such that

$$\chi_k^W(\phi) = \begin{cases} 1, & \text{if } \xi_i^{-1} > \theta(I_i + W),\ \forall i \leq k \\ 0, & \text{otherwise,} \end{cases}$$

where $\phi = \{\xi_i\}$ and $\xi_i < \xi_j,\ \forall i < j$.

Note that $\chi_k^W(\phi) \leq \chi_k^W(C\phi),\ \forall C \in (0, 1)$, where $C\phi = \{C\xi_i\}$. To show that, assume that $\chi_k^W(\phi) = 1$, *i.e.,* $\xi_i^{-1} > \theta(\sum_{j=i+1}^{\infty} \xi_j^{-1} + W),\ \forall i \leq k$, which is equivalent to $(C\xi_i)^{-1} > \theta(\sum_{j=i+1}^{\infty} (C\xi_j)^{-1} + C^{-1}W),\ \forall i \leq k$. It follows that $\chi_k^W(C\phi) = 1$ since $C^{-1}W > W$.

Therefore, we have

$$p_k(\Xi) = \mathbb{E}[\chi_k^W(\Xi)] \overset{\text{(a)}}{\leq} \mathbb{E}[\chi_k\left(f(\Xi)\right)] \overset{\text{(b)}}{=} \mathbb{E}[\chi_k\left(\bar{\Xi}\right)] = p_k(\bar{\Xi}),$$

where (a) is due to $a_1 < a_2$ and thus $(a_1/a_2)^{1/\beta} < 1$ and (b) is because both $f(\Xi)$ and $\bar{\Xi}$ are PPPs on $\mathbb{R}^+$ with intensity measure $\mu([0,r]) = a_2 r^\beta$.

Combining Lemma 11 and Proposition 19 yields the following corollary, since $\mathbb{E}[h^\beta] \leq 1$ given that $\mathbb{E}[h] = 1$.

**Corollary 11.** *In a noisy PPNF, fading reduces $p_k^W$, the mean number of users that can be successively decoded, and the aggregate throughput.*

Since random power control, *i.e.,* randomly varying the transmit power at each transmitter under some mean and peak power constraint [77], can be viewed as a way of manipulating the fading distribution, Corollary 11 also indicates that random power control cannot increase the network throughput in a noisy PPNF.

## 4.8 Conclusions

Using a unified PLPF-based framework, this chapter analyzes the performance of SIC in $d$-dimensional fading networks with power law density functions. We show that the probability of successively decoding at least $k$ users decays super-exponentially with $k^2$ if high-rate codes are used, and it decays especially fast under small path loss exponent in high dimensional networks, which suggests the marginal gain of adding more SIC capability diminishes very fast. On the other hand, SIC is shown to be especially beneficial if very low-rate codes are used or the active transmitters are clustered around the receiver.

Since SIC can be considered not only as an interference mitigation technique but also as a multiple packet reception (MPR) scheme, we also investigate the performance gain of SIC in terms of aggregate throughput at the receiver. We observe

that, in interference-limited networks, the aggregate throughput (or, sum rate) is a monotonically decreasing function of the per-user information rate and the asymptotic sum rate is $\frac{1}{\beta} - 1$ as the per-user information rate goes to 0, where $\beta = \frac{b+d}{\alpha}$, $\alpha$ is the pathloss exponent and $b$ determines the network geometry (clustering). Since $b$ can be manipulated by distance-dependent access control or power control[39], the result shows that properly designed MAC or power control schemes can significantly increase the network performance when combined with low rate codes and SIC.

On the other hand, in noisy networks, there exists at least one positive optimal per-user rate which maximizes the aggregate throughput. Moreover, different from interference-limited networks where fading does not affect the performance of SIC, we prove fading to be harmful in noisy networks. This suggests communication schemes that eliminate (average out) the channel randomness are desirable in noisy networks with SIC capability.

# CHAPTER 5

# SIC IN HETEROGENEOUS CELLULAR NETWORKS

The results we derived in Chapter 4 apply to many types of wireless networks. In this chapter, we provide a nontrivial application of the technical results in Chapter 4 to the downlink of heterogeneous cellular networks (HCNs). The results demonstrate that SIC can boost the coverage probability in heterogeneous networks with overloaded or closed-configured base stations. However, SIC is not very helpful in terms of average throughput for typical system parameters. Moreover, for typical contemporary OFDM-based systems, most of the gain of SIC comes from canceling a single interferer.

## 5.1 Modeling Heterogeneous Cellular Networks Using PPP

We model the base stations (BSs) in a $K$-tier HCN as a family of marked Poisson point processes (PPP) $\{\hat{\Phi}_i,\ i \in [K]\}$, where $\hat{\Phi}_i = \{(x_j, h_{x_j}^{(i)}, t_{x_j}^{(i)})\}$ represents the BSs of the $i$-th tier, $\Phi_i = \{x_j\} \subset \mathbb{R}^2$ are uniform[1] PPPs with intensity $\lambda_i$, $h_x^{(i)}$ is the iid (subject to distribution $f_h^{(i)}(\cdot)$) fading coefficient of the link from $x$ to $o$, and $t_x^{(i)}$ is the *type* of the BS and is an iid Bernoulli random variable with $\mathbb{P}(t_x^{(i)} = 1) = \pi^{(i)}$ and $\mathbb{P}(t_x^{(i)} = 0) = 1 - \pi^{(i)}$. If $t_x^{(i)} = 1$, we call the BS $x$ *accessible* and otherwise *non-accessible*[2]. For a typical receiver (UE) at $o$, the received power from BS $x \in \Phi_i$

[1] Although we only consider uniformly distributed BSs in this chapter, with the results in Chapter 4, generalizing the results to non-uniform (power-law density) HCNs is straightforward.

[2] The non-accessible BSs can be interpreted as overloaded/biased BSs [29], femtocells with closed-access configuration, or simply interferers outside the cellular system.

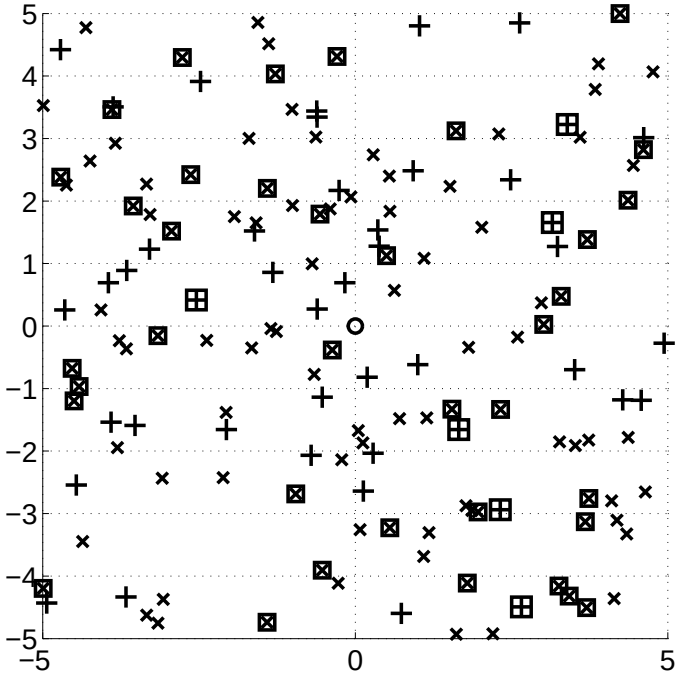


Figure 5.1. An 2-tier HCN with 10% of Tier 1 (macrocell) BSs (denoted by +) overloaded and 30% of Tier 2 (femtocell) BSs (denoted by ×) configured as closed. A box is put on the BS whenever it is non-accessible (*i.e.,* either configured as closed or overloaded). The o at origin is a typical receiver.

is $P^{(i)}h_x^{(i)}\|x\|^{-\alpha}$, where $P^{(i)}$ is the transmit power at BSs of tier $i$, and $\alpha$ is the path loss exponent. Also note that since this chapter focuses on 2-dimensional uniform networks, we have $\beta = 2/\alpha$. An example of a two tier HCN is shown in Fig. 5.1.

## 5.2 The Marked Path Loss Process with Fading

An important quantity that will simplify our analysis in the $K$-tier HCN is the *equivalent access probability* (EAP) defined as below.

**Definition 12.** *Let*

$$Z \triangleq \sum_{i=1}^{K} \lambda_i \mathbb{E}[(h^{(i)})^{\beta}](P^{(i)})^{\beta}.$$

*The* equivalent access probability *(EAP) is the following weighted average of the*

*individual access probabilities* $\pi^{(i)}$*:*

$$\eta = \frac{1}{Z}\sum_{i=1}^{K}\pi^{(i)}\lambda_i\mathbb{E}[(h^{(i)})^{\beta}](P^{(i)})^{\beta}.$$

Thanks to the obvious similarity between this HCN model and our PPNF model introduced in Section 4.3, we can define the *marked* PLPF as follows.

**Definition 13.** *The* marked PLPF *corresponding to the tier* $i$ *network is* $\hat{\Xi}_i = \{(\frac{\|x\|^{\alpha}}{h_x P^{(i)}}, t_x) : x \in \Phi_i\}$*, with* $\Xi_i \triangleq \{\frac{\|x\|^{\alpha}}{h_x P^{(i)}} : x \in \Phi_i\}$ *being the (ground) PLPF.*

Furthermore, we denote the union of the $K$ marked PLPFs and ground PLPFs as $\hat{\Xi} \triangleq \bigcup_{i=1}^{K}\hat{\Xi}_i$ and $\Xi \triangleq \bigcup_{i=1}^{K}\Xi_i$, respectively. Then, we have the following lemma.

**Lemma 20.** *The PLPF corresponding to the* $K$*-tier heterogeneous cellular BSs is a marked inhomogeneous PPP* $\hat{\Xi} = \{(\xi_i, t_{\xi_i})\} \subset \mathbb{R}^{+} \times \{0, 1\}$*, where the intensity measure of* $\Xi = \{\xi_j\}$ *is* $\Lambda([0, r]) = Z\pi r^{\delta}$ *and the marks* $t_{\xi}$ *are iid Bernoulli with* $\mathbb{P}(t_{\xi} = 1) = \eta$*.*

Based on the mapping theorem, the independence between $t_x^i$ and the fact that the superposition of PPPs is still a PPP, the proof of Lemma 20 is straightforward and thus omitted from the thesis. Despite the simplicity of the proof, the implication of Lemma 20 is significant: the effect of the different transmit powers, fading distributions and access probabilities of the $K$-tiers of the HCN can all be subsumed by the two parameters $Z$ and $\eta$.

## 5.3 The Coverage Probability

An important quantity in the analysis of the downlink of heterogeneous cellular networks is the coverage probability, which is defined as the probability of a typical UE successfully connecting to (at least) one of the accessible BSs (after possibly canceling some of the non-accessible BSs).

### 5.3.1 Without SIC

Using the PLPF framework we established above and assuming that the UE *cannot* do SIC and the system is interference-limited, we can simplify the coverage probability in the $K$-tier cellular network to

$$P_c = \mathbb{P}\left(\frac{\xi_*^{-1}}{\sum_{\xi\in\Xi\setminus\{\xi_*\}}\xi^{-1}} > \theta\right), \tag{5.1}$$

where $\xi_* \triangleq \arg\max_{\xi\in\Xi} t_\xi \xi^{-1}$, and $\theta$ is the SIR threshold.

Note that the coverage probability in (5.1) does not yield a closed-form expression in general [23]. However, for $\theta \geq 1$, we have

$$P_c = \eta p_1 = \frac{\eta \operatorname{sinc}\beta}{\theta^\beta}, \tag{5.2}$$

which can be straightforwardly obtained by combining Lemma 16, Corollary 8 and the fact that the marks $\{t_i\}$ are independent from $\Xi$.

### 5.3.2 With SIC

Similar to (5.1), we can define the coverage probability when the UE has SIC capability. In particular, the coverage probability $P_c^{\mathrm{SIC}}$ is the probability that after cancellation a number of non-accessible BSs, the signal to (residual) interference ratio from the any of the accessible BSs is above $\theta$. Formally, with the help of the PLPF, we can define the following event of coverage which happens with probability $P_c^{\mathrm{SIC}}$.

**Definition 14** (Coverage with (infinite) SIC capability)**.** *A UE with infinite SIC capability is* covered *iff there exists* $l \in \mathbb{N}$ *and* $k \in \{i : t_i = 1\}$ *such that* $\xi_i^{-1} > \theta I_i$, $\forall i \leq l$ *and* $\xi_k^{-1} > \theta I_l^{!k}$, *where* $I_l^{!k} \triangleq \sum_{j\geq l+1}^{j\neq k} \xi_j^{-1}$.

With the help of PLPF and the parameters we defined in the analysis of the PPNF, the following lemma describes this probability in a neat formula.

**Proposition 20.** *In the $K$-tier heterogeneous cellular network, the coverage probability of a typical UE with SIC is*

$$P_c^{\mathrm{SIC}} = \sum_{k=1}^{\infty} (1-\eta)^{k-1} \eta p_k,$$

*where $p_k = p_k(\Xi)$ is the probability of successively decoding at least $k$ users in a PLPF on $\mathbb{R}^+$ with intensity measure $\Lambda([0,r]) = Z\pi r^\beta$.*

*Proof.* Without loss of generality, we consider the marked PLPF corresponding to the $K$-tier heterogeneous cellular BSs $\hat{\Xi} = \{(\xi_i, t_i)\}$, where the index $i$ is introduced such that $\{\xi_i\}$ are increasingly ordered. Let $\vartheta_k : \mathcal{N} \to \{0,1\},\ k \in \mathbb{N}$, be an indicator function such that

$$\vartheta_k(\phi) \triangleq \begin{cases} 1, & \text{if } \exists l \in \mathbb{N} \text{ s.t. } \chi_l(\phi) = 1 \text{ and } \xi_k^{-1} > \theta I_l^{!k} \\ 0, & \text{otherwise,} \end{cases} \tag{5.3}$$

where $\chi_k(\cdot)$ is defined in (4.2). Furthermore, we define a random variable $M = \min\{i : t_i = 1\}$, where $t_i$ is the mark of the $i$th element in $\hat{\Xi}$. Note that since, according to Lemma 20, $t_i$ are iid (also independent from $\Xi$), $M$ is geometrically distributed with parameter $\eta$ and is independent of $\Xi$. Then, it is easy to check with Definition 14 that the coverage probability can be written as

$$P_c^{\mathrm{SIC}} = \mathbb{P}(\vartheta_M(\Xi)) = \mathbb{E}_M\left[\mathbb{P}(\vartheta_M(\Xi) \mid M)\right],$$

where the probability inside the expectation is the probability of decoding the $M$th strongest BS (with the help of SIC) conditioned on the fact that this BS is the strongest accessible BS.

Moreover, we have $\vartheta_k(\cdot) = \chi_k(\cdot),\ \forall k \in \mathbb{N}$. To see this, we first notice that, by the definition of the two functions, $\chi_k(\phi) = 1 \ \Rightarrow\ \vartheta_k(\phi) = 1$. Conversely, assuming

$\vartheta_k(\phi) = 1$, which by definition means $\exists l \in \mathbb{N}$ s.t. $\chi_l(\phi) = 1$ and $\xi_k^{-1} > \theta I_l^{!k}$, we immediately notice that $\chi_k(\phi) = 1$ if $l \geq k$. If $l < k$, we have $\xi_{l+1}^{-1} \geq \xi_k^{-1} > \theta I_l^{!k} \geq \theta I_{l+1}$, *i.e.*, $\chi_{l+1}(\phi) = 1$, which, by induction, leads to the fact that $\chi_k(\phi) = 1$. Since both $\chi_k(\cdot)$ and $\vartheta_k(\cdot)$ are indicator functions on the domain of all countable subsets of $\mathbb{R}^+$, we have established the equivalence of the two functions.

Therefore, we have $P_c^{\mathrm{SIC}} = \mathbb{E}_M\left[\mathbb{P}(\chi_M(\Xi) \mid M)\right] = \mathbb{E}_M[p_M]$, which completes the proof.

Thanks to Proposition 20 we can quantify the coverage probability of the HCN downlink using the bounds on $p_k$ we obtained in Section 4.5. In particular, based on Proposition 9, a lower bound can be found as

$$P_c^{\mathrm{SIC}} \geq \sum_{k=1}^{K} (1-\eta)^{k-1} \eta (1+\theta)^{-\frac{\beta k(k-1)}{2}} \Delta_1(k), \tag{5.4}$$

where the choice of $K$ affects the tightness of the bound. Although a rigorous upper bound cannot be obtained by simply discarding some terms from the sum, we can easily upper bound the tail terms of it. For example, based on Proposition 11 we have

$$P_c^{\mathrm{SIC}} \leq \sum_{k=1}^{K} (1-\eta)^{k-1} \eta \bar{\theta}^{-\frac{\beta}{2}k(k-1)} \Delta_2(k) + (1-\eta)^{K+1}, \tag{5.5}$$

where $\bar{\theta} = \max\{\theta, 1\}$ and $(1-\eta)^{K+1}$ bounds the residual terms in the infinite sum.

Besides these bounds, we can also use the approximation established in Section 4.6.3 to obtain an approximation on the coverage probability in closed-form. In particular, we had

$$p_k \approx \mathcal{L}_{\xi_k I_k}(s)|_{s=\theta} = \frac{1}{\left(c(\theta)+1\right)^k},$$

where $c(\theta) = \theta^\beta \gamma(1-\beta, \theta) - 1 + e^{-\theta}$. Combing this with Proposition 21, we have

$$P_c^{\mathrm{SIC}} \approx \frac{\eta}{1-\eta} \sum_{k=1}^{\infty} \left(\frac{1-\eta}{1+c(\theta)}\right)^k = \frac{\eta}{\eta + c(\theta)}. \tag{5.6}$$

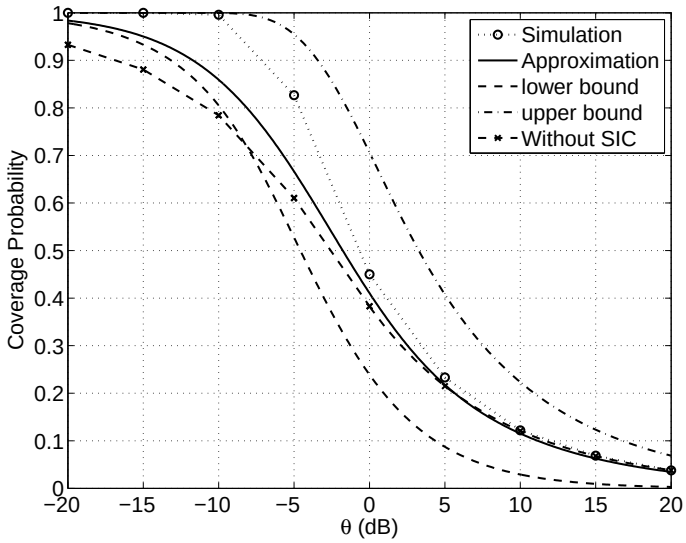


Figure 5.2. The coverage probability (with infinite SIC capability) as a function of SIR threshold $\theta$ in HCNs with $\eta = 0.6$ and $\alpha = 4$. The (Laplace-transform-based) approximation, lower bound and upper bounds of $P_c^{\text{SIC}}$ is calculated according to (5.6), (5.4) and (5.5), respectively. The coverage probability in the case without SIC (a problem also studied in [23, 24]) is also plotted for comparison, where the $\theta \geq 0$dB part is analytically obtained by (5.2) and the $\theta < 0$dB part is based on simulation.

In Fig. 5.2, we compare these bounds and the approximation with simulation results. These bounds give reasonably good estimates on the coverage probability throughout the full range of the SIR threshold $\theta$. In comparison with the coverage probability when no SIC is available, we see that a significant gain can be achieved by SIC when the SIR threshold $\theta$ is between $-10$dB and $-5$dB. This conclusion is, of course, affected by $\eta$. The effect of $\eta$ will be further explored in Section 5.6.

## 5.4 The Effect of the Path Loss Exponent $\alpha$

We can also use the bounds in Proposition 12 to estimate the coverage probability. In particular,

$$P_c^{\mathrm{SIC}} \geq \frac{\eta}{1-\eta} \sum_{k=1}^{K} \frac{1}{(1+\theta)^{\frac{\beta}{2}k(k-1)}\Gamma(1+k\beta)} \left( \frac{1-\eta}{\theta^{\beta}\Gamma(1-\beta)} \right)^k, \ \forall K \geq 1, \tag{5.7}$$

where we take a finite sum in the place of an infinite one. The error term assoicated with this appoximation is upper bounded as

$$\sum_{k=K+1}^{\infty} \frac{1}{(1+\theta)^{\frac{\beta}{2}k(k-1)}\Gamma(1+k\beta)} \left( \frac{1-\eta}{\theta^{\beta}\Gamma(1-\beta)} \right)^k \leq \frac{1}{\Gamma(1+(K+1)\beta)} \frac{C_2^{K+1}}{1-C_2}, \tag{5.8}$$

where $C_2 = \frac{1-\eta}{(1+\theta)^{\frac{\beta}{2}K}\theta^{\beta}\Gamma(1-\beta)}$. Since (5.8) decays super-exponentially with $K$, a small $K$ typically ends up with a quite accurate estimate.

For the upper bound, we can reuse the calculation in Proposition 16 and obtain

$$\begin{aligned} P_c^{\mathrm{SIC}} \leq & \frac{\eta}{1-\eta} \sum_{k=1}^{K-1} \left( \frac{(1-\eta)C(k)}{\Gamma(1-\beta)} \right)^k \frac{1}{\Gamma(1+k\beta)} \\ & + \frac{\eta}{1-\eta} \frac{1}{\Gamma(1+K\beta)} \left( \frac{(1-\eta)C(K)}{\Gamma(1-\beta)} \right)^K \frac{\Gamma(1-\beta)}{\Gamma(1-\beta)-(1-\eta)C(K)}, \end{aligned} \tag{5.9}$$

where $C(k) \triangleq \theta^{-\beta}\bar{\theta}^{-\frac{\beta}{2}(k-1)}$.

Fig. 5.3 plots the coverage probability as a function of the path loss exponent $\alpha$. Here, the coverage probability without SIC $P_c^{\mathrm{SIC}}$ is given by (5.2). The figure shows that the absolute gain of coverage probability due to SIC is larger for larger path loss exponent $\alpha$. Although our model here does not explicitly consider BS clustering, by the construction of the PLPF in Section 4.4, we can expect a larger gain due to SIC for clustered BSs. Further numerical results also show that the gain is larger when $\eta$ is smaller, *i.e.,* there are more non-accessible BSs.

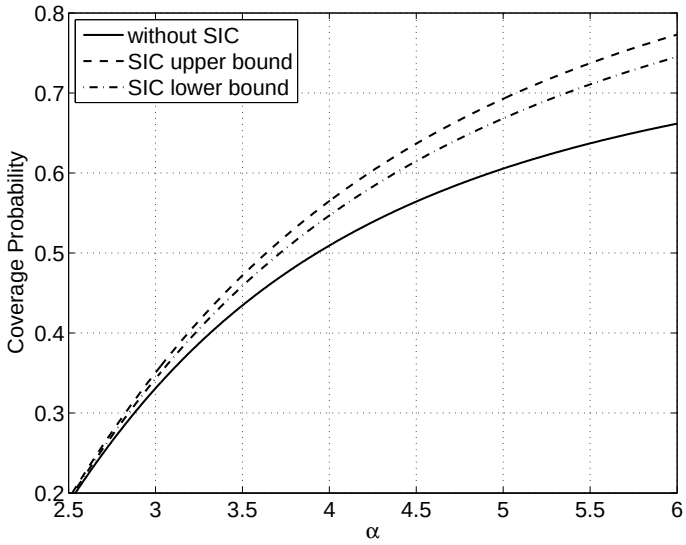


Figure 5.3. Comparison between coverage probability with and without SIC in HCNs with $\eta = 0.8$, $\theta = 1$. Here, the upper and lower bounds are based on (5.9) and (5.7), respectively.

## 5.5 Average Throughput

Reducing the SIR threshold $\theta$ puts a penalty on the throughput of the users under coverage. Similar to our analyses to the aggregate throughput, we can define the average throughput as

$$T \triangleq \log(1+\theta) P_c^{\mathrm{SIC}}.$$

For the case without SIC, the definition is simplified as $T \triangleq \log(1+\theta) P_c$. The average throughput is different from the aggregate throughput defined in Section 4.6.2 in that we do not allow multiple packet reception in this case.

Fig. 5.4 shows how the average throughput change as a function of $\theta$ with the same set of parameters as in Fig. 5.2. Comparing these two figures, we find that while SIC is particularly useful in terms of coverage in combination with low-rate codes (low $\theta$), the usefulness of SIC in terms of average throughput can be marginal. For this particular set of parameters, the average throughput is maximized at $\theta$ about

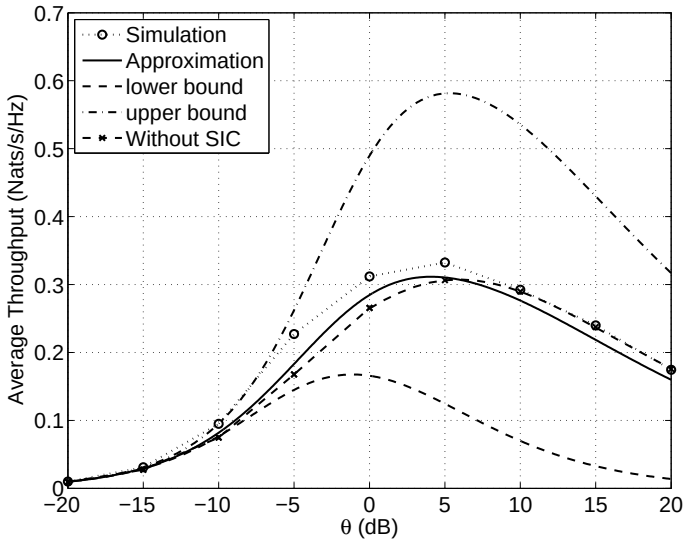


Figure 5.4. The average throughput as a function of SIR threshold $\theta$ in HCNs with $\eta = 0.6$ and $\alpha = 4$. The (Laplace-transform-based) approximation, lower bound and upper bounds of $P_c^{\mathrm{SIC}}$ is calculated according to (5.6), (5.4) and (5.5), respectively. The non-outage throughput in the case without SIC is plotted for comparison, where the $\theta \geq 0$dB part is analytically obtained by (5.2) and the $\theta < 0$dB part is based on simulation.

5dB, a regime where SIC is not very useful. On the positive side, as we will show in Section 5.6, for such $\theta$, most of the gain of SIC can be obtained by simply canceling a very small number of non-accessible BSs.

## 5.6 Finite SIC Capabilty

In real cellular network settings, the assumption that the UEs have the ability to successively decode an infinite number of interferers is impractical and conceivably unnecessary in achieving the coverage gain. Thus, it is important to evaluate the performance gain of SIC when the UEs have only a limited ability of interference cancellation. Since the latency is likely to be the most critical factor in practical systems, we consider the case where the UE can cancel at most $n-1$ interferers.

Formally, we define the event of coverage for a UE with $n$-layer SIC capability as follows.

**Definition 15** (Coverage with $n$-layer SIC capability)**.** *A UE with $n$-layer SIC capability is* covered *iff there exists $l \in [n-1]$ and $k \in \{i : t_i = 1\}$ such that $\xi_i^{-1} > \theta I_i$, $\forall i < l$ and $\xi_k^{-1} > \theta I_l^{!k}$.*

We will use $P_{c,n}^{\mathrm{SIC}}$ to denote the coverage probability for a typical UE with $n$-layer SIC capability. As two special cases, we have $P_{c,1}^{\mathrm{SIC}} = P_c$ and $P_{c,\infty}^{\mathrm{SIC}} = P_c^{\mathrm{SIC}}$.

Following a similar procedure in the proof of Proposition 20, we find a lower bound on $P_{c,n}^{\mathrm{SIC}}$ which is exact when $\theta \geq 1$.

**Proposition 21.** *In the $K$-tier heterogeneous cellular network, the coverage probability of a typical UE with $n$-layer SIC capability is*

$$P_{c,n}^{\mathrm{SIC}} \geq \sum_{k=1}^{n} (1-\eta)^{k-1} \eta p_k, \tag{5.10}$$

*where the equality holds when $\theta \geq 1$.*

*Proof.* Similar to the definition of $\vartheta_k(\cdot)$ in (5.3). We define

$$\vartheta_{n,k}(\phi) \triangleq \begin{cases} 1, & \text{if } \exists l < n \text{ s.t. } \chi_l(\phi) = 1 \text{ and } \xi_k^{-1} > \theta I_l^{!k} \\ 0, & \text{otherwise.} \end{cases} \tag{5.11}$$

Then, we have

$$\begin{aligned} P_{c,n}^{\mathrm{SIC}} &\overset{\text{(a)}}{=} \mathbb{E}_M \left[ \mathbb{P}(\vartheta_{n,M}(\Xi) \mid M) \right] \\ &\overset{\text{(b)}}{=} \sum_{k=1}^{\infty} \eta(1-\eta)^{k-1} \mathbb{P}(\vartheta_{n,k}(\Xi)) \\ &\overset{\text{(c)}}{\geq} \sum_{k=1}^{n} \eta(1-\eta)^{k-1} \mathbb{P}(\chi_k(\Xi)) \\ &\overset{\text{(d)}}{=} \sum_{k=1}^{n} \eta(1-\eta)^{k-1} p_k. \end{aligned}$$

where (a) is due to Definition 15, (b) is due to the independence between the marks and the process $\Xi$ and (d) is due to the definition of $p_k$. To show (c), we note that $\vartheta_{n,k}(\cdot) = \chi_k(\cdot)$ for all $k \leq n$, which can be shown in a way analogous to the way we establish the equivalence between $\vartheta_k(\cdot)$ and $\chi_k(\cdot)$ in the proof of Proposition 20. In addition, when $\theta \geq 1$, for all $k > n > l$, $\xi_k^{-1} < \theta \sum_{j \geq l+1}^{j \neq k} \xi_j^{-1}$ almost surely. In other words, $\mathbb{P}(\vartheta_{n,k}(\cdot)) = 0$ for all $k > n$ and the equality in (c) is attained for $\theta \geq 1$.

Comparing Propositions 20 and 21, it is obvious that the inequality in Proposition 21 is asymptotically tight as $n \to \infty$. More precisely, since $P_c^{\mathrm{SIC}} \geq P_{c,n}^{\mathrm{SIC}}$, we have

$$\sum_{k=1}^{n} (1-\eta)^{k-1} \eta p_k \leq P_{c,n}^{\mathrm{SIC}} \leq \sum_{k=1}^{\infty} (1-\eta)^{k-1} \eta p_k,$$

and the difference between the upper and lower bound decays (at least) exponentially with $n$. Thus, the lower bound in Proposition 21 converges to the true value at least exponentially fast with $n$.

Combining Propositions 20 and 21 with the results given before, we can estimate the performance gain of SIC in the HCN downlink. In the following, we focus on two different scenarios to analyze the performance of finite SIC capability.

### 5.6.1 The High SIR Case

First, we focus on the case with $\theta \geq 1$. Thanks to Proposition 12, this case has extra tractability since $\mathbb{P}(\xi_k^{-1} > \theta I_k)$ can be expressed in closed-form. Thus, by applying Proposition 21, we obtain a set of upper bounds on the coverage probability with finite SIC capability

$$P_{c,n}^{\mathrm{SIC}} \leq \frac{\eta}{1-\eta} \sum_{k=1}^{n} \frac{1}{\Gamma(1+k\beta)} \left( \frac{1-\eta}{\theta^{\frac{\beta}{2}(k+1)}\Gamma(1-\beta)} \right)^k. \tag{5.12}$$

For infinite SIC capability, by the same procedule, a closed-form upper bound on the coverage probability can also be obtained when $\alpha = 4$ (or, $\beta = \frac{1}{2}$)

$$\begin{aligned} P_c^{\mathrm{SIC}} &= \sum_{k=1}^{\infty} (1-\eta)^{k-1} \eta p_k \\ &\leq \sum_{k=1}^{\infty} (1-\eta)^{k-1} \eta \frac{(\pi\theta)^{-k/2}}{\Gamma(k/2+1)} \\ &= \frac{\eta}{1-\eta} \left( \exp\left( \frac{(1-\eta)^2}{\pi\theta} \right) \left( 1 + \mathrm{erf}\left( \frac{1-\eta}{\sqrt{\pi\theta}} \right) \right) - 1 \right). \end{aligned} \tag{5.13}$$

Fig. 5.5 plots the coverage probability with different levels of SIC capability as a function of $\eta$ for $\theta$ =0dB and 2dB. Here, we plot the upper bounds on $P_{c,n}^{\mathrm{SIC}}$ according to (5.12) for $n = 1, 2$, the upper bound on $P_c^{\mathrm{SIC}}$ according to (5.13), and simulated value of $P_{c,n}^{\mathrm{SIC}}$ for $n = 1, 2, 10$. The problem of $n = 1$ is already studied in [24].

Taking $n = 1$ and $\beta = \frac{1}{2}$ in (5.12) and comparing it with (5.2) shows that the upper bound in (5.12) is tight for $n = 1$. This explains why the lowest solid lines (upper bound on $P_{c,1}^{\mathrm{SIC}}$) and the lowest dashed lines (simulated $P_{c,1}^{\mathrm{SIC}}$) in Fig. 5.5 overlap.

Fig. 5.5 shows that $P_{c,n}^{\mathrm{SIC}} - P_{c,1}^{\mathrm{SIC}}$, the absolute coverage probability gain of SIC, is much larger when $\eta$ is close to $\frac{1}{2}$ than when $\eta$ is close to 0 or 1. This phenomenon can be observed within a much wider range of system parameters. Intuitively, this

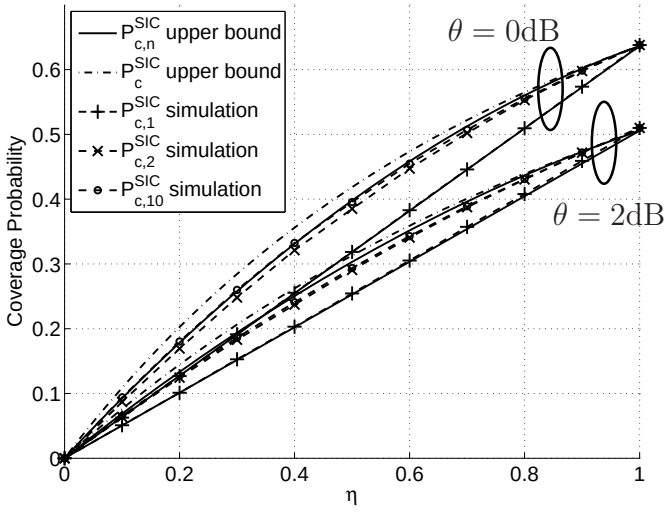


Figure 5.5. Comparison between the upper bound on the coverage probabilities and the simulated coverage probability of femto-cell networks with different levels of SIC capability when $\alpha = 4$. The upper bounds on $P_{c,n}^{\text{SIC}}$ is calculated according to (5.12) for $n = 1, 2$ (coverage probability is higher for larger $n$). The upper bound on $P_{c}^{\text{SIC}}$ is calculated by (5.13). The simulated value of $P_{c,n}^{\text{SIC}}$ is plotted for $n = 1, 2, 10$. When $\theta = 2$dB, the curves for $n = 2$ and $n = 10$ almost completely overlap.

observation can be explained as follows: On the one hand, when $\eta \to 1$, most of the BSs in the network are accessible. Thus, SIC will not significantly improve the coverage probability. On the other hand, when $\eta \to 0$, most of the BSs in the network are non-accessible. In this case, UE coverage can only be significantly improved if many BSs are expected to be successively canceled. As is shown in Section 4.6, the number of BSs that can be successively decoded is fundamentally limited by the choice of $\theta$, and in this particular case ($\theta \geq 1$), very few, if any, non-accessible BSs are expected to be canceled, leaving very little space for SIC to improve the coverage probability.

Moreover, it is worth noting that with $\theta \geq 1$ and $\beta = \frac{1}{2}$, most of the gain of SIC is achieved by the ability of canceling only a single non-accessible BS. This is

consistent with observations reported in [71] where a different model for SIC is used and the transmission capacity is used as the metric. The fundamental reason of this observation can be explained by Proposition 21. The difference in coverage probability between infinite SIC capability and the capability of canceling $n-1$ UEs is $\sum_{k=n+1}^{\infty}(1-\eta)^{k-1}\eta p_k$, which, due to the super-exponential decay of $p_k$ (Proposition 12), decays super-exponentially with $n$. Thus, most of the additional coverage probability comes from canceling a small number of non-accessible BSs. Since $\theta$ affects the rate at which $p_k$ decays, we can expect that the ability of successively decoding more than one non-accessible BS becomes even less useful for larger $\theta$, which is also demonstrated in Fig. 5.5.

Of course, with the same logic and analytical bounds, *e.g.,* the one in Proposition 9 or the one in Proposition 10, we would expect that the ability to successively decode a large number of users does help if $\beta \to 0$ and/or $\theta \to 0$. $\beta \to 0$ could happen if the path loss exponent $\alpha$ is very large and/or the BSs are clustered around the receiver and/or the network dimension is low (*e.g.* for vehicular networks, it is reasonable to take $d = 1$). $\theta \to 0$ happens when very low-rate codes are used.

### 5.6.2 More Realistic Cases

Since the different values of $\theta$ and $\beta$ can result in different usefulness of the finite SIC capability at the HCN downlink, it is worthwhile to discuss most realistic parameter choices in contemporary systems.

The exact values of $\theta$ and $\beta$ depends on many facts including modulation and coding schemes, receiver sensitivity, BS densities and propagation environment. However, in practical OFDM-type HCNs (*e.g.,* LTE and 802.11 networks), the SIR threshold $\theta$ is typically larger than $-3$dB and often more than 0dB [23][3]. For the indoor propagation, $\alpha$ is typically between 3 and 4. Therefore, the system parameters used

[3]The small $\theta$ regime is more applicable to wide-band systems, *e.g.,* CDMA or UWB systems.

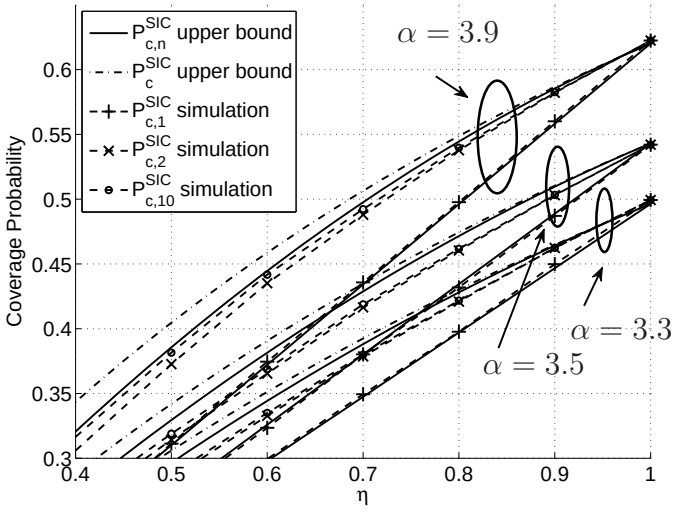


Figure 5.6. Comparison between the upper bound on the coverage probabilities and the simulated coverage probability of femto-cell networks with different path loss exponent $\alpha$ when $\theta = 0$dB. The upper bounds on $P_{c,n}^{\text{SIC}}$ is calculated according to (5.14) for $n = 1, 2$ (coverage probability is higher for larger $n$). The upper bound on $P_{c}^{\text{SIC}}$ is calculated by (5.15). The simulated value of $P_{c,n}^{\text{SIC}}$ is plotted for $n = 1, 2, 10$. For $\alpha \leq 3.5$, the curves for $n = 2$ and $n = 10$ almost completely overlap.

in the high SIR case (Fig. 5.5) are already reasonably realistic.

To have a closer look at the impact of $\alpha$, we fix $\theta = 1$. Then, (5.12) can be simplified as

$$P_{c,n}^{\text{SIC}} \leq \frac{\eta}{1-\eta} \sum_{k=1}^{n} \frac{1}{\Gamma(1+k\beta)} \left( \frac{1-\eta}{\Gamma(1-\beta)} \right)^{k}. \tag{5.14}$$

which in the case of $n \to \infty$ gives an upper bound on the coverage probabilty with infinite SIC capability,

$$P_{c}^{\text{SIC}} \leq \frac{\eta}{1-\eta} \left( \mathbf{E}_{\beta,1} \left( \frac{1-\eta}{\Gamma(1-\beta)} \right) - 1 \right), \tag{5.15}$$

where $\mathbf{E}_{a,b}(z) = \sum_{k=0}^{\infty} \frac{z^k}{\Gamma(ak+b)}$ is the Mittag-Leffler function.

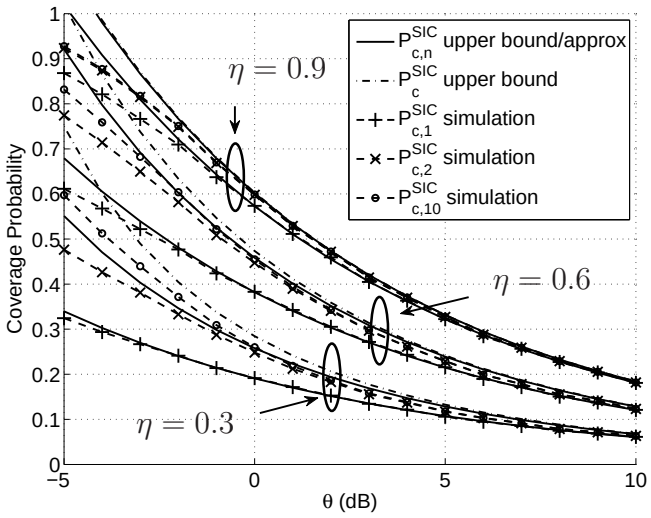


Figure 5.7. Coverage probability of femto-cell networks with SIR threshold $\theta \geq -5$dB with $\alpha = 4$. The solid lines are calculated for $n = 1, 2$ according to (5.14) (the lines are higher for larger $n$), which are an upper bounds on $P_{c,n}^{\text{SIC}}$ when $\theta \geq 0$dB. For $\theta \leq 0$, these lines should be considered as approximations. The upper bound on $P_{c}^{\text{SIC}}$ is calculated by (5.15). The simulated value of $P_{c,n}^{\text{SIC}}$ is plotted for $n = 1, 2, 10$. For $\eta \leq 0.9$, the curves for $n = 2$ and $n = 10$ almost completely overlap throught the simulated SIR range.

Fig. 5.6 compares the coverage probabilities with different levels of SIC capability for different path loss exponents $\alpha$ when $\theta = 1$. As expected, as $\alpha$ decreases, both the coverage probability and the gain of additional SIC capability decrease. The former is due to the fact that with a smaller $\alpha$ the far users contribute more to the interference. The latter can be explained by the fact that when $\alpha$ is smaller, the received power from different users are more comparable, leaving less structure in the received signal that can be exploited by SIC.

Similarly, we can apply the bounds in (5.14) and (5.15) to even smaller $\alpha$ which may apply to outdoor environments, and conceivably the gain of SIC will becomes even more marginal. Therefore, *SIC is more useful in an indoor environment.*

Generally speaking, accurately estimating $P_{c,n}^{\text{SIC}}$ is more difficult when $\theta < 1$. One

of the reasons is that the upper bound in Theorem 6 becomes increasingly loose as $\theta$ decreases. However, within the realistic parameters, *i.e.,* $\theta > -3$dB, the values calculated by (5.14)[4] and (5.15) are still informative as is shown in Fig. 5.7. This figure shows the coverage probability as a function of $\theta \geq -5$dB for $\eta = 0.3, 0.6, 0.9$. We found that most of the the conclusions we made for $\theta \geq 1$ still hold when $\theta \geq -5$dB. For example, we can still see that most of the gain of SIC comes from canceling a single interferer and that the gain is larger when $\eta$ is close to 0.5.

Quantitatively, we found that when $\eta$ is relatively small ($\eta = 0.3, 0.6$) the analytical results still track the results obtained by simulation closely for $\theta > -3$dB. The analytical results are less precise when $\eta$ is large. However, large $\eta$ characterizes a regime where most of the BSs are accessible. In this case, it is conceivable that SIC is often unnecessary, which can be verified by either the simulation results or the analytical results in Fig. 5.7. Therefore, overall, the analytical results generates enough quantitative insights for the most interesting set of parameters.

## 5.7 Conclusions

Building upon the theoretical results derived in Chapter 4, this chapter demonstrates how a marked PLPF framework can be used to generate insights in designing heterogeneous cellular networks (HCNs) with SIC capability at the UE side. We show that the code rate can significantly impact the usefulness of successively canceling a large number of non-accessible BSs. In particular, SIC in combination with low rate codes can boost the coverage probability of the HCN to a large extent. We also observe that, for contemporary OFDM-based cellular systems, most of the gain of SIC comes from canceling a single non-accessible BS.

An important contribution of this chapter is the demonstration of a general ap-

[4] (5.14) can only be considered as an approximation on $P_{c,n}^{\text{SIC}}$ when $\theta < 1$ since Proposition 21 only gives a lower bound in this regime.

proach to analyze HCNs based on constructing the (marked) PLPF and calculating the *equivalent access probability* (EAP). We show that the complexity introduced by the network heterogeneity can be elegantly addressed through this approach and the coverage probability with SIC can be evaluated based on the knowledge about the same problem in the homogeneous networks. In addition to SIC, this approach can be used to analyze many other techniques in HCNs and has the potential to generalize many known results from homogeneous networks to heterogeneous networks.

# CHAPTER 6

# CONCLUDING REMARKS AND FUTURE WORK

## 6.1 Random Power Control in Networks with Both Noise and Interference

In Chapter 2, we show that random power control can significantly reduce the local delay in noise-limited networks and in many cases the optimal memoryless random power control strategy is an ALOHA-type random on-off policy. Under a game theoretic formulation, Chapter 3 shows similar results in interference-limited networks. In particular, we show that in many cases, ALOH-type random on-off power control policies are the single node optimal power control (SNOPC) and Nash equilibrium power control (NEPC) strategies. These results provide a new view of ALOHA as a efficient power control scheme. The gain of random power control in interference-limited networks are also demonstrated numerically.

A natural extension of these results is to consider the (more realistic) case with both noise and interference. In the case of Rayleigh fading, similar results can be obtained by a relatively straightforward extension of the results in Chapter 3. To see this, recall that the success probability of a transmission attempt over link distance $r$ with power $P$ is

$$\mathbb{P}(Phr^{-\alpha} > \theta I) = \mathcal{L}_I(s)|_{s=\frac{\theta r^\alpha}{P}}. \tag{6.1}$$

In the presence of noise of power $N_0$, the success probability becomes

$$\mathbb{P}\left(\frac{Phr^{-\alpha}}{I+N_0} > \theta\right) = \mathcal{L}_I(s)e^{-N_0 s}|_{s=\frac{\theta r^\alpha}{P}},$$

which can be considered as a noiseless link with another interference distribution. Therefore, although the analytical results in previous chapters will become more cumbersome if noise is included, the method will be the same.

For other fading distributions, the approaches we used in Chapter 3 are not directly applicable. Further investigation is needed to obtain deeper understanding in such cases. However, based on the results in Chapter 2 and 3, it is reasonable to conjecture that the optimality of random on-off power control still hold at least in the sense as stated in Chapter 3.

## 6.2 Practical Aspects of Random on-off Power Control

### 6.2.1 Adaptive Modulation

The optimality of random on-off power control strategies is to some extent a result of the fixed SNR (SIR) threshold $\theta$. If there are more than one possible rate, *i.e.,* more than one threshold, the optimal power control strategies need to be redefined, as it is reasonable to consider different pay-offs (utility) for successful transmission at different rates.

Since real wireless systems typically have more than one modulation and coding schemes (MCSs), it is of interest to understand how to jointly choose MCS and random power control schemes to maximize the utility.

### 6.2.2 RF Constraints

The linear regime of practical RF devices is always limited. This is an important concern in real-world wireless networks especially when the power efficiency is critical. On the one hand, the optimality of random on-off schemes raises hope that the benefits of random power control can be fully harnessed using existing RF hardware. On the other hand, since the transmit power and probability of the optimal schemes

derived in Chapter 2 and 3 are typically a function of the knowledge regarding the channel fading and network geometry statistics, the implementation of random power control may require more than one power amplifiers (PAs) in order to be truly power efficient. Thus, there exists a trade-off between the cost (of the RF components) and performance (of random power control). Such trade-off is of practical interest and remains for future investigation.

## 6.3 More Detailed Modeling of SIC in Random Wireless Networks

### 6.3.1 Centralized Rate Assignment and Scheduling

Chapter 4 and 5 assume all the transmitters in the network are transmitting at the same rate. In some cases, it is more likely (and potentially more desirable) to allow transmitters to transmit at different rates. For example, in cellular uplinks, the BSs may assign different users with different rates according to the channel quality and thus significantly boost the expected aggregate throughput at the receiver. Similarly, by scheduling users with significantly different received powers at the same time, the BS can potentially improve the expected number of users that can be successively decoded.

Although such rate assignment and scheduling is unlikely in the cellular downlinks, modeling the centralized rate assignment and scheduling properly would be an important step toward understanding the fundamental limits of SIC in the cellular uplinks.

### 6.3.2 Power Control and SIC

#### 6.3.2.1 Deterministic Power Control

Similar to rate assignment and scheduling, power control can have a big impact on the gain of SIC. Letting stronger users to transmit at higher power while reducing

the power at the weaker users can increase the received power differences and thus increase the probability of successively decoding a large number of users. In fact, this is another way of manipulating $\beta$ in Chapter 4.

However, if there are more than one receivers in the network, the favorable power control strategy for one receiver may create unfavorable condition for another. Investigation on power control schemes that benefits the global performance of multi-receiver wireless networks remains for future work.

#### 6.3.2.2 Random Power Control

Random power control can be considered as a way of manipulating the fading distribution. Therefore, as a result of Corollary 7, any *global* random power control scheme will not improve the performance of SIC in interference-limited network. In noisy networks, the outlook of such random power control schemes are even more pessimistic: as pointed out in Section 4.7, *global* random power control is often likely to deteriorate the gain of SIC.

Nevertheless, the above arguments only account for the case where all the transmitters in the networks apply the *same* random power control strategy. If the transmitters in the networks can determine their own power control strategy based on the (local) information, a non-trivial (additional) gain in the performance of SIC is still conceivable. How to maximize and quantify such gain is still an unsolved interesting problem, remaining for future research.

# BIBLIOGRAPHY


1. N. Abramson. The ALOHA system: another alternative for computer communications. In *AFIPS '70 (Fall): Proceedings of the November 17-19, 1970, fall joint computer conference*, pages 281–285, New York, NY, USA, 1970. ACM.

2. K. Akkarajitsakul, E. Hossain, D. Niyato, and D. Kim. Game theoretic approaches for multiple access in wireless networks: A survey. *IEEE Communications Surveys & Tutorials*, 13(3):372–395, Mar. 2011. ISSN 1553-877X. doi: 10.1109/SURV.2011.122310.000119.

3. E. Altman and Z. Altman. S-modular games and power control in wireless networks. *IEEE Transactions on Automatic Control*, 48(5):839–842, May 2003. ISSN 0018-9286. doi: 10.1109/TAC.2003.811264.

4. J. Andrews. Interference cancellation for cellular systems: a contemporary overview. *IEEE Wireless Communications0*, 12(2):19 – 29, april 2005. ISSN 1536-1284. doi: 10.1109/MWC.2005.1421925.

5. J. Andrews and T. Meng. Optimum power control for successive interference cancellation with imperfect channel estimation. *IEEE Transactions on Wireless Communications*, 2(2):375 – 383, mar 2003. ISSN 1536-1276. doi: 10.1109/TWC.2003.809123.

6. M. Andrews and M. Dinitz. Maximizing capacity in arbitrary wireless networks in the SINR model: Complexity and game theory. In *28th IEEE International Conference on Computer Communications (INFOCOM'09)*, pages 1332–1340, april 2009. doi: 10.1109/INFCOM.2009.5062048.

7. B. C. Arnold, N. Balakrishnan, and H. N. Nagaraja. *A First Course in Order Statistics (Classics in Applied Mathematics)*. SIAM, 2008. ISBN 0898716489, 9780898716481.

8. E. Asgeirsson and P. Mitra. On a game theoretic approach to capacity maximization in wireless networks. In *30th IEEE International Conference on Computer Communications (INFOCOM'11)*, pages 3029–3037, april 2011. doi: 10.1109/INFCOM.2011.5935146.

9. F. Baccelli and B. Baszczyszyn. A new phase transitions for local delays in manets. In *INFOCOM, 2010 Proceedings IEEE*, pages 1 –9, march 2010. doi: 10.1109/INFCOM.2010.5462132.

10. F. Baccelli, B. Blaszczyszyn, and P. Muhlethaler. An ALOHA protocol for multihop mobile wireless networks. *IEEE Transactions on Information Theory*, 52 (2):421–436, Feb. 2006. ISSN 0018-9448. doi: 10.1109/TIT.2005.862098.

11. F. Baccelli, B. Baszczyszyn, and M.-o. Haji-mirsadeghi. optimal paths on the space-time SINR random graph. *Advances in Applied Probability*, 43(1):131 – 150, 2011. ISSN 00018678.

12. F. Baccelli, A. El Gamal, and D. Tse. Interference networks with point-to-point codes. *IEEE Transactions on Information Theory*, 57(5):2582–2596, May 2011. ISSN 0018-9448. doi: 10.1109/TIT.2011.2119230.

13. R. Berry and R. Gallager. Communication over fading channels with delay constraints. *Information Theory, IEEE Transactions on*, 48(5):1135 –1149, may 2002. ISSN 0018-9448. doi: 10.1109/18.995554.

14. J. Blomer and N. Jindal. Transmission capacity of wireless ad hoc networks: Successive interference cancellation vs. joint detection. In *IEEE International Conference on Communications, 2009. (ICC '09)*, pages 1 –5, june 2009. doi: 10.1109/ICC.2009.5199541.

15. V. Cadambe and S. Jafar. Interference alignment and the degrees of freedom of wireless x networks. *IEEE Transactions on Information Theory*, 55(9):3893 –3908, sept. 2009. ISSN 0018-9448. doi: 10.1109/TIT.2009.2025541.

16. G. Caire, G. Taricco, and E. Biglieri. Optimum power control over fading channels. *IEEE Transactions on Information Theory*, 45(5):1468 –1489, jul 1999. ISSN 0018-9448. doi: 10.1109/18.771147.

17. R. Cheng and S. Verdu. Gaussian multiaccess channels with ISI: capacity region and multiuser water-filling. *IEEE Transactions on Information Theory*, 39(3): 773–785, May 1993. ISSN 0018-9448. doi: 10.1109/18.256487.

18. M. Chiang, P. Hande, T. Lan, and C. W. Tan. *Power Control in Cellular Networks*. NOW: Foundations and Trends in Networking, 2008.

19. B. E. Collins and R. L. Cruz. Transmission policies for time varying channels with average delay constraints. In *Annual Allerton Conference on Communication, Control, and Computing*, pages 709–717, 1999.

20. M. Costa. Writing on dirty paper (corresp.). *IEEE Transactions on Information Theory*, 29(3):439 – 441, may 1983. ISSN 0018-9448. doi: 10.1109/TIT.1983.1056659.

21. T. Cover. Broadcast channels. *IEEE Transactions on Information Theory*, 18 (1):2 – 14, jan 1972. ISSN 0018-9448. doi: 10.1109/TIT.1972.1054727.

22. T. M. Cover and J. A. Thomas. *Elements of Information Theory*. John Wiley & Sons, Inc., New York, 1991.

23. H. Dhillon, R. Ganti, F. Baccelli, and J. Andrews. Coverage and ergodic rate in K-tier downlink heterogeneous cellular networks. In *2011 49th Annual Allerton Conference on Communication, Control, and Computing (Allerton)*, pages 1627–1632, Sept. 2011. doi: 10.1109/Allerton.2011.6120363.

24. H. S. Dhillon, R. K. Ganti, F. Baccelli, and J. G. Andrews. Modeling and analysis of K-tier downlink heterogeneous cellular networks. *IEEE Journal on Selected Areas in Communications*, 30(3):550–560, Apr. 2012.

25. M. Dinitz. Distributed algorithms for approximating wireless network capacity. In *29th IEEE International Conference on Computer Communications (INFOCOM'10)*, pages 1–9, march 2010. doi: 10.1109/INFCOM.2010.5461905.

26. M. Elmusrati, N. Tarhuni, and R. Jantti. Performance analysis of random uniform power allocation for wireless networks in Rayleigh fading channels. *European Transactions on Telecommunications*, 20(4):457–462, 2009. ISSN 1541-8251.

27. G. J. Foschini and Z. Miljanic. A simple distributed autonomous power control algorithm and its convergence. *IEEE Transactions on Vehicular Technology*, 42 (4):641–646, Nov. 1993.

28. A. Fu, E. Modiano, and J. Tsitsiklis. Optimal energy allocation for delay-constrained data transmission over a time-varying channel. In *INFOCOM 2003. Twenty-Second Annual Joint Conference of the IEEE Computer and Communications. IEEE Societies*, volume 2, pages 1095 – 1105 vol.2, march-3 april 2003. doi: 10.1109/INFCOM.2003.1208946.

29. A. Ghosh, J. G. Andrews, N. Mangalvedhe, R. Ratasuk, B. Mondal, M. Cudak, E. Visotsky, T. A. Thomas, P. Xia, H. S. Jo, H. S. Dhillon, and T. D. Novlan. Heterogeneous cellular networks: From theory to practice. *IEEE Communications Magazine*, June 2012.

30. A. Goldsmith and P. Varaiya. Capacity of fading channels with channel side information. *Information Theory, IEEE Transactions on*, 43(6):1986 –1992, nov 1997. ISSN 0018-9448. doi: 10.1109/18.641562.

31. A. Goldsmith, S. Jafar, N. Jindal, and S. Vishwanath. Capacity limits of MIMO channels. *IEEE Journal on Selected Areas in Communications*, 21(5):684 – 702, june 2003. ISSN 0733-8716. doi: 10.1109/JSAC.2003.810294.

32. Z. Gong and M. Haenggi. The local delay in mobile poisson networks. *IEEE Transactions on Wireless Communications*, 2013. Accepted. Available at `http://www.nd.edu/~mhaenggi/pubs/twc13.pdf`.

33. I. S. Gradshteyn and I. M. Ryzhik. *Table of Integrals, Series, and Products*. Academic Press, 7th edition edition, 2007.

34. M. Haenggi. On distances in uniformly random networks. *IEEE Transactions on Information Theory*, 51(10):3584–3586, Oct. 2005.

35. M. Haenggi. A geometric interpretation of fading in wireless networks: Theory and applications. *IEEE Transactions on Information Theory*, 54(12):5500–5510, Dec. 2008.

36. M. Haenggi. Local delay in static and highly mobile poisson networks with ALOHA. In *IEEE International Conference on Communications (ICC)*, pages 1 –5, may 2010. doi: 10.1109/ICC.2010.5502205.

37. M. Haenggi. Local delay in Poisson networks with and without interference. In *Annual Allerton Conference on Communication, Control, and Computing (Allerton)*, pages 1482 –1487, 29 2010-oct. 1 2010. doi: 10.1109/ALLERTON.2010.5707088.

38. M. Haenggi. Diversity loss due to interference correlation. *IEEE Communications Letters*, 16(10):1600–1603, Oct. 2012.

39. M. Haenggi. *Stochastic Geometry for Wireless Networks*. Cambridge University Press, 2012.

40. M. Haenggi. The local delay in Poisson networks. *IEEE Transactions on Information Theory*, 59(3):1788–1802, Mar. 2013. Available at `http://www.nd.edu/~mhaenggi/pubs/tit13.pdf`.

41. M. Haenggi and R. K. Ganti. *Interference in Large Wireless Networks*. Foundations and Trends in Networking. NOW, 2008.

42. M. Haenggi, J. G. Andrews, F. Baccelli, O. Dousse, and M. Franceschetti. Stochastic geometry and random graphs for the analysis and design of wireless networks. *IEEE Journal on Selected Areas in Communications*, 27(7):1029–1046, Sept. 2009.

43. P. Hande, S. Rangan, M. Chiang, and X. Wu. Distributed uplink power control for optimal SIR assignment in cellular data networks. *IEEE/ACM Transactions on Networking*, 16(6):1420–1433, Dec. 2008. ISSN 1063-6692. doi: 10.1109/TNET.2008.918070.

44. T. Holliday, A. Goldsmith, P. Glynn, and N. Bambos. Distributed power and admission control for time varying wireless networks. In *Global Telecommunications Conference, 2004 (GLOBECOM'04)*, volume 2, pages 768–774, Dec. 2004. doi: 10.1109/GLOCOM.2004.1378064.

45. J. Huang, R. Berry, and M. Honig. Distributed interference compensation for wireless networks. *IEEE Journal on Selected Areas in Communications*, 24(5):1074–1084, May 2006. ISSN 0733-8716. doi: 10.1109/JSAC.2006.872889.

46. K. Huang, J. Andrews, D. Guo, R. Heath, and R. Berry. Spatial interference cancellation for multiantenna mobile ad hoc networks. *IEEE Transactions on Information Theory*, 58(3):1660 –1676, march 2012. ISSN 0018-9448. doi: 10.1109/TIT.2011.2178140.

47. A. Hunter, S. Weber, and J. Andrews. Transmission capacity of wireless ad hoc networks with spatial diversity. *IEEE Transactions on Wireless Communications*, 7(12):5058–5071, Dec. 2008.

48. V. Kawadia and P. Kumar. Principles and protocols for power control in wireless ad hoc networks. *IEEE Journal on Selected Areas in Communications*, 23(1): 76–88, Jan. 2005. ISSN 0733-8716. doi: 10.1109/JSAC.2004.837354(410)23.

49. M. Khojastepour and B. Aazhang. The capacity of average and peak power constrained fading channels with channel side information. In *Wireless Communications and Networking Conference, 2004. WCNC. 2004 IEEE*, volume 1, pages 77 – 82 Vol.1, march 2004. doi: 10.1109/WCNC.2004.1311521.

50. T.-S. Kim and S.-L. Kim. Random power control in wireless ad hoc networks. *Communications Letters, IEEE*, 9(12):1046–1048, Dec. 2005. ISSN 1089-7798. doi: 10.1109/LCOMM.2005.1576583.

51. J. Lee and N. Jindal. Energy-efficient scheduling of delay constrained traffic over fading channels. *Wireless Communications, IEEE Transactions on*, 8(4):1866 –1875, april 2009. ISSN 1536-1276. doi: 10.1109/T-WC.2008.080037.

52. L. Li and A. Goldsmith. Capacity and optimal resource allocation for fading broadcast channels .I. ergodic capacity. *Information Theory, IEEE Transactions on*, 47(3):1083 –1102, mar 2001. ISSN 0018-9448. doi: 10.1109/18.915665.

53. A. MacKenzie and S. Wicker. Game theory in communications: motivation, explanation, and application to power control. In *IEEE Global Telecommunications Conference, 2001 (GLOBECOM'01)*, volume 2, pages 821–826, Dec. 2001. doi: 10.1109/GLOCOM.2001.965533.

54. P. Madhusudhanan, J. G. Restrepo, Y. E. Liu, and T. X. Brown. Downlink coverage analysis in a heterogeneous cellular network. In *IEEE Global Communications Conference (GLOBECOM'12)*, 2012.

55. M. Medard and R. Gallager. Bandwidth scaling for fading multipath channels. *Information Theory, IEEE Transactions on*, 48(4):840 –852, apr 2002. ISSN 0018-9448. doi: 10.1109/18.992769.

56. F. Meshkati, H. Poor, S. Schwartz, and N. Mandayam. An energy-efficient approach to power control and receiver design in wireless data networks. *IEEE Transactions on Communications*, 53(11):1885–1894, Nov. 2005. ISSN 0090-6778. doi: 10.1109/TCOMM.2005.858695.

57. V. Mhatre, K. Papagiannaki, and F. Baccelli. Interference mitigation through power control in high density 802.11 WLANs. In *26th IEEE International Conference on Computer Communications (INFOCOM'07)*, pages 535–543, May 2007. doi: 10.1109/INFCOM.2007.69.

58. N. Miridakis and D. Vergados. A survey on the successive interference cancellation performance for single-antenna and multiple-antenna OFDM systems. *IEEE Communications Surveys and Tutorials*, 15(99):1–24, 2012. ISSN 1553-877X. doi: 10.1109/SURV.2012.030512.00103.

59. D. Rajan, A. Sabharwal, and B. Aazhang. Delay-Bounded Packet Scheduling of Bursty Traffic over Wireless Channels. *IEEE Transactions on Information Theory*, 50(1):125–144, Jan. 2004.

60. B. Rimoldi and R. Urbanke. A rate-splitting approach to the Gaussian multiple-access channel. *IEEE Transactions on Information Theory*, 42(2):364 –375, mar 1996. ISSN 0018-9448. doi: 10.1109/18.485709.

61. Z. Shen, J. Andrews, and B. Evans. Optimal power allocation in multiuser OFDM systems. In *IEEE Global Telecommunications Conference, 2003 (GLOBECOM '03)*, volume 1, pages 337–341, Dec. 2003. doi: 10.1109/GLOCOM.2003.1258257.

62. V. Srivastava, J. Neel, A. Mackenzie, R. Menon, L. Dasilva, J. Hicks, J. Reed, and R. Gilles. Using game theory to analyze wireless ad hoc networks. *IEEE Communications Surveys & Tutorials*, 7(4):46–56, fourth quarter 2005. ISSN 1553-877X. doi: 10.1109/COMST.2005.1593279.

63. D. Stoyan, W. S. Kendall, and J. Mecke. *Stochastic Geometry and Its Applications*. New York: Wiley, 2nd edition, 1995.

64. V. Subramanian and B. Hajek. Broad-band fading channels: signal burstiness and capacity. *Information Theory, IEEE Transactions on*, 48(4):809 –827, apr 2002. ISSN 0018-9448. doi: 10.1109/18.992762.

65. E. Telatar. Capacity of multi-antenna gaussian channels. *European Transactions on Telecommunications*, 10(6):1–28, 1999.

66. I. Telatar and D. Tse. Capacity and mutual information of wideband multipath fading channels. *Information Theory, IEEE Transactions on*, 46(4):1384 –1400, jul 2000. ISSN 0018-9448. doi: 10.1109/18.850678.

67. D. Tse and P. Viswanath. *Fundamentals of wireless communication*. Cambridge university press, 2005.

68. S. Vanka, S. Srinivasa, Z. Gong, P. Vizi, K. Stamatiou, and M. Haenggi. Superposition coding strategies: Design and experimental evaluation. *IEEE Transactions on Wireless Communications*, 11(7):2628–2639, July 2012.

69. R. Vaze and R. Heath. Transmission capacity of ad-hoc networks with multiple antennas using transmit stream adaptation and interference cancellation. *IEEE Transactions on Information Theory*, 58(2):780 –792, Feb. 2012. ISSN 0018-9448. doi: 10.1109/TIT.2011.2173712.

70. A. Viterbi. Very low rate convolution codes for maximum theoretical performance of spread-spectrum multiple-access channels. *IEEE Journal on Selected Areas in Communications*, 8(4):641–649, 1990.

71. S. Weber, J. Andrews, X. Yang, and G. D. Veciana. Transmission capacity of wireless ad hoc networks with successive interference cancellation. *IEEE Transactions on Information Theory*, 53(8):2799–2814, Aug. 2007.

72. A. Zanella and M. Zorzi. Theoretical analysis of the capture probability in wireless systems with multiple packet reception capabilities. *IEEE Transactions on Communications*, 60(4):1058 –1071, april 2012. ISSN 0090-6778. doi: 10.1109/TCOMM.2012.021712.100782.

73. X. Zhang and M. Haenggi. ALOHA performs delay-optimum power control. In *IEEE Global Communications Conference (GLOBECOM'11)*, Houston, TX, Dec. 2011.

74. X. Zhang and M. Haenggi. A location-based MAC scheme for random networks. In *IEEE International Conference on Communications (ICC'11)*, Kyoto, Japan, June 2011.

75. X. Zhang and M. Haenggi. The performance of successive interference cancellation in random wireless networks. In *IEEE Global Telecommunications Conference (GLOBECOM'12)*, Dec. 2012.

76. X. Zhang and M. Haenggi. ALOHA performs optimal power control in Poisson networks. In *2012 Information Theory and Applications Workshop (ITA'12)*, 2012.

77. X. Zhang and M. Haenggi. Random power control in Poisson networks. *IEEE Transactions on Communications*, 60(9):2602–2611, Sept. 2012.

78. X. Zhang and M. Haenggi. Delay-optimal power control policies. *IEEE Transactions on Wireless Communications*, 11(10):3518–3527, Oct. 2012.

79. X. Zhang and M. Haenggi. The aggregate throughput in random wireless networks with successive interference cancellation. In *IEEE International Symposium on Information Theory (ISIT'13)*, July 2013.

80. X. Zhang and M. Haenggi. On decoding the $k$th strongest user in Poisson networks with arbitrary fading distribution. In *47th Asilomar Conference of Signals, Systems and Computers (Asilomar'13)*, Pacific Grove, CA, Nov. 2013.

81. X. Zhang and M. Haenggi. The performance of successive interference cancellation in random wireless networks. *IEEE Transactions on Information Theory*, 2013. Submitted. Available at `http://www.nd.edu/~mhaenggi/pubs/tit14.pdf`.

82. Y. Zhong, W. Zhang, and M. Haenggi. Managing interference correlation through random medium access. *IEEE Transactions on Wireless Communications*, 2013. Submitted. Available at `http://www.nd.edu/~mhaenggi/pubs/twc13c.pdf`.